Engineering Lib

UNITED STATES DEPARTMENT OF COMMERCE

Journal of Research

of the

National Bureau of Standards

Vol. 30, No. 6 June 1943

CONTENTS

RP	TITLE AND AUTHOR	Page
1541.	Thermal expansivity and density of indium. Peter Hidnert and Mary Grace Blair.....[Price 5c]	427
1542.	Measurements of ultraviolet solar radiation in Washington, 1936 to 1942. W. W. Coblentz and R. Stair.....[Price 5c]	434
1543.	A tungsten-in-quartz lamp and its applications in photoelectric radiometry. R. Stair and Wm. O. Smith.....[Price 10c]	449
1544.	Effect of turbulence and channel slope on translation waves. Garbis H. Keulegan and George W. Patterson.....[Price 10c]	461
	Index to volume 30 (January to June 1943) Research Papers RP1513 to RP1544.....	513

The articles listed May be purchased separately (see cover page II) at the prices stated

A monthly periodical of pure and applied science published by our National Government

Journal of Research
of the
National Bureau of Standards

The January 1943 issue of the JOURNAL OF RESEARCH of the National Bureau of Standards began the thirtieth semiannual volume of this periodical. Fundamental researches in progress in the Bureau's laboratories are reported in this JOURNAL. If you are interested in new developments in science and technology, you should receive the JOURNAL. If you are not already a subscriber, you are invited to send in your subscription.

Technical News Bulletin

This is a monthly publication containing short articles reporting progress of work in the Bureau laboratories, abstracts of papers which appear in the JOURNAL OF RESEARCH, accounts of scientific and technical meetings in which the Bureau has taken part, a list of all publications by members of the staff, and other items within the Bureau's fields. The BULLETIN is designed primarily to give a general and timely review of the activities of the Bureau in brief form. It is a prompt and reliable source of official information. If you have not already subscribed for the BULLETIN, you are invited to do so.

ANNUAL SUBSCRIPTION	Price	
	United States, Canada, Cuba, Mexico, Newfoundland, Republic of Panama	Other countries
JOURNAL OF RESEARCH of the National Bureau of Standards:		
12 monthly issues (2 volumes), paper covers	$3.50	$4.50
Bound volume (½ year, 1 volume) blue buckram	3.00	3.50
Technical News Bulletin, 12 monthly issues	.50	.70

Research Papers, reprinted individual articles appearing in the JOURNAL OF RESEARCH, are available from the Superintendent of Documents shortly after appearance of monthly issue of the JOURNAL

Address orders only to
Superintendent of Documents, U. S. Government Printing Office,
Washington, D. C.

UNITED STATES DEPARTMENT OF COMMERCE
JESSE H. JONES, Secretary
NATIONAL BUREAU OF STANDARDS
Lyman J. Briggs, Director

✦

Journal of Research

of the

National Bureau of Standards

✦

Volume 30, Number 6

June 1943

[Published with the approval of the Director of the Budget]

UNITED STATES
GOVERNMENT PRINTING OFFICE
WASHINGTON : 1943

For sale by the Superintendent of Documents, U. S. Government Printing Office
Washington, D. C. - Price 30 cents - $3.50 per year on subscription

The prices of the separate Research Papers appearing in this JOURNAL are given on the front cover page. If 100 or more copies of any separate are ordered, a discount of 25 percent is allowed. Those who desire copies of separate Research Papers should send their orders and remittances without delay to the Superintendent of Documents, U. S. Government Printing Office, Washington, D. C. This will aid him to determine the number of copies to be printed for sale. Research Papers are not printed from electrotypes, and usually no more reprints can be had when the first and only printing is exhausted.

MATHEMATICAL TABLES

A list of the mathematical tables now obtainable from the National Bureau of Standards is printed on pages 3 and 4 of the JOURNAL cover. New tables will be announced from time to time as they become available.

U. S. DEPARTMENT OF COMMERCE NATIONAL BUREAU OF STANDARDS

RESEARCH PAPER RP1541

Part of Journal of Research of the National Bureau of Standards, Volume 30, June 1943

THERMAL EXPANSIVITY AND DENSITY OF INDIUM

By Peter Hidnert and Mary Grace Blair

ABSTRACT

The linear thermal expansion of cast indium of high purity was investigated between −190° and +100°C and the cubical thermal expansion between 0° and 50°C. The following equation was derived for the linear expansion of indium:

$$L_t = L_0[1 + (28.9_3 t + 0.013_4 t^2)10^{-6}],$$

where L_0 represents the length of the metal at 0°C, and L_t the length at any temperature, t, within the range of the observations. The average coefficients of cubical expansion of indium were found to be 77×10^{-6} and 101×10^{-6} per degree centigrade for the ranges 0° to 25°C and 25° to 50°C, respectively. These coefficients of cubical expansion are not equal to three times the coefficients of linear expansion for the corresponding temperature ranges on account of the anisotropy of indium.

The density of cast indium was found to be 7.281 g/cm³ at 22.6°C. The density of indium calculated from the best available data on atomic weights and lattice constants is 7.40 g/cm³. Observed densities at 0°, 25°, and 50°C are also given in this paper.

CONTENTS

	Page
I. Introduction	427
II. Material investigated	428
III. Apparatus	428
IV. Results	428
1. Thermal expansion	428
2. Density	432
V. References	432

I. INTRODUCTION

In 1869 Fizeau [1] [1] reported the value 41.7×10^{-6} per degree centigrade for the coefficient of linear thermal expansion of cast indium at 40° C and the value 0.4238×10^{-6} as the change per degree centigrade in the coefficient, or rate, of expansion. He computed the value 45.9×10^{-6} per degree centigrade for the average coefficient of expansion of indium between 0° and 100° C. The work described in the present paper was undertaken in order to obtain data on the linear thermal expansion of high-purity indium over a wide range of temperature (−190° to +100° C). Data on the cubical thermal expansion and density of indium between 0° and 50° C were also obtained.

Industrial applications of indium have been indicated by Murray [2], Williams [3], Linford [4], Dyer [5], and Ludwick [6]. A compilation of some of the physical properties of indium was given by Westbrook [7].

[1] Figures in brackets indicate the literature references at the end of this paper.

II. MATERIAL INVESTIGATED

A rod of cast indium loaned to the National Bureau of Standards by the Indium Corporation of America, Utica, N. Y., was used for the determinations of thermal expansion and density. A spectrochemical analysis [2] was made on a piece cut from the rod of indium. Traces of Ag, Ca, Cr, Mg, and Tl, small amounts (less than 0.01 percent) of Al, Cd(?), Co(?), Cu, Mn, Si, and Sn, and larger amounts of Fe, Ni, and Pb, were reported. The results of a chemical analysis [3] were: Fe, 0.01 percent; Pb, 0.01 percent; and Ni, not detected. The indium content was estimated to be 99.9 percent.

X-ray diffraction patterns [4] obtained on a piece cut from the rod of indium, after the second expansion test had been completed, indicated large crystals. A subsequent examination (see footnote 4) of an etched section of the piece of indium indicated that the average diameter of the crystals was 1 to 2 mm.

III. APPARATUS

Five linear expansion tests were made on the rod of indium (10 mm in diam). The length of the sample was 250 mm for tests 1 and 2, which were made from 20° to 100° C with the precision micrometric thermal-expansion apparatus described by Souder and Hidnert [8]. The details of the specimen mounting for use in the furnace are illustrated in figure 4 of their publication.

Tests 3 [5] to 5 were made at low temperatures with the fused-quartz-tube thermal-expansion apparatus [6] described by Hidnert and Sweeney [9]. Liquid air, solid carbon dioxide in a mixture of equal parts of carbon tetrachloride and chloroform, and ice and water were used for low temperature baths at about −190°, −78°, and 0° C, respectively.

IV. RESULTS

1. THERMAL EXPANSION

Figures 1 and 2 show the linear expansion and contraction curves of the sample of indium on two cycles of heating and cooling between 20° and 100° C and on three cycles of cooling and heating at low temperatures. Table 1 gives the coefficients of expansion and contraction obtained from these curves.

[2] By Dorothy Grosch, of the National Bureau of Standards.
[3] By R. K. Bell, of the National Bureau of Standards.
[4] By H. C. Vacher, of the National Bureau of Standards.
[5] Before test 3, the rod of indium was cut to a length of 200 mm.
[6] This apparatus was found to be unsatisfactory for determinations of the linear thermal expansion of indium above room temperature on account of flow of the sample caused by the combined weight of the foot of the dial indicator and the movable fused-quartz rod of the apparatus.

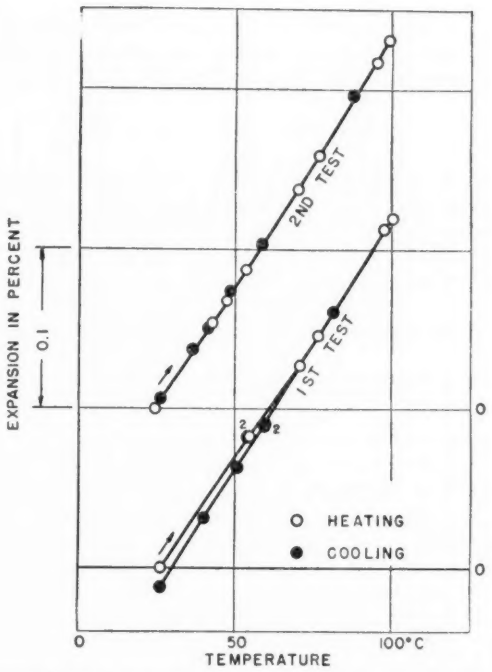

FIGURE 1.—*Linear thermal expansion of indium on heating from room temperature to 100° C and contraction on subsequent cooling from 100° C to room temperature.*

Each number adjacent to a point on the curve represents the number of observations at the temperature. The variations in these observations were too small to be indicated on this scale.

TABLE 1.—*Coefficients of linear expansion and contraction of a sample of indium*

Test	Treatment [a]	Average coefficients of expansion and contraction per degree centigrade					
		−190° to −80° C	−80° to 0° C	−80° to +20° C	20° to 60° C	60° to 100° C	20° to 100° C
		×10⁻⁶	×10⁻⁶	×10⁻⁶	×10⁻⁶	×10⁻⁶	×10⁻⁶
1 Heating	As cast				29.0	30.3	29.7
1 Cooling	As cast				30.5	31.6	31.0
2 Heating	Heated to 100° C and cooled slowly				29.8	31.4	30.6
2 Cooling	Heated to 100° C and cooled slowly				30.2	31.2	30.7
3, Cooling	Reheated to 100° C and cooled slowly		28.2	28.4			
4 Cooling	Cooled to −80° C and heated to +20° C	25.6	29.1				
4 Heating	Cooled to −80° C and heated to +20° C	24.8	28.0	28.1			
5 Cooling	Cooled to −190° C and heated to +20° C	25.1	28.2	28.5			
5 Heating	Cooled to −190° C and heated to +20° C	25.4	26.9	27.1			
Values from equation 2		25.3	27.9	28.1	30.0	31.1	30.5

[a] All heat treatments on the cast sample were incident to the tests on thermal expansion.

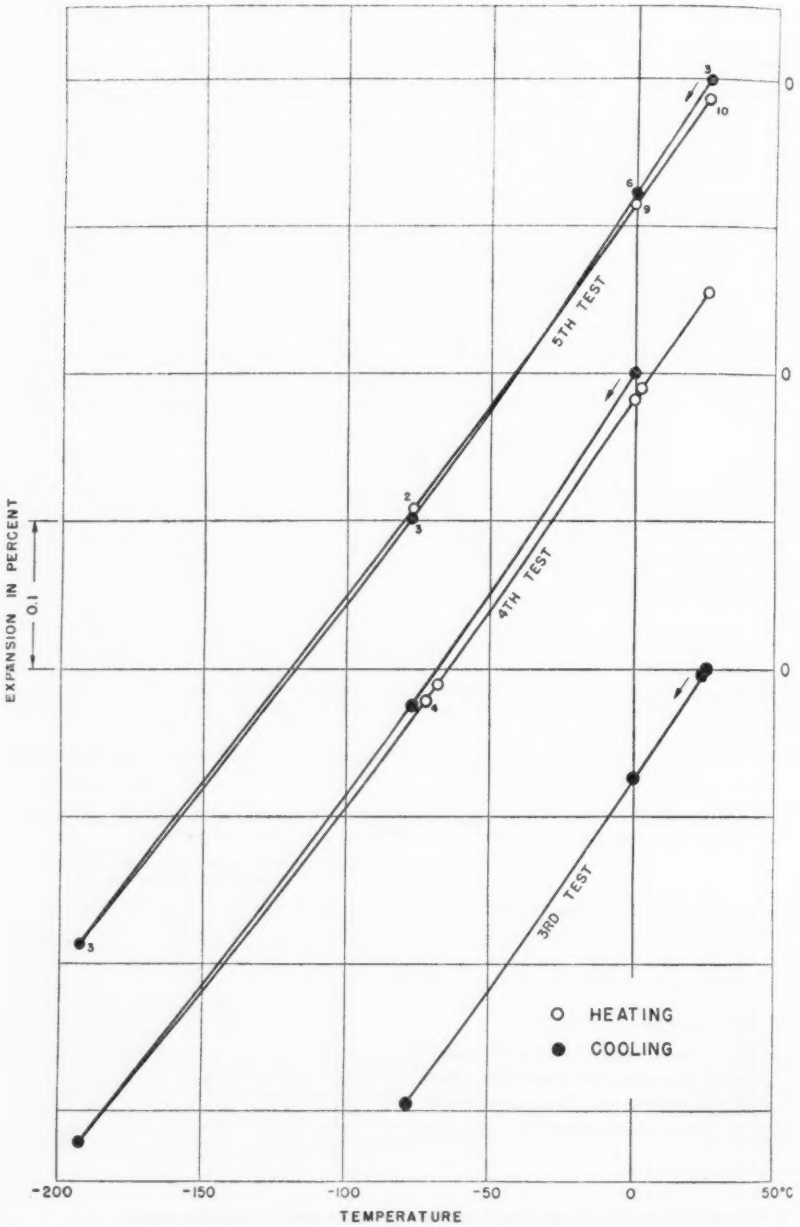

FIGURE 2.—*Linear thermal contraction on cooling to low temperatures and expansion on subsequent heating to room temperature.*

Each number adjacent to a point on the curve represents the number of observations at the temperature. The variations in these observations were too small to be indicated on this scale.

From the average coefficients of linear expansion and contraction obtained in the five tests on indium (table 1), the following linear equation was derived by the method of least squares:

$$a_t = (28.9_3 + 0.026_8 t)10^{-6}, \quad (1)$$

where a_t is the instantaneous coefficient of expansion (contraction) or the rate of expansion (contraction) at any temperature, $t°$ C, between $-135°$ and $+80°$ C. The probable error of a_t is $\pm 0.4 \times 10^{-6}$. The differences in the coefficients of expansion (table 1) and the magnitude of the probable error of a_t indicate that this metal failed to give reproducible results on heating and cooling.

The following second-degree equation was obtained by integration of equation 1:

$$L_t = L_0[1 + (28.9_3 t + 0.013_4 t^2)10^{-6}]. \quad (2)$$

In this equation, L_0 represents the length at 0° C and L_t the length at any temperature, $t°$ C, within the range of the observations.

After the determinations on linear thermal expansion had been completed, the cubical expansion of the sample of indium was determined between 0° and 50° C by weighing the sample in air at room temperature and in water at 0°, 25°, and 50° C. Table 2 gives the coefficients of cubical expansion. These coefficients of cubical expansions [7] are not equal to three times the coefficients of linear expansion of the sample of indium on account of the anisotropy [8] of indium.

TABLE 2.—*Coefficients of cubical expansion of indium*

Temperature range	Average coefficient of cubical expansion per degree centigrade
°C	$\times 10^{-6}$
0 to 25	77
25 to 50	101
0 to 50	89

The coefficient of linear expansion of indium (30.0×10^{-6}) at 40° C, computed from equation 1, is considerably less than the coefficient 41.7×10^{-6} reported by Fizeau [1]. The large divergence between these values may be ascribed to different orientations of the crystals in the two samples.

Frevel and Ott [10] determined the coefficients of linear thermal expansion of crystal indium along the *a*-axis and the *c*-axis from X-ray measurements on the cell dimensions of 99.9-percent-pure indium. They reported 56×10^{-6} and 13×10^{-6} for the coefficients of linear expansion along the *a*-axis and *c*-axis, respectively, for the range [9] from $-17°$ to $+9°$ C. From these coefficients of linear

[7] Except the coefficient of cubical expansion for the range 0° to 50°C.
[8] Crystal structure of indium is face-centered tetragonal [10, 11].
[9] This range of temperature was reported in a private communication by L. K. Frevel, The Dow Chemical Co., Midland, Mich.

expansion, the computed coefficient of cubical expansion is 125×10^{-6} for the range from $-17°$ to $+9°$ C. The coefficients of cubical expansion given in table 2 are less than the value calculated from the results of Frevel and Ott [10] at a lower range of temperature.

2. DENSITY

Before the determinations of thermal expansion were made, the density of the 250-mm rod of indium was found to be 7.281 g/cm³ at 22.6° C. The density of indium was also calculated from the equation

$$D=\frac{nw(H/N_0)}{a^2c}, \tag{3}$$

where D is the density, n is the number of atoms included within the unit cell of the metal, w is the atomic weight of the metal, H is the atomic weight of hydrogen, N_0 is the Avogadro number, and a and c are the lattice constants of the metal. If the following values [10] are substituted in this equation:

$$\begin{aligned} n&=4\\ w&=114.76\\ H&=1.0080\\ N_0&=6.023\times10^{23}\\ a&=4.58_5\times10^{-8}\text{ cm}\\ c&=4.94_1\times10^{-8}\text{ cm}, \end{aligned}$$

the computed density is 7.39_6 g/cm³. This value agrees within 2 percent of the observed density. Observed densities reported in the literature [14] range from about 7.12 to 7.42 g/cm³.

After the completion of the thermal-expansion determinations, the density of the 200-mm rod of indium was calculated at several temperatures from the data obtained in the determinations of cubical expansion. The results are given in table 3.

TABLE 3.—*Density of indium*

Temperature	Density
°C	g/cm³
25	7.275
0	7.289
50	7.257
25	7.274

V. REFERENCES

[1] H. Fizeau, *Tableau des dilatations par la chaleur de divers corps simples métal liques ou non métalliques, et de quelques composés hydrogénés du carbone,* Compt. rend. **68,** 1125 (1869) or *Wärme-Ausdehnungen verschiedener einfacher, metallischer und nicht-metallischer Körper, so wie einiger Kohlenwasserstoff-Verbindungen,* Ann. Physik u. Chem. **18,** [5] (**138**), 26 (1869).

[2] W. S. Murray, *Indium available in commercial quantities,* Ind. Eng. Chem. **24,** 686 (1932).

[3] R. V. Williams, *Use of indium in dental alloys,* J. Am. Coll. Dentists **5,** 78 (1938).

[4] H. B. Linford, *Indium,* Chem. & Chem. Eng., News Ed. **18,** 624 (1940).

[10] Values for H and N_0 complied by Birge [12] and those for a and c by Neuburger [13].

[5] J. R. Dyer, Jr., *Indium*, Iron Age **146,** 35 (Dec. 19, 1940).
[6] M. T. Ludwick, *Indium*, Steel **111, 80** (Nov. 9, 1942).
[7] L. R. Westbrook, *Indium: Recovery by electrodeposition*, Trans. Am. Electrochem. Soc. **57,** 289 (1930).
[8] W. Souder and P. Hidnert, *Measurements on the thermal expansion of fused silica*, Sci. Pap. BS **21,** 1 (1926–27) S524.
[9] P. Hidnert and W. T. Sweeney, *Thermal expansion of magnesium and some of its alloys*, BS J. Research **1,** 771 (1928) RP29.
[10] L. K. Frevel and E. Ott, *The X-ray study of indium and the indium-silver system*, J. Am. Chem. Soc. **57,** 228 (1935).
[11] E. Zintl and S. Neumayr, *Gitterstruktur des Indiums*, Z. Elektrochem. **39,** 81 (1933).
[12] R. T. Birge, *A new table of values of the general physical constants*, Rev. Modern Phys. **13,** 233 (1941).
[13] M. C. Neuburger, *Gitterkonstanten für das Jahr 1936*, Z. Krist. **93,** 1 (1936).
[14] J. W. Mellor, A Comprehensive Treatise on Inorganic and theoretical Chemistry **5,** 390 (Longman, Green, & Co., London and New York, 1924).

WASHINGTON, January 21, 1943.

U. S. DEPARTMENT OF COMMERCE NATIONAL BUREAU OF STANDARDS

RESEARCH PAPER RP1542

Part of Journal of Research of the National Bureau of Standards, Volume 30, June 1943

MEASUREMENTS OF ULTRAVIOLET SOLAR RADIATION IN WASHINGTON, 1936 TO 1942

By W. W. Coblentz and R. Stair

ABSTRACT

Continuing earlier measurements of ultraviolet solar radiation (RP877), a summary is given of similar measurements made during the years 1936 to 1942, in Washington, D. C. Marked variations in the spectral quality and total intensity of ultraviolet solar radiation, attributable to variations in atmospheric turbidity, and, to a less extent, to well-known cyclonic and seasonal changes in ozone concentrations in the stratosphere, are recorded. On the clearest days the biologically effective ultraviolet of wavelengths shorter than 3132 A, incident directly from the sun and the surrounding sky at midday, ranges from about 75 microwatts per square centimeter ($\mu w/cm^2$) in midsummer to about 12 $\mu w/cm^2$ in midwinter.

CONTENTS

		Page
I.	Introduction	435
II.	Apparatus and methods	436
III.	Discussion of ultraviolet solar intensity data	443
IV.	References and notes	447

I. INTRODUCTION

The evaluation of the biologically effective component of ultraviolet in sunlight is still in its infancy. The difficulties and uncertainties involved in present-day measurements of the ultraviolet component of sunlight are somewhat comparable with those experienced in the beginning of the evaluation of the total incident solar radiation of all wavelengths, half a century ago.

For some years the present writers have been engaged in an investigation of instruments and methods of evaluating the biologically effective component of ultraviolet solar and sky radiation useful in heliotherapy.

In a previous paper [1] [1] measurements were given of the biologically effective ultraviolet solar radiation of wavelengths 3132 A and shorter, incident normally in Washington, during the years 1934 and 1935. The present paper summarizes similar measurements made on some of the clearest days during the years 1936 to 1942, inclusive.

The hereindescribed measurements of ultraviolet solar intensities, incident normally upon the earth's surface, were obtained principally for three purposes:

(a) to secure data on the intensities, incident directly from the sun and from a small contiguous portion of the sky, that may be expected on relatively clear days at a sea-level station in midlatitude (which in-

[1] Figures in brackets indicate the literature references and notes at the end of this paper.

formation is of important in biological and photochemical irradiation experiments using a small exposure aperture);

(b) to secure data required in working out methods of evaluating the biologically effective component of ultraviolet solar radiation [1]—required particularly in one method of standardizing ultraviolet dosage-intensity meters [4, 11]; and

(c) to determine whether, with the accuracy attainable in the radiometric measurements, the reduction factors (F, G) used in the calculations of ultraviolet intensities, will require modifications with changes in the spectral quality of the biologically effective ultraviolet radiation, which varies with the ozone concentration in the stratosphere, which, in turn, varies with the latitude, the season, the barometric pressure (movements of masses of polar air) and, less systematically, with the sunspot cycle [5, 6, 18].

II. APPARATUS AND METHODS

In previous publications, descriptions were given of the instruments used in making ultraviolet solar-intensity measurements and the methods of evaluating the biologically effective spectral component of wavelengths 3132 A and shorter [1, 2, 7]. It will therefore suffice to recall that the intensity measurements were made with a spectrally selective radiometer [2] consisting of Ti-photoelectric cells sensitive to wavelengths 3500 A and shorter, and suitable glass filters that exclude ultraviolet radiation of wavelengths 3150 A and shorter.

The photoelectric cell in its mounting is shown in figure 1 of reference [7]. The aperture exposed to the sun and surrounding sky is about 22°. As shown in previous papers, at high elevations the amount of ultraviolet sky radiation is small (p. 142 of ref. [7]). On the other hand, at a sea-level station even a slightly hazy atmosphere greatly increases the amount of ultraviolet sky radiation; but the total ultraviolet radiation from the sun and from a small part of the surrounding sky, incident normal upon the photocell receiver, is greatly reduced—see the measurements of April 13 and 16, 1942, depicted in figure 10.

Using a photoelectric cell and filter method [1, 2], the separation of the amount of biologically effective ultraviolet solar radiation of wavelengths 3132 A and shorter from the total amount of all wavelengths measured by a particular photoelectric cell (having a threshold of response at 3200 to 3500 A), requires measurements of the total intensity of the radiation to which the photoelectric cell responds and the amount transmitted through the filters at various solar altitudes. A knowledge is required also of: (a) the spectral response of the photoelectric cell, (b) the ultraviolet spectral transmissions of the filters, (c) the ultraviolet spectral-energy distribution at different solar heights (air masses), and (d) calibration of the ultraviolet meter, in absolute value, against a standard of ultraviolet radiation [8].

At the beginning of these investigations [20], based upon the spectral range of the erythemic and antirachitic responses, the intense emission line in the mercury arc at 3132 A was adopted as the long-wavelength limit of biological effectiveness. In the meantime, it has been established that the spectral range of the tanning reaction extends to longer wavelengths [9], upon which basis it seemed logical to place the limit of biological effectiveness at 3200 A [10]. Another reason for considering the adoption of a threshold of biological effectiveness at longer wavelengths was the development of photocells sensitive

only to wavelengths shorter than about 3200 A, for use in measuring solar and sky radiation on a horizontal plane [11]. If reproducible photoelectric cells with the same threshold of response were available, ultraviolet radiometry would be greatly simplified. Thus far, however, it has been impossible to make photocells having the same threshold of response. Hence, in view of the well-established use of 3132 A in specifying the long-wavelength limit of biological effectiveness, it seems desirable to continue the use of this wavelength limit. This, of course, requires the continuation of the use of complicated factors for reducing the measurements obtained with various photoelectric cells and filters. In the present paper (figs. 4 to 9, inclusive) the data are given for both spectral ranges—to 3132 A and to 3200 A, respectively.

The procedure employed in calculating the factor P, used in calibrating the photoelectric cell against a primary standard of ultraviolet radiation, and the factor G, used in evaluating the ultraviolet solar radiation of wavelengths shorter than 3132 A (or 3200 A) relative

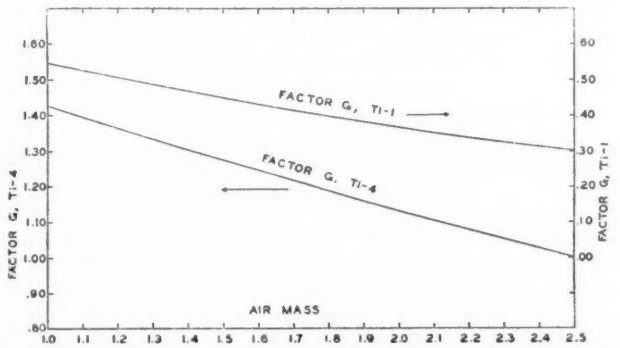

FIGURE 1.—*Reduction factors, G, used in determining the amount of ultraviolet solar radiation of wavelengths shorter than and including 3200 A relative to the total spectral range measured with photoelectric cells Ti–1 and Ti–4.*

to the total range of wavelengths to which the photocell responds, is described in previous papers [1, 13]. As a matter of record, in figure 1 are illustrated the reduction factors G for the spectral band of 3200 A and shorter wavelengths for comparison with figure 5 of reference [1] for the band of 3132 A and shorter wavelengths. Obviously, if photocells can be developed having the same threshold response (say 3200 A) for use as comparison standards, the same factor G can be used for all or be eliminated entirely by comparison with primary standards.

The weak point in the calculation of the factor G is the lack of exact knowledge of the spectral distribution of energy in the extreme ultraviolet of solar radiation at the observing station. The method of deducing the solar spectral-energy distribution by means of various photoelectric cells and filters is described in previous publications ([7] and p. 323 of ref. [1]). To simplify the calculations, a smooth spectral-energy distribution is assumed, although from the very beginning [20] it was noted that the energy curve is deeply indented (see fig. 2 of ref. [7] and p. 167 of RP1367 [18]) by numerous Fraunhofer and ozone absorption lines.

This method of checking the ultraviolet spectral-energy distribution may be criticized because of the difficulty in determining the threshold and the shape of the spectral photoelectric response. The recent determinations of the spectral responses of our photoelectric cells, using a monochromator and a mercury- or cadmium-arc lamp, are therefore supplemented by integrated filter-transmission measurements of the

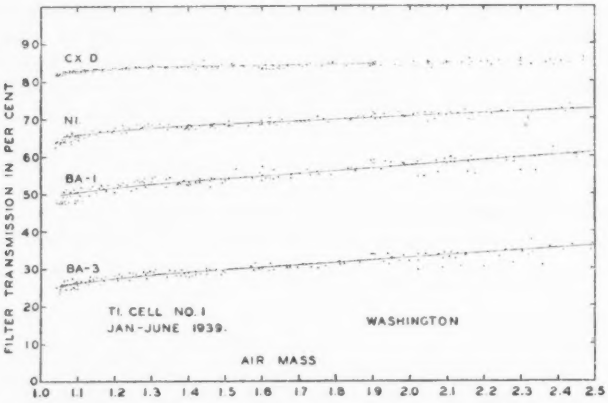

FIGURE 2.—*Diurnal variation in transmission of ultraviolet solar radiation through standard filters, from January to June 1939, observed in Washington.*

See fig. 3 for seasonal variation.

ultraviolet radiation emitted by a tungsten-ribbon-filament lamp operated at a high temperature (2,900°K), and using the spectral-

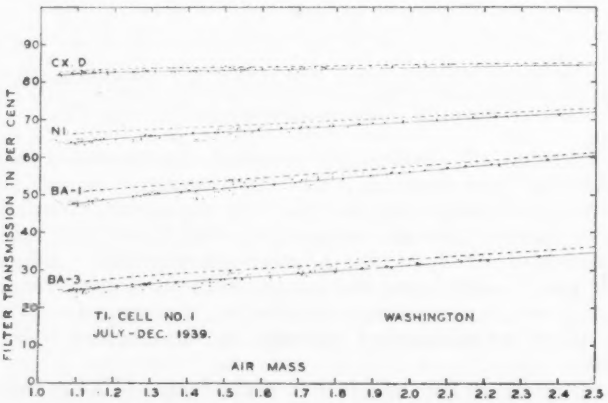

FIGURE 3.—*Diurnal and (dotted curves from fig. 2) seasonal variation in transmission of ultraviolet solar radiation through standard filters, observed from July to December 1939, in Washington, D. C.*

energy data observed by Hamaker [14] (communicated by Ornstein [14]) and by Hoffmann and Willenberg [15].

As shown elsewhere [16, 17], based upon integrated ultraviolet-transmission measurements made with four filters of known spectral ultraviolet transmissions and eight photoelectric cells differing widely

in spectral photoelectric response, the average values of the spectral emissivities of tungsten, in the band of wavelengths extending from 2,400 to 3,500 A, observed by Hoffmann and Willenberg appear to be substantially correct. Hence, as mentioned above, in recent determinations of the spectral response of a photoelectric cell, the wide gaps between the response measurements, made with the spectrally isolated emission lines of the mercury and the cadmium arc (at 3,024, 3,132, 3,261, 3,342, and 3,663 A) are filled in on the basis of a smooth spectral photoelectric response curve that is adjusted to give calculated filter transmissions in agreement with the integrated filter transmissions observed on the ultraviolet radiation from a tungsten-ribbon lamp operated at a known temperature.

From our most recent studies it appears that the ultraviolet solar spectral-energy distributions, published in table 2 (p. 323 of ref. [1]), remain unchanged for air masses $m=2$, and less; but for air masses, $m=2.3$ and larger, the data appear to belong to air masses about 0.3 larger, e. g., $m=3.3$ instead of $m=3.0$. However, for these large air masses the spectral intensities of the shortest wavelengths are so small that this uncertainty seems relatively negligible in the present-day stage of evaluation of biologically effective ultraviolet solar radiation. As noted in earlier papers [1, 12], the good agreement in the measurements of the biologically effective component of ultraviolet solar radiation of wavelengths shorter than 3,132 A, obtained with spectrally nonselective thermopiles and with wavelength-selective radiometers differing greatly in range of spectral photoelectric response, appears to be real and not the result of a fortuitous combination of factors, including (a) the spectral responses of the photoelectric cells, (b) the spectral transmissions of the filters, and (c) the transmissions of the integrated ultraviolet solar radiation through the various filters.

In figures 4 to 10, inclusive, the ultraviolet intensities are given in the two above-mentioned spectral ranges, extending from the shortest incident wave lengths (at about 2900 A) to 3132 A and to 3200 A, respectively. The values of the intensities in these two spectral ranges differ by about 40 percent, varying from about 33 percent for air mass, $m=3$, to about 48 percent for $m=1.05$. In these illustrations the scale on the right-hand side is to the nearest rounded numbers. Based upon some preliminary trials [4], it is believed that when satisfactory photoelectric cells are obtainable for use as primary standards, the calibration of meters for measuring ultraviolet solar and sky radiation incident on a horizontal plane will be greatly simplified.

During the 7 years of measurements included in the present report, two of the filters (Ba–1 and Ba–3, a soft glass) became slightly scratched from frequent wiping with a fine-haired brush and were replaced by others of practically the same thickness. No difference was observed in the ultraviolet intensities deduced from the measurements with the old and new filters. Furthermore, frequent calibration against a primary standard of ultraviolet radiation showed no systematic change in the sensitivity of the photocells (Ti–1 and Ti–4, illustrated in figs. 1 and 2 of ref. [7]) used throughout these researches. From this it appears that the instrumental precision from year to year was maintained within 10 percent, or even closer.

The accuracy attained in the measurements of ultraviolet solar intensities was limited entirely by meteorological conditions. As

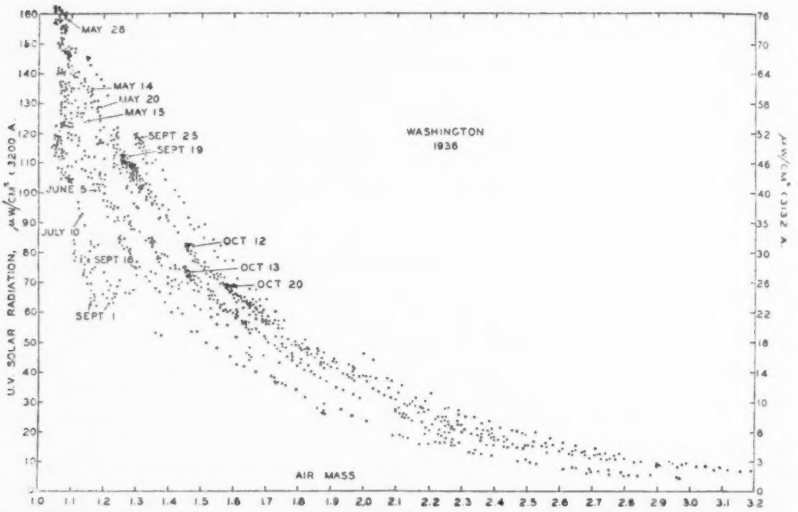

FIGURE 4.—*Measurements of ultraviolet solar radiation of wavelengths shorter than 3132 A, also 3200 A and shorter, during some of the clearest days in 1936.*

noted in previous papers, on the clearest days at high elevations (Flagstaff, Ariz.) where the measurements could be repeated to 0.1 to 0.2 percent, a change in spectral quality and total intensity, result-

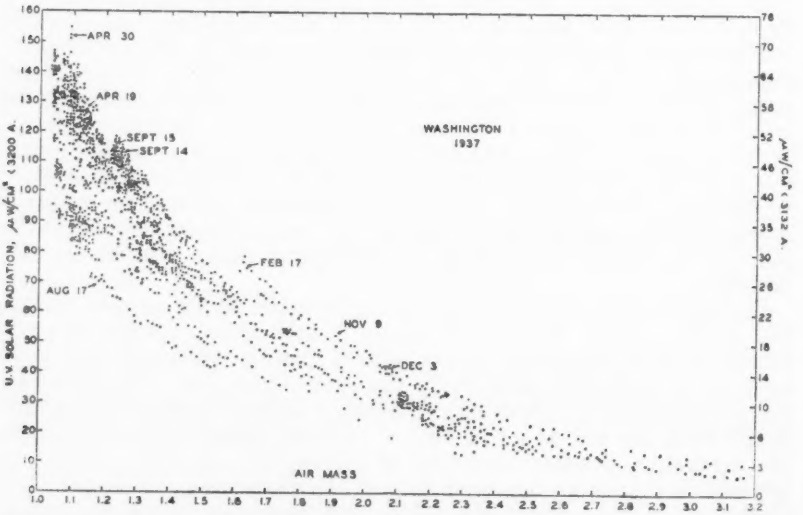

FIGURE 5.—*Measurements of ultraviolet solar radiation of wavelengths shorter than 3132 A, also 3200 A and shorter, during some of the clearest days in 1937.*

ing from a change in solar height, was observed from minute to minute.

In contrast, at sea-level stations (San Juan, P. R., and Washington, D. C.) with a continual variation in turbidity in the lower atmos-

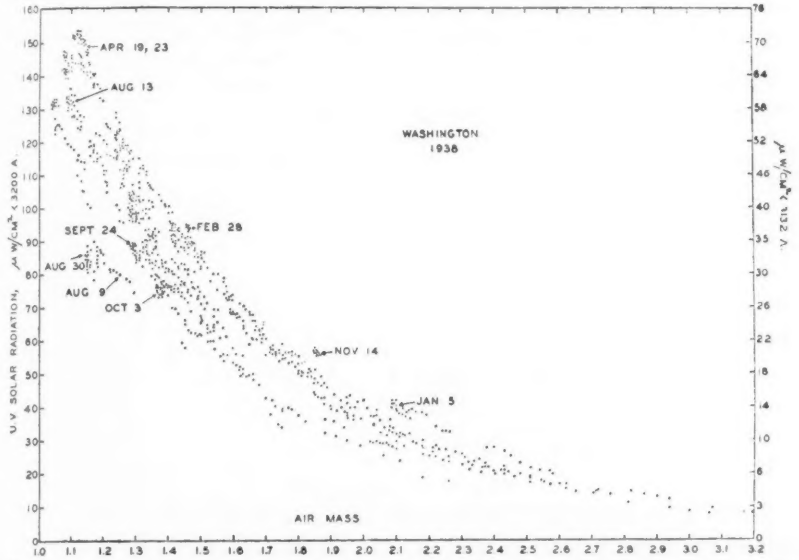

FIGURE 6.—*Measurements of ultraviolet solar radiation of wavelengths shorter than 3132 A, also 3200 A and shorter, during some of the clearest days in 1938.*

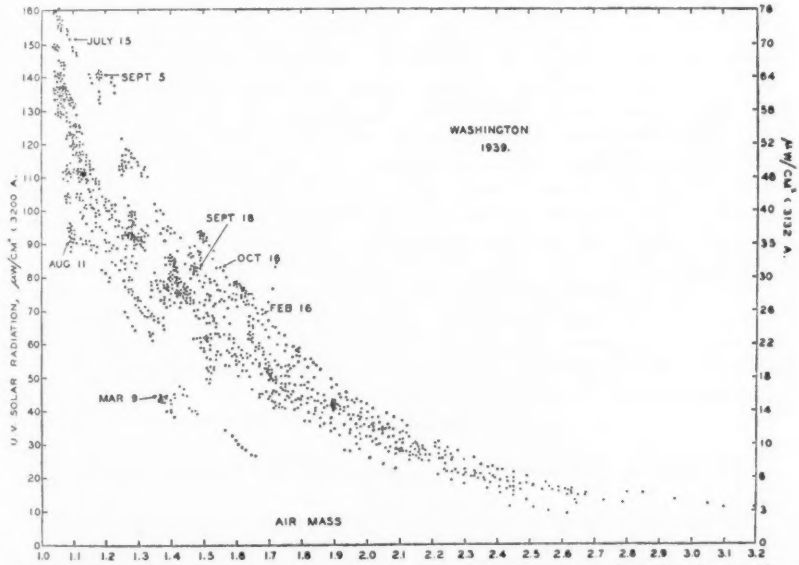

FIGURE 7.—*Measurements of ultraviolet solar radiation of wavelengths shorter than 3132 A, also 3200 A and shorter, during some of the clearest days in 1939.*

phere, the precision attained is best shown graphically in the measurements of April 13 and 16, 1942, figure 10, where each measurement (the

instantaneous value in the group, say at $m=1.2$ and at $m=1.3$) is probably accurate to 1 percent. Nevertheless, because of atmos-

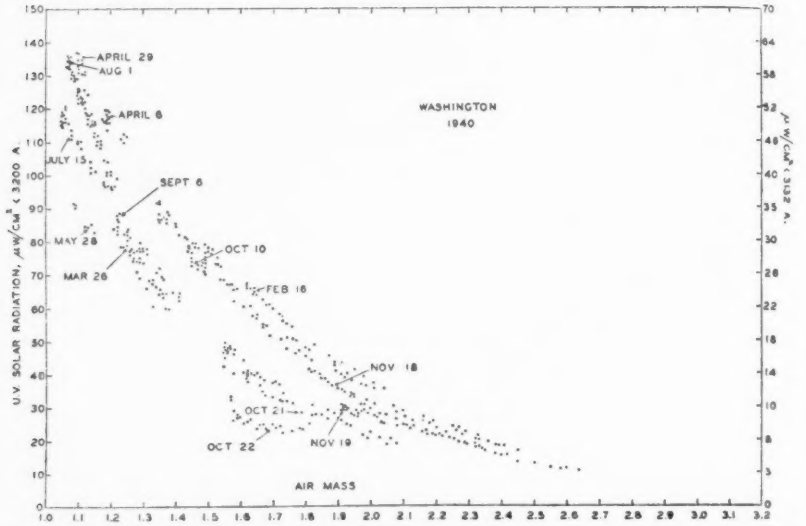

FIGURE 8.—*Measurements of ultraviolet solar radiation of wavelengths shorter than 3132 A, also 3200 A and shorter, during some of the clearest days in 1940.*

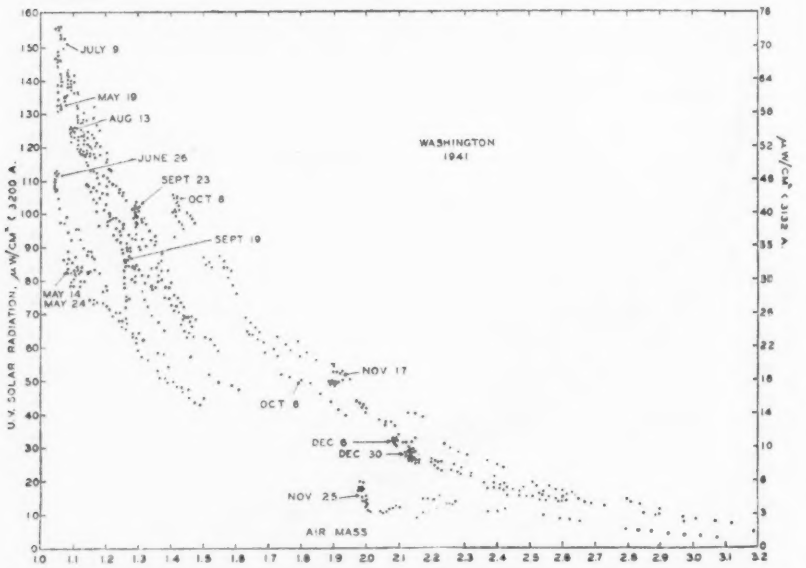

FIGURE 9.—*Measurements of ultraviolet solar radiation of wavelengths shorter than 3132 A, also 3200 A and shorter, during some of the clearest days in 1941.*

pheric conditions the average values for these two days are best represented by the two lines drawn through these measurements.

The wide spread in the values of the ultraviolet solar intensities depicted in figures 4 to 10, inclusive, is attributable to constantly varying meteorological conditions. This was shown in an earlier paper (fig. 6 of ref [1], where a detailed description is given of the effect of a slight change in turbidity upon the ultraviolet intensities observed throughout an exceptionally clear day, May 18, 1935.

The accuracy attained in the absolute values of the herein-described measurements of ultraviolet solar intensities is somewhat of a conjecture. As noted in a previous paper (p. 335 and fig. 6 of ref. [1]), using three distinctly different methods of evaluation (thermoelectric

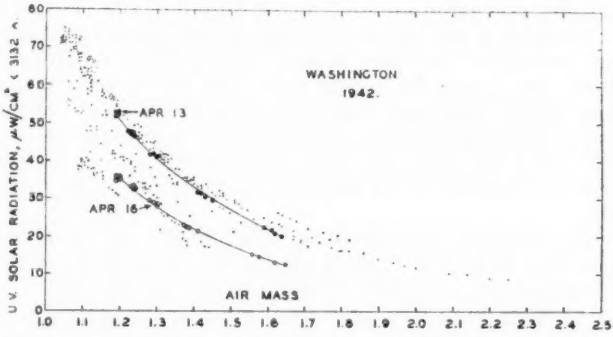

FIGURE 10.—*Measurements of ultraviolet solar radiation of wavelengths shorter than 3132 A, during some of the clearest days in 1942.*

The large black dots, and the circles, connected with lines, indicate measurements on 2 days, differing greatly in atmospheric turbidity.

and photoelectric), the ultraviolet solar intensities, of wavelengths 3132 A and shorter, observed at midday in Washington during the clearest midsummer weather, range from 75 to 78 $\mu w/cm^2$.

Using measured intensities of ultraviolet solar radiation, from erythematogenic tests made at two sea-level stations (San Juan, P. R., and Washington, D. C.) and at two high elevations (7,300 and 10,000 ft.; Flagstaff and the San Francisco Peaks, Ariz.), the uncertainty in the radiometric evaluation seems to be no greater than the uncertainty in the biological evaluation used in checking the radiometric measurements, viz., 10 to 15 percent [1]. This uncertainty is due to a lack of knowledge of the spectral-energy distribution of solar radiation in the biologically effective range of wavelengths 3200 A and shorter. Similar radiometric and biologic comparisons made by Greider and Downs, by Luckiesh, and by Pettit (discussed on p. 973 of ref. [20], reduced to the same range of wavelengths, are in good agreement with the foregoing data.

III. DISCUSSION OF ULTRAVIOLET SOLAR INTENSITY DATA

In previous papers it was shown that, for the same solar altitudes, the atmosphere is more transparent to ultraviolet radiation of short wavelengths in the afternoon than in the forenoon and more transparent in the autumn than in the spring (p. 144 and fig. 5 of ref. [7]). The reason therefor is the presence of less ozone in the stratosphere in

the autumn than in the spring [5, 6], and presumably less in the afternoon than in the forenoon. While, in the present stage of evaluation of ultraviolet solar radiation, this difference in atmospheric transparency is not taken into consideration (see figs. 2 and 5 of ref. [1]), it is evident that, at stations where atmospheric conditions are sufficiently constant to warrant such refinements in reducing the observations, this variation in ultraviolet transparency should be included in the calculations.

In figure 2 of a previous publication [1] a sudden, presumably seasonal, change in atmospheric transparency was observed in the tropics. Similar changes are evident from the filter measurements made at Flagstaff, Ariz., elevation about 7,300 ft (fig. 5 of ref. [7] and fig. 3 of ref. [18]). In spite of the great variation in the dirunal measurements, the average values of the filter transmissions observed from January to June 1939 (fig. 2 and the dotted curves in fig. 3) are conspicuously higher than those observed from July to December 1939 (fig. 3). This seasonal difference in filter transmissions is equivalent to a difference of about 0.2 air mass (3° to 5° in solar height) or a decrease of perhaps 8 to 10 percent in the amount of ozone in the stratosphere in the autumn.

The measurements of ultraviolet solar radiation of wavelengths shorter than and including 3132 A, also in the spectral range of 3200 A and shorter wavelengths, made on some of the clearest days during the years 1936 to 1942, inclusive, in Washington, are depicted in figures 4 to 10.

The wide difference in the ultraviolet intensities observed from day to day at any given solar height (air mass in these illustrations) is attributed primarily to variations in atmospheric turbidity, although changes in the amount of ozone in the stratosphre also cause variations in ultraviolet intensities. Even a slight increase in atmospheric scattering (as judged by the solar corona) greatly decreases the intensity of ultraviolet radiation incident on a surface exposed normal to the sun's rays. This was repeatedly observed in the measurements of 1942 (fig. 10), the most of which were made in connection with the calibration of a photoelectric cell used for measuring ultraviolet solar and sky radiation incident on a horizontal plane (4, 11]. In the course of these measurements of solar and sky radiation it was repeatedly observed (by shadowing the receiver from the direct solar rays) that it was only during the noon hours of the clearest days in early summer that the ultraviolet radiation from the whole sky incident on a horizontal surface was slightly less than the directly incident solar rays, and that when the sky was slightly turbid, the ultraviolet radiation from the whole sky was at least 2.5 times greater than the directly incident solar rays [3, 4].

A specific example of the decrease in intensity caused by atmospheric scattering is illustrated in the measurements of April 13 and 16, 1942, depicted in figure 10. On April 13 (sky blue; no corona) the ratio of the ultraviolet in sky radiation to direct solar radiation was 1:1. On April 16 (sky turbid; white corona) the ultraviolet sky radiation was 2.5 times greater than the direct solar radiation. In this instance, however, contrary to general experience, the filter transmissions were lower on April 16 than on April 13, indicating the presence of a relatively greater amount of ultraviolet of the shortest wavelengths on April 16. This might be due to selective atmospheric (Rayleigh)

scattering (see p. 146, of ref. [7]). On the other hand, the barometer was higher (760 mm for 2 days; hence, there probably was less ozone) on April 16 than on April 13, when the barometer (759 mm) was rising from a (cyclonic) barometric low that occurred on April 10 to 11. It is therefore probable that on April 16 the reduction in ultraviolet intensities by atmospheric scattering was compensated for appreciably by an increased transparency (caused by a decreased ozone content) of the stratosphere to ultraviolet solar radiation. In this connection, reference is made to measurements procured at high altitudes (Flagstaff, Ariz., elevation 7,300 ft) showing the effect of (a) scattering by atmospheric water vapor and (b) variation in barometric pressure, and an accompanying variation in ozone content of the stratosphere, upon the incident ultraviolet solar radiation (see figs. 1 to 5, inclusive, of ref. [18]).

With constantly changing atmospheric pollution and cloudiness, especially at sea-level stations, great variations in ultraviolet intensities may be expected. Hence, the measurements depicted in figures 4 to 10 represent only what may be expected under the most favorable atmospheric conditions.

As already mentioned, because of the seasonal decrease in ozone content and, hence, increase in transparency of the stratosphere, the ultraviolet intensities should be systematically higher in the autumn than for similar solar heights at other seasons. This is shown in figure 4 (Sept. 25, Oct. 20), figure 5 (Nov. 9, Dec. 3), figure 7 (Sept. 5, Oct. 16), figure 9 (Oct. 8, Nov. 17), etc. However, while high ultraviolet solar intensities seem to predominate in the autumn, they occur frequently in the late winter and early spring (e. g., February and April; figs. 5, 6, 7, and 8), when the highest concentration of ozone usually prevails in the stratosphere (see fig. 1 of ref. [4]). Correcting for solar distance, the ultraviolet intensities in March, relative to September, would be reduced by about 2 percent. Evidently this does not explain the high ultraviolet solar intensities in February, which, more logically, are explainable on the basis of a temporary reduction in the ozone content (the "ozone holes" observed by Kiepenheuer [19]) and a concomitant increase in transparency of the stratosphere to ultraviolet radiation of very short wavelengths [19].

These measurements were begun when the relative numbers of sunspots were low (minimum in 1934). They include the maximum of the sunspot cycle (April 1937; secondary maximum January 1939) and the period of rapidly decreasing sunspot numbers in 1941 and 1942—predicated minimum about 1944.

The clearest weather is usually associated with a high or average barometric pressure. It is therefore rare to secure ultraviolet solar-intensity measurements during a cyclonic disturbance, when atmospheric ozone is higher than normal (see fig. 5 and discussion on p. 575 to 577 of ref. [18].

The seasonal variation in atmospheric ozone, especially in midlatitude (see fig. 1 of ref. [4]), also must be considered. Since the time of making the hereindescribed measurements, from season to season, could not be selected (for example, there were but few clear days during the summer of 1940—see fig. 8, $m=1.05$) only generalized comparisons can be made. It therefore seems illusory to attempt to seek a correlation of these data with the sunspot cycle. For example, in the measurements of 1938 (fig. 6) the noon-hour ultraviolet inten-

sities (u.v.Q.) for $m=1.1$ are higher than for $m=1.05$. This was owing to clearer weather in April than in June, and not because of the effect of sunspots upon the ultraviolet intensity. Selecting 2 years having the same sunspot numbers, in 1936 the u.v.Q. for $m=1.05$ is higher than in 1941; but in September the intensities are the same as, or they are higher than, observed during some other years. Again, in comparison with 1941, the u.v.Q. values of 1937 are low in April and September; and they are practically the same in February, November, and December.

In the absence of factors for eliminating the effect of atmospheric turbidity and the variability (seasonal and meteorological) of atmospheric ozone, it is impracticable to determine from these data the effect of sunspots upon the amount of ultraviolet emitted. In the few instances when observations could be made near the time when the ionosphere (and radio transmission) was disturbed by large outbursts of sunspots, the ultraviolet intensities showed nothing conspicuously different from the usual values.

The measurements depicted in figures 4 to 10 indicate what intensities may be expected in irradiation experiments using biological effective ultraviolet radiation incident from the sun and from a narrow portion of the surrounding sky, practically free from pollution by smoke, on relatively cloud-free days, at a practically sea-level station, Washington, D. C. The great variations in intensities from day to day, for the same solar height (air mass, in these illustrations), is caused primarily by differences in atmospheric turbidity. A specific example is illustrated in figure 10; April 13 and 16, 1942, described on a preceding page. At the same solar height (air mass traversed) the intensity differs by 30 to 35 percent, primarily because of atmospheric scattering. As will be shown in a subsequent paper, the total incident ultraviolet solar and sky radiation, integrated for the whole day, was 16 percent less on April 16 when the sky was more turbid.

In figures 4 to 10, inclusive, the dates attached to the low intensities indicate days that were conspicuously hazy; with no attempt at correlating the low values with atmospheric scattering and with increased ozone in the atmosphere as indicated by a decrease in barometric pressure.

From the data depicted in figures 4 to 10, inclusive, it appears that at a sea-level station in midlatitude, on exceptionally clear days, the noon-hour intensity of biologically effective ultraviolet radiation of wavelengths less than 3132 A, incident directly from the sun and a small portion of the surrounding sky, varies from about 75 $\mu w/cm^2$ in June (air mass, $m=1.05$) to about 12 $\mu w/cm^2$ in December ($m=2.1$). For similar measurements, made during 1934 and 1935, with noon-hour designations of intensities for all the months, reference is made to figure 7 of ref. [1].

In a previous paper (fig. 6 of ref. [4]) data were given showing that, in high latitudes (78° N) at the noon-hour on the clearest days in midsummer, the intensity of the biologically effective ultraviolet radiation of wavelengths shorter than 3200 A from the sun and the whole sky, incident on a horizontal plane, ranged from 30 to 40 $\mu w/cm^2$. As shown in the figures 4 to 10 of the present paper for the band of wavelengths shorter than 3132 A, the corresponding values range from 10 to 14 $\mu w/cm^2$. The longer spectral range includes more of the ultra-

violet rays that produce tanning. The shorter spectral range is of more significance in the prevention of rickets.

As noted in the previous paper [4], the intensity and biological effectiveness of ultraviolet solar and sky radiation, in midsummer, in high latitudes (78° N) is not markedly different from that observed at the same solar height in December ($m=2.1$) in Washington. It was shown also that while these intensities are low, if long exposures can be made, they are effective in heliotherapy.

IV. REFERENCES AND NOTES

[1] W. W. Coblentz and R. Stair, *Evaluation of ultraviolet solar radiation of short wave lengths*, J. Research NBS **16,** 315 (1936) RP877. See p. 339 for accuracy attained in erythema tests.

[2] W. W. Coblentz and R. Stair, *A portable ultraviolet meter, consisting of a balanced amplifier, photoelectric cell, and microammeter*, BS J. Research **12,** 231 (1934) RP647.

[3] *Instruments and methods of radiometry*, NBS Tech. News Bul. No. 289, p. 41 (May 1941). Reference to the use of an automatic inpulse ("traffic") counter in recording ultraviolet intensities [4].

[4] W. W. Coblentz, F. R. Gracely, and R. Stair, *Measurements of ultraviolet solar and sky radiation intensities in high latitudes*, J. Research NBS **28,** 581 (1942) RP1469.

[5] G. M. B. Dobson, *Measurements of the amount of ozone in the earth's atmosphere and its relation to other geophysical conditions*, pt. IV, Proc. Roy. Soc. (London) [A] **129,** 411 (1930). Appendix I, by H. H. Kimball, p. 418; appendix II, by E. Kidson, p. 421.

[6] F. W. P. Götz, Zum Strahlungsklima des Spitzbergensommers, Gerlands Beitr. Geophys. **31,** 119 (1931).

[7] W. W. Coblentz and R. Stair, *Factors affecting ultraviolet solar-radiation intensities*, J. Research NBS **15,** 123 (1935) RP816. See p. 142 for erythema tests, and figure 2 for photograph of the ultraviolet solar spectrum.

[8] W. W. Coblentz and R. Stair, *A standard source of ultraviolet radiation for calibrating photoelectric dosage intensity meters*, J. Research NBS **16,** 83 (1936) RP858.

[9] M. Luckiesh and A. H. Taylor, *Production of erythema and tan by ultraviolet energy*, J. Am. Med. Assn. **112,** 2510 (1939); I. Hausser, Strahlentherapie **62,** 315 (1938).

[10] W. W. Coblentz, *The spectral range of ultraviolet solar radiation useful in climatology*, Bul. Am. Meteorol. Soc. **22,** 316 (1941).

[11] W. W. Coblentz and R. J. Cashman, *A photoelectric cell for measuring ultraviolet solar and sky radiation on a horizontal plane*, Bul. Am. Meteorol. Soc. **21,** 149 (1940).

[12] W. W. Coblentz and R. Stair, *Distribution of the energy in the extreme ultraviolet of the solar spectrum*, J. Research NBS **17,** 1 (1936) RP899.

[13] R. Stair and W. W. Coblentz, *Radiometric measurements of ultraviolet solar intensities in the stratosphere*, J. Research NBS **20,** 185 (1938) RP1075.

[14] H. C. Hamaker, Reflectivity and Emissivity of Tungsten. Inaug. Diss., Utrecht, Holland (1934). L. S. Ornstein, Physika **3,** 561 (1936).

[15] F. Hoffman and H. Willenberg, *Ultraviolet emissivity of tungsten at high temperatures*, Physik. Z. **35,** 1 and 711 (1934).

[16] R. Stair and W. W. Coblentz, *Spectral energy distribution of the standard comparison lamp used in evaluating the flash spectrum of the solar eclipse of 1940*, Nat. Geographic Soc., Contrib. Tech. Papers, Solar Eclipse Series No. 2, 48 (1942).

[17] W. W. Coblentz, *The emissivity and energy distribution of tungsten in the photographic region of the spectrum*, Pub. Am. Astronom. Soc. **10,** 222 (1942).

[18] W. W. Coblentz and R. Stair, *Distribution of ozone in the stratosphere*, J. Research NBS **22,** 573 (1939) RP1207; **26,** 161 (1941) RP1367.

[19] Ozone clouds and holes in the stratosphere: K. O. Kiepenheuer, Z. Astrophysik **14,** 348 (1937); F. W. P. Götz, Helv. Phys. Acta **13,** 3 (1940).

[20] W. W. Coblentz and R. Stair, *Measurements of extreme ultraviolet solar radiation by a filter method*, BS J. Research **6,** 951 (1931) RP318.

WASHINGTON, January 8, 1943.

U. S. Department of Commerce National Bureau of Standards

RESEARCH PAPER RP1543

Part of Journal of Research of the National Bureau of Standards, Volume 30, June 1943

A TUNGSTEN-IN-QUARTZ LAMP AND ITS APPLICATIONS IN PHOTOELECTRIC RADIOMETRY

By R. Stair and W. O. Smith*

ABSTRACT

This paper gives constructional data relating to a tungsten-filament-in-quartz lamp and a discussion of its applications to precision filter radiometry. This lamp is adapted for use in the calibration of the spectral and total radiation sensitivity of phototubes. In its applications, it supplements the spectroradiometer for calibrating phototubes while employing the tubes with the associated filters used in measuring the radiation under investigation.

The spectral radiation output from such a lamp depends upon the temperature of the filament, the emissivity of tungsten, and the transmission of the fused-quartz envelope. A table of relative blackbody radiation intensities has been calculated for the temperature range 2,500° to 2,900° K in the wavelength interval 2300 to 3500 angstroms.

CONTENTS

		Page
I.	Introduction	449
II.	Description of lamp	450
III.	Spectral-energy distribution of the lamp	452
IV.	Application of the lamp to the spectral calibration of phototubes	455
V.	Application of the lamp for the total radiation calibration of phototubes	458
VI.	References	459

I. INTRODUCTION

The phototube has attained a place of great importance for making radiation measurements in the ultraviolet, visible, and near-infrared regions of the spectrum. The field of application is continually extending. Electronic devices for the amplification of the photoelectric current allow measurements of energies many thousand times smaller than are possible with the most sensitive thermopiles and galvanometers available. Reliable results are obtained by using stable amplifiers with microammeters or stable d'Arsonval galvanometers in cases where, because of mechanical vibrations, temperature changes, air currents, and the like, it is impossible to employ a sensitive thermopile-galvanometer radiometer.

Phototubes, however, have a selective response with respect to wavelength, which varies from tube to tube and also from point to point on the surface of the same electrode, both as to absolute intensity and as to wavelength range of sensitivity, even in tubes of the same type and process of manufacture. It is, therefore, necessary not only to calibrate individual tubes for the specific purpose to which they are to be applied, but the identical portion of the surface of the phototube that is to be used must be calibrated.

* Associate Physicist, Bureau of Plant Industry, U. S. Department of Agriculture.

None of the existing procedures for the calibration of phototubes appears to be adequate. Accurate calibration has become an important problem in the field of photoelectric radiometry. Radiation from an ordinary Mazda CX lamp, used with filters, has been employed in the spectral calibration of some of the phototubes used for the measurement of short wavelength ultraviolet solar radiation and the determination of the amount of ozone in the stratosphere. [1].[1] More recently a tungsten-ribbon-filament lamp, with a fused-quartz window, has been used in the measurement of the spectral transmission of spectroradiometers [2]. The limitations of transmission of glass are removed, but since auxiliary diaphragms must be employed, in many cases it is possible to irradiate only a small part of the active surface of the phototube. The sensitivity of different parts of the active surface is known to vary considerably, and calibrations made for a portion of the active surface are not valid when the entire, or even another, portion of the active surface is used.

To eliminate the difficulties just mentioned, a tungsten-filament lamp, enclosed by a fused-quartz envelope, was constructed. Since this type of lamp appears to be a satisfactory standard source of continuous radiation, it will be fully described, and its properties and use discussed. Other types of tungsten-filament lamps with fused-quartz envelopes have been designed and used for other purposes [5, 17] with practical results.

II. DESCRIPTION OF LAMP

The lamp constructed is shown in figures 1 and 2.[2] It consists of an 8-mil straight filament of pure tungsten wire enclosed in a spherical fused-quartz envelope 4 inches in diameter. A straight round wire rather than a coiled filament was chosen to insure relatively even temperatures at all points on the wire. Black tungsten shields cover the filament ends and loops, as well as the molybdenum supporting hooks, and prevent radiation from these cooler areas of the filament reaching the receiver being calibrated. The filament consists of four evenly spaced "hairpin" loops arranged, in a plane, over an area approximately ¾ by 1½ inches. The blackened tungsten shields were placed inside the lamp for simplicity in the use of the lamp. It was realized that these shields would become heated and reradiate energy at long wavelengths. Since not more than 10 percent of the total energy radiated from the lamp filament can be absorbed by each shield, and since the surface of each shield is more than 10 times the total surface area of the filament, it follows that the total energy radiated per unit area of the shields is less than 1 percent of that for the filament. Hence the temperature reached by the shields cannot be very high, and therefore the spectral distribution of the radiation is limited to long wavelengths in the infrared, which do not excite available phototubes.

The lamp is filled with nitrogen at a pressure of 0.6 atmosphere. The filament was "flashed" in nitrogen, prior to sealing it in the fused-quartz envelope, at a temperature of about 3,000° K for 1 hour

[1] Figures in brackets indicate the literature references at the end of this paper.

[2] The advice and assistance of R. A. Nelson, of the Bureau of Plant Industry, in the construction of this lamp is gratefully acknowledged.

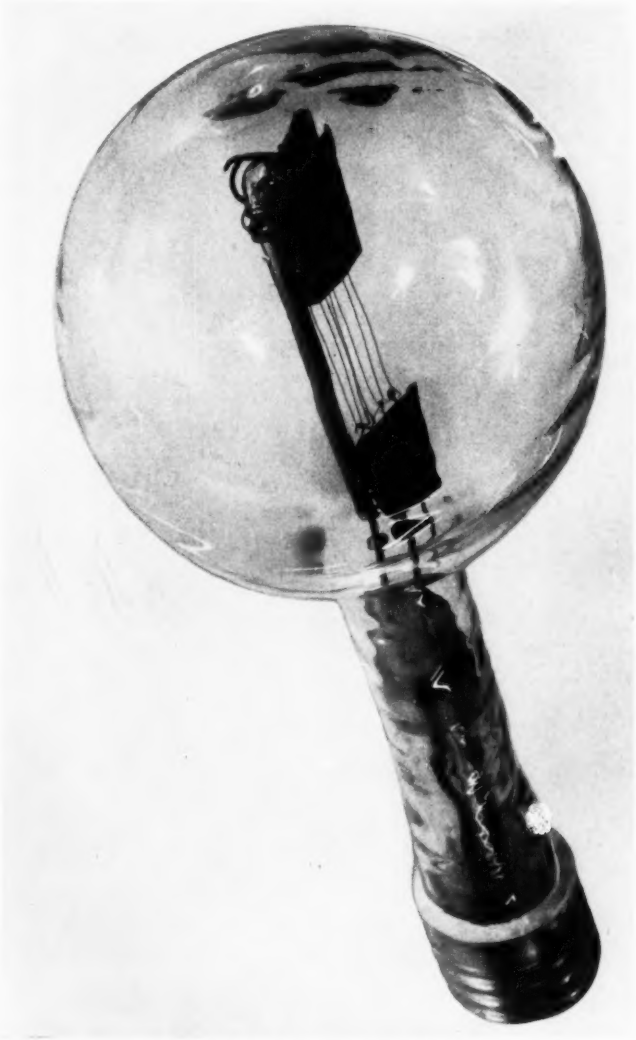

FIGURE 1.—*Tungsten-in-quartz lamp.*

UNIV. OF MICH.

to free it of any impurities. It has been shown [2, 5] that different lots of tungsten agree in spectral emissivity, probably because at high temperatures most impurities are evaporated, leaving practically pure tungsten [5, 7]. To extend the useful life of such a lamp, it should not be operated at a temperature exceeding 2,800° K after flashing.

A lamp of this type, as shown by experience, should have a power input of about 500 watts to insure sufficient radiation output for the calibration of the relative spectral response of phototubes by the filter method, especially the types of tubes sensitive only to ultraviolet radiation. The problem of a source of power and its control must be considered when designing a lamp. It is convenient to have a lamp operating somewhat below 100 volts and at the same time requiring less than 10 amperes, so that it may be controlled with the common

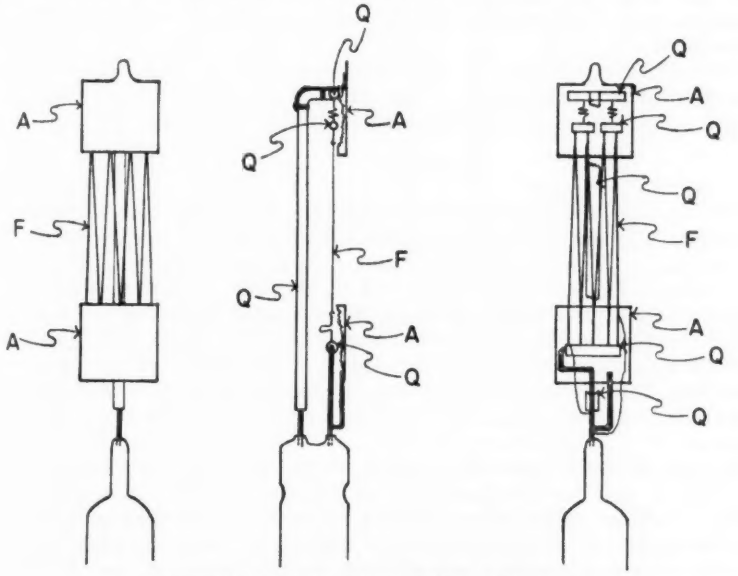

FIGURE 2.—*Constructional details of the lamp.*
A, Shields; F, filament; Q, quartz supports.

type of laboratory equipment. This is realized by using about 16 to 18 inches of 8-mil tungsten wire as a filament. A short ribbon filament operated at a low voltage and high current requires special control equipment.

The entire lamp envelope, except for the Pyrex press, is constructed of high quality fused quartz, since it has a high transmission throughout the region from below 2500 to above 20 000 A. This construction, together with shields which prevent radiation from the cooler ends and loops of the lamp filament reaching the phototube, eliminates the need of an additional diaphragm, or lens, between the lamp and tube under examination and thus the phototube is completely and uniformly irradiated with radiation of known spectral quality. Inhomogeneity and variations in the thickness of the quartz envelope render an image of the lamp filament distorted (see Fig. 1). This makes no difference, however, in the use of the lamp in the calibration

of phototubes. If it is desired to use an image of the filament for some purpose, the lamp could be provided with a sealed-in window of polished fused quartz.

Finally, this lamp may be operated at any temperature from 2,000° K to about 2,800° K without excessive depreciation of the tungsten filament or blackening of the lamp envelope.

III. SPECTRAL-ENERGY DISTRIBUTION OF THE LAMP

In applications such as the calibration of phototubes, an accurate knowledge of the distribution of the energy radiated from the lamp is required. For the particular type of lamp considered in this paper, it is a function of the filament temperature, the emissivity of the material composing the filament, and the transmission of the envelope. For this purpose, therefore, blackbody radiation, the emissivity of tungsten, and the transmission of the fused-quartz envelope must be considered.

The spectral quality of the radiation from a blackbody depends only upon the temperature. The intensity J_λ of the energy at wavelength λ, according to Planck's radiation law, is given by

$$J_\lambda = C_1 \lambda^{-5} (e^{C_2/\lambda T} - 1)^{-1}, \tag{1}$$

where C_1 is the first radiation constant, C_2 is the second radiation constant, T is the absolute temperature, and e is the base of the natural logarithms. If λ is in microns, and T in degrees Kelvin, then C_1 has the value 3.732×10^4 watt cm^2 and C_2 the value 14,360μ deg [3]; J_λ is then the radiant power, in watts, over a solid angle 2π, for unit area (cm^2) of the blackbody per micron of wavelength. Values of J_λ can be calculated directly from eq 1. The value of the radiation constant C_2 was taken as 1.436 cm deg (14,360 μ deg), which has been shown in a recent summary by Wensel [3] to be the most probable value.

Values of the relative intensities, from eq 1, for wavelengths 2300 to 3500 A and for temperatures of 2,500° to 2,900° K are given in table 1. This table was calculated for use in studies of the short wavelengths of ultraviolet solar radiation and should be very helpful when ultraviolet radiation from the lamp is used.[3] Values of J_λ relative to that for $\lambda = 0.3500$ micron are given for the temperature range 2,500° to 2,900° K in 50° increments. Wavelengths are given from 2300 to 3500 A in increments of 50 A.

The values given in table 1 are $(J_\lambda / J_{0.3500}) \times (10^4)$; or what is equivalent, $J_{0.3500}$ has been set equal to 10,000. The constant C_1, it is to be observed, is not used in the calculations, since these are relative values. Values of e^x used to compute the data of these tables were taken from tables [11] recently published by the Work Projects Administration.

The values tabulated in table 1 are, in most cases, considered to be accurate to better than one in the final significant figure.

[3] Complete tables to 4 significant figures over the range 2,000° to 3,100° K, in 25° steps, in the wavelength interval 2300 to 3500 angstroms, may be obtained upon application to the National Bureau of Standards.

TABLE 1.—*Relative values of J_λ based on a value of J_λ at $\lambda = 0.3500$ micron of 10,000*

Wave lengths (λ)	Blackbody temperatures								
	2,500° K	2,550° K	2,600° K	2,650° K	2,700° K	2,750° K	2,800° K	2,850° K	2,900° K
A									
2300	16	18	22	25	29	34	39	45	51
2350	24	28	32	38	43	49	56	64	72
2400	36	41	48	55	62	71	80	90	101
2450	52	60	69	78	88	99	112	125	138
2500	76	86	98	110	123	138	153	170	188
2550	108	122	136	152	169	188	207	228	250
2600	151	169	188	208	230	253	277	303	330
2650	208	231	255	280	307	336	366	397	430
2700	283	311	341	373	406	440	476	514	553
2750	380	415	451	490	529	571	614	659	705
2800	504	547	591	636	683	732	783	835	888
2850	662	712	764	818	873	930	988	1048	1109
2900	859	918	978	1040	1104	1169	1235	1303	1371
2950	1103	1171	1240	1311	1383	1456	1530	1605	1681
3000	1402	1480	1558	1637	1716	1798	1880	1962	2045
3050	1767	1853	1940	2027	2114	2202	2291	2379	2468
3100	2207	2301	2395	2488	2582	2676	2770	2863	2956
3150	2734	2834	2953	3032	3130	3227	3324	3421	3516
3200	3361	3464	3565	3666	3766	3865	3963	4059	4155
3250	4099	4202	4303	4403	4501	4597	4693	4786	4878
3300	4964	5062	5157	5250	5343	5434	5522	5609	5694
3350	5970	6057	6141	6224	6304	6382	6459	6534	6607
3400	7134	7201	7267	7332	7393	7454	7512	7569	7625
3450	8472	8511	8549	8586	8622	8657	8690	8723	8754
3500	10000	10000	10000	10000	10000	10000	10000	10000	10000

Data [12, 13, 14, 15] are to be found elsewhere that contain similar blackbody calculations for longer wavelengths. The tables of Skogland [13], for example, list values of $(J_\lambda/J_{0.5900}$ from 3200 to 7600 A for a temperature range of 2,000° K to 3,120° K. A slightly different value of the second radiation constant C_2 is used in most published work, but a correction factor has been determined [14]. Where it is desired to calculate a specific value, a short method of calculation given by Coblentz [12] is useful.

The emissivity of tungsten has been determined by several workers [4, 5, 6, 7] for different temperatures. The data which appear to best represent the published values for the temperature range 2,700° to 2,900° K are tabulated in table 2. These values may be used in work of this kind throughout the range 2,500° to 2,900° K, since only relative values enter into the calculations.

As the transmission in the spectral region 2500 to 20000 A of fused quartz of the thickness (about 1 mm) employed in this lamp is nearly uniform, no correction is necessary for most practical purposes. The transmission of the fused-quartz envelope of the lamp must be taken into consideration, however, when a phototube has its major response in the short wavelengths, for example, a tungsten or tantalum phototube in a quartz or special ultraviolet transmitting glass envelope.

TABLE 2.—*An example of the application of the tungsten-in-quartz lamp in the determination of the spectral response of a phototube*

[The spectral-response data (col. 5) are adjusted until the observed and calculated filter transmissions are in close agreement]

Wavelength	Relative radiation from black body at 2,737° K	Emissivity factor for tungsten	Relative radiation from tungsten at 2,737° K (col. 2 × col. 3)	Relative response of titanium phototube *A*	Filter transmissions				Relative radiation from tungsten times relative response of phototube (col. 4×col. 5)	Relative radiation from tungsten times relative response of phototube times filter transmissions			
					Cx-D	Ni	Ba-1	Ba-3		Cx-D	Ni	Ba-1	Ba-3
1	2	3	4	5	6	7	8	9	10	11	12	13	14
A					%	%	%	%					
2560	19.5	0.393	7.66	6	------	------	------	------	0.5	------	------	------	------
2580	22.1	.394	8.71	8	------	------	------	------	.7	------	------	------	------
2600	24.7	.395	9.76	10.5	------	------	------	------	1.0	------	------	------	------
2620	27.7	.397	11.00	13	------	------	------	------	1.4	------	------	------	------
2640	31.1	.398	12.38	16	------	------	------	------	2.0	------	------	------	------
2660	35.0	.399	13.96	19.5	------	------	------	------	2.7	------	------	------	------
2680	39.0	.400	15.6	23	0.6	------	------	------	3.6	------	------	------	------
2700	43.2	.401	17.3	28	1.7	------	------	------	4.8	0.1	------	------	------
2720	48.0	.402	19.3	34	3.0	------	------	------	6.6	.2	------	------	------
2740	53.4	.403	21.5	41	4.3	------	------	------	8.8	.4	------	------	------
2760	59.3	.405	24.0	47.5	6.2	------	------	------	11.4	.7	------	------	------
2780	65.5	.406	26.6	53.5	8.2	------	------	------	14.2	1.2	------	------	------
2800	72.0	.407	29.3	60	11	------	------	------	17.6	1.9	------	------	------
2820	79.3	.408	32.4	66	14.5	------	------	------	21.4	3.1	------	------	------
2840	87.0	.410	35.7	71	18.5	------	------	------	25.3	4.7	------	------	------
2860	95.0	.411	39.0	76	23	0.3	------	------	29.6	6.8	0.1	------	------
2880	103.0	.412	42.4	79	28	1.7	------	------	35.5	9.4	.6	------	------
2900	115.3	.413	47.6	79.5	33	3.3	------	------	37.8	12.5	1.2	------	------
2920	125	.415	51.9	79	38	5.3	------	------	41.0	15.6	2.2	------	------
2940	137	.417	57.1	78	43	7.6	------	------	44.6	19.2	3.4	------	------
2960	150	.419	62.9	74.5	47.5	10.0	------	------	46.9	22.3	4.7	------	------
2980	163	.420	68.5	70.5	52	13.2	------	------	48.3	25.1	6.4	------	------
3000	178	.422	75.1	66	56.3	16.5	------	------	49.6	27.9	8.2	------	------
3020	193	.423	81.6	61.5	60.2	21	0.3	------	50.2	30.2	10.5	0.2	------
3040	211	.424	89.5	58	63.5	26	1.4	------	51.9	33.0	13.5	.7	------
3060	229	.426	97.6	52.5	66.6	31.5	3.0	------	51.2	34.1	16.1	1.5	------
3080	248	.427	105.9	48.5	69.5	36.5	5.5	------	51.4	35.7	18.8	2.8	------
3100	265	.428	113.4	44	72.3	41.8	9.3	------	49.9	36.1	20.9	4.6	------
3120	289	.429	124.0	40	74.8	46.5	14.5	0.1	49.6	37.1	23.1	7.2	0.05
3140	311	.430	133.8	36.5	76.8	51.5	21.5	.8	48.9	37.5	25.2	10.5	.39
3160	335	.431	144.4	32	78.7	56	28	2.5	46.2	36.4	25.9	12.9	1.16
3180	360	.432	155.5	28.5	80.0	60	34.5	5	44.3	35.4	26.6	15.3	2.22
3200	384	.433	166.3	24.5	81.3	64	41	8	40.8	33.2	26.1	16.7	3.26
3220	412	.434	178.9	21	82.4	67	47	12	37.6	31.0	25.2	17.7	4.51
3240	442	.435	192.3	17	83.4	70	53.5	18	32.7	27.3	22.9	17.5	5.89
3260	473	.436	206.2	13.5	84.4	73	59	25	27.8	23.5	20.3	16.4	6.96
3280	506	.437	221.2	10	85	75.8	64	32	22.1	18.8	16.8	14.1	7.07
3300	541	.438	237.0	7.3	85.5	77.8	68	39	17.3	14.8	13.5	11.8	6.75
3320	580	.439	254.7	4.6	86.3	79.5	71.5	45.5	11.7	10.1	9.3	8.4	5.33
3340	620	.440	272.8	2.5	86.7	81	74.5	51	6.8	5.9	5.5	5.1	3.48
3360	662	.441	292.0	1.3	87.3	82.5	77	56	3.8	3.3	3.1	2.9	2.13
3380	703	.442	300.8	0.6	87.7	83.6	79	60	1.7	1.5	1.4	1.3	0.99
3400	744	.433	329.7	.3	88.3	84.5	80.5	64	0.9	0.8	0.8	0.7	.59
Total									1100.1	636.8	352.3	168.3	50.78
Calculated percentage transmission									------	57.9	32.0	15.3	4.61
Observed percentage transmission									------	59.0	31.9	14.8	5.83

The relative spectral emission from the lamp, for a given temperature, is the product of the relative blackbody radiation intensities, the emissivity of the tungsten filament (each for the given temperature), and the transmission of the fused-quartz lamp envelope. In table 2, the blackbody radiation and the emissivity values for a temperature of 2,737° K (which was the mean true temperature of the lamp filament in this case) are given, together with their product. The transmission of the quartz envelope has been neglected in this case, and for all practical purposes this product represents the relative spectral emission of the lamp for that temperature, since the transmission of the fused-quartz envelope varies but slightly throughout the spectral range in which this phototube is sensitive.

IV. APPLICATION OF THE LAMP TO THE SPECTRAL CALIBRATION OF PHOTOTUBES

The use of a continuous spectrum source in conjunction with filters to supplement the spectroradiometer in the determination of the spectral response of phototubes was discussed in detail in a previous publication [1]. Since the tungsten-in-quartz lamp is calibrated by a single measurement of the mean filament temperature, its spectral emission is readily determined and kept constant by controlling the voltage. As the result of heat conduction along the filament to the supporting elements within the lamp, and because of variations in filament thickness and absorption of radiation from other elements of the filament assembly, there is always a certain amount of variation in the temperature of different sections of the filament. Hence it becomes necessary to obtain a mean, or average, value for the filament temperature. This may be obtained by different methods, but for the purposes for which this lamp is to be employed it is probably most practically obtained by observing the color temperature [4] of the total visible radiation from the lamp and reducing this value to true temperature [6, 16].

Some calculations, in which the published values of emissivity were used [5], on filament sections having assumed differences in temperature of the magnitude for the type of lamp described in this paper, indicate that mean true temperature values obtained from color-temperature measurements also accurately apply in the ultraviolet spectral range 2500 to 3500 A.

The authors have considered the use of a ribbon instead of a round-wire filament in order to reduce the end and loop-cooling effects, but because of difficulties in keeping different sections of the filament in the same plane, it appears that the round wire is more desirable from the standpoint of the stability of the radiation received by the radiometer. The end cooling effects are reduced to a low value if the shields cover ¼ to ½ inch of the filament ends and loops. The temperature variation between different sections of the filament could be reduced by a wider spacing of the filament loops.

Since it is usually impossible to irradiate evenly the entire surface of the cathode of the phototube in the spectroradiometric method of calibration of the relative spectral response, the response curve obtained applies only to the portion of the phototube irradiated, and for

[4] These color temperature measurements were made by Deane B. Judd, of the National Bureau of Standards.

accurate work it becomes necessary to correct this curve so that it will apply to the entire phototube surface as used in practice.

Phototubes, as pointed out in the previous paper [1], often possess a long wavelength "tail" in their relative spectral-response curves which is not detected in the spectroradiometric calibration of the relative spectral response, but which in the use of the tubes may produce very large errors, especially if the source of radiation has a relatively high emission in this spectral region. Not only is the presence of a long wavelength "tail" to the spectral-response curve of a phototube simply detected by means of this lamp in conjunction with a set of calibrated filters, but the magnitude of its effect may be closely evaluated, so that the phototube may be used in precision work.

Since, as illustrated by the data of tables 3 and 4, the true photoelectric-response curve may, for all practical purposes, be much different from the spectroradiometrically observed curve, especially near the long wavelength limit of the tube, extra precautions in the use of double monochromators, etc., in the determination of phototube response curves would be useless effort unless the data were supplemented by other means, for example, by observations using a tungsten lamp and calibrated filters. The use of a tungsten lamp and calibrated filters to supplement the results obtained appears to be required with even the best of spectroradiometers if high precision is to result. It would be very much better to use monochromator data, although it may not be of high accuracy, supplemented by lamp and filter measurements, than to rely solely on the best double monochromator.

TABLE 3.—*Results of comparative tests of two phototubes for agreement between calculated and observed filter transmissions*

[The data for tube *A* were taken from table 2, and show close agreement between observed and calculated transmissions. The data for tube *B* show a large discrepancy, although the response curve was obtained with great care on a good spectroradiometer. The calculations marked I were made upon the basis of a smooth spectral-response curve drawn through the spectroradiometrically observed points. Calculations II were made upon an adjusted curve (see table 4). Tube *B* appeared to have a slight amount of "fatigue," which probably accounts for part of the discrepancy between the calculated and observed filter transmissions]

Filter	Phototube *A* (no filter)		Phototube *B* (no filter)			Phototube *B* (Nillite filter)		
	Obs.	Calc. I	Obs.	Calc. I	Calc. II	Obs.	Calc. I	Calc. II
Cx-D	59.0	57.9	38.2	24.9	34.0	75.6	63.5	75.1
Ni	31.9	32.0	19.0	6.7	15.4	53.8	31.4	53.8
Ba-1	14.8	15.3	8.8	1.2	7.6	31.3	9.1	34.8
Ba-3	5.8	4.6	3.3	0.1	3.1	13.4	1.0	15.6

TABLE 4.—*Adjustment of phototube spectral response*

[The values indicate the adjustment in the relative spectral response of phototube *B* required to give filter transmissions which approximate the observed values when using the tungsten-in-quartz lamp and calibrated filters, see tables 2 and 3]

Wavelength	Spectroradiometrically observed response, curve I	Adjusted response, curve II
A		
2600	133	108
2640	121	103
2680	110	98
2720	97	90
2760	85	83
2800	72	72
2840	60	60
2880	48	48
2920	37	37
2960	26.5	26.5
3000	18	18
3040	12	13
3080	7	9.5
3120	3.5	7
3160	2	5
3200	0.8	4
3240	.2	3
3280	.....	2
3320	.....	1.5
3360	.....	1
3400	.....	0.5

By measuring the integrated transmissions of a set of calibrated filters with this lamp as a source, and by calculating the integrated transmissions of the same filters from a knowledge of their spectral transmission, the spectral-energy emission of the lamp, and the spectral response of the phototube (based upon an arbitrary curve drawn through the values for the wavelengths at which the response was determined spectroradiometrically), the shape of the phototube response may be altered until the observed and calculated transmissions are in agreement.

For all practical purposes, the number of filters can be increased by $(n-1)$ by using combinations of each filter with the one having the nearest long (or short) wavelength cutoff. In certain cases more remote combinations can also be employed to advantage. This is especially true where filters having bands of selective absorption are employed in evaluating radiation over a long wavelength range of the spectrum. The particular problem in hand, together with the characteristics of the available filters, will determine the most useful combinations. A great amount of labor may be saved by using a combination filter rather than calibrating a new one where the combination gives the desired spectral transmission.

In this method of determining the relative spectral response of a phototube the entire electrode of the cell is fully and evenly irradiated, so that any local variations in the relative spectral response are averaged into the final response curve for the cell as used in practice. This is important, since in the manufacture of cells a uniform cathode surface is rarely obtained. Differences in the thickness of the sensitive layer or the presence of impurities modify the relative spectral response of one area of the receiving surface relative to another adjoining area in the same phototube.

524586—43——3

Having obtained a careful evaluation of the spectral photoelectric response and the transmissions of the available filters, the problem of the measurement of ultraviolet radiation from a given source requires a certain amount of information concerning the spectral quality of the source under investigation. If the source is a temperature radiator, as, for example, an incandescent-filament lamp of unknown filament temperature, a smooth curve may be assumed and adjusted to its true relative spectral value through a set of observations and calculations on the filter transmissions. For a discontinuous source, as, for example, a metallic arc, the wavelength and a knowledge of the relative intensity of the emission lines are necessary. In the case of a source of intermediate type, as a carbon arc or the sun, where there are emission bands with intervening regions of low intensity, a knowledge of the shape of the emission curve is essential.

In the calculations on the sun [1, 8, 9] a smooth curve was assumed (because the true shape of the curve was unknown), and the results are given in terms of the equivalent radiation for a definite wavelength interval on the basis of that assumption. This has a shortcoming, in that it is impossible to evaluate accurately the intensity of the radiation in any definite wavelength interval, since ultraviolet solar radiation is not distributed according to a smooth curve but is concentrated in definite bands with relatively low intensities at intermediate wavelengths. The accuracy of any evaluation of this type will therefore depend upon the wavelength interval chosen and upon the range of spectral sensitivity of the phototube employed.

Therefore, it at once becomes obvious that to evaluate ultraviolet solar radiation accurately in a definite wavelength interval an approximate shape of the true spectral solar radiation emission curve should be obtained. Since it is impossible to obtain this curve by means of an ordinary spectroradiometer (because of scattering within the instrument), it would be a valuable contribution in this field for someone having available a quartz lens and prism double monochromator to make this determination for (different air masses) several altitudes of the sun. Photoelectric filter radiometry in solar radiation studies will, with this accomplishment, be put on a practical scientific basis.

V. APPLICATION OF THE LAMP FOR THE TOTAL RADIATION CALIBRATION OF PHOTOTUBES

A practical method of using a standard quartz mercury-arc lamp for calibrating the total response of phototubes, together with the associated amplifier or other indicating or recording instrument, has been described in detail elsewhere [8, 9, 10]. The herein-described tungsten-filament-in-quartz lamp may be used in a similar manner and may have advantages in some cases over the mercury lamp. The radiation intensity is more constant, both in relative spectral quality and in total intensity, and its operation requires less care in the control of room temperature and circulating air currents. Furthermore, since the tungsten lamp emits radiation throughout the range of sensitivity of the phototube, the calibration applies to the total integrated curve rather than to a few isolated wavelengths. If the cell is employed in work involving a more or less continuous spectrum, or one which is at least different from the mercury arc, the advantage of using this type of spectrum in the calibration is obvious.

Since the lamp envelope absorbs the long infrared radiation emitted by the filament and emits some infrared radiation, of very long wavelength, characteristic of the temperature of the quartz envelope, the lamp is more easily calibrated, for absolute radiation intensity per unit wavelength at a fixed position relative to the lamp, by employing a 1-centimeter water cell over the thermopile. Phototubes are insensitive to this infrared radiation, and a water cell is not required in the use of the lamp with them.

If the sensitivity of the phototube is confined to a narrow range of the spectrum, as in the case of the two titanium tubes referred to above (see tables 2 and 3), additional filters may be employed to evaluate the limited range of the spectrum of the lamp radiation covering that to which a particular phototube is sensitive. Since the relative emissivity of tungsten is known none too well over the total spectral range from 2300 to 15 000 A, it is obviously an advantage to limit the range of calibration of the lamp to the spectral range over which the phototube responds.

The authors thank Leonardo Testa, of the Bureau of Plant Industry, for the glass and quartz work required in the construction of the lamp; also E. S. Shipley and Joseph F. Mullins, of the Bureau of Plant Industry, for constructing the filament, shields, and mountings of the lamp.

VI. REFERENCES

[1] R. Stair and I. F. Hand, *Methods and results of ozone measurements over Mount Evans, Colo.*, Monthly Weather Rev. **67,** 331 (1939).
[2] R. Stair and W. W. Coblentz, *Spectral energy distribution of the standard comparison lamp used in evaluating flash spectrum of the solar eclipse of 1940,* Nat. Geog. Soc., Contr. Tech. Papers, Solar Eclipse Series No. 2, p. 48 (1942).
[3] H. T. Wensel, *International Temperature Scale and some related physical constants,* J. Research NBS **22,** 375 (1939) RP1189.
[4] F. Hoffman and H. Willenberg, Physik. Z. **35,** 1, 711 (1934).
[5] H. C. Hamaker, Reflectivity and Emissivity of Tungsten, Inaug. Diss Utrecht, Holland (1934).
[6] W. E. Forsythe and A. G. Worthing, Astrophys. J. **61,** 146 (1925).
[7] L. S. Ornstein, Physica **3,** 561 (1936).
[8] W. W. Coblentz and R. Stair, J. Research NBS **16,** 315 (1936) RP877; BS J. Research **6,** 951 (1931) RP318; J. Research NBS **15,** 123 (1935) RP816.
[9] R. Stair and W. W. Coblentz, J. Research NBS **20,** 185 (1938) RP1075.
[10] R. Stair and I. F. Hand, Bul. Am. Met. Soc. **22,** 259 (1941).
[11] Federal Works Agency, Work Projects Administration, Table of the Exponential Function e^x (1939).
[12] W. W. Coblentz, BS Sci. Pap. **15,** 617 (1920) S360.
[13] J. F. Skogland, Misc. Pub. BS M86 (1929).
[14] Parry Moon, Table of Planck's Function from 3,500° to 8,000° K (Mass. Inst. of Tech., Cambridge, Mass.)
[15] M. Katherine Frehafer and Chester L. Snow, Misc. Pub. BS M56 (1925).
[16] H. T. Wensel, D. B. Judd and Wm. F. Roeser, *Establishment of a scale of color temperature,* BS J. Research **12,** 527 (1934) RP677.
[17] John Strong, Procedures in Experimental Physics (Prentice-Hall, Inc., New York, N. Y., 1942).

WASHINGTON, February 25, 1943.

U. S. Department of Commerce National Bureau of Standards

RESEARCH PAPER RP1544

Part of Journal of Research of the National Bureau of Standards, Volume 30, June 1943

EFFECT OF TURBULENCE AND CHANNEL SLOPE ON TRANSLATION WAVES

By Garbis H. Keulegan and George W. Patterson

ABSTRACT

This paper is the second of a series dealing with the motion of flood waves and other waves of translation in open channels. The first paper considered waves controlled solely by inertia forces; the present one is an analysis of the combined effects of turbulent friction and inertia. The basic equation of motion for gradually varied unsteady flow in prismatic channels is derived from fundamental principles. The effect of the velocity distribution in the original undisturbed current on the motion of short waves is investigated, and the effects of wave height, curvature of profile, and fluid friction on the celerity of a wave-volume element is analyzed in detail. The deformation of a straight sloping front and the change of height of an abrupt wave front is treated. Special emphasis is laid on disturbances of negligible curvature and practical methods of handling engineering problems arising in connection with the operation of locks or hydroelectric canals are given.

CONTENTS

	Page
List of symbols	462
I. Introduction	462
II. Fundamental principles	464
1. Reynolds equation of mean motion	464
2. Equation of continuity for mean flow in channels	470
III. First-order theory of wave propagation	471
1. The equation of mean flow in prismatic channels	471
2. Coefficient of resistance as a function of H	477
3. Velocity of propagation of short waves of negligible curvature	478
4. Propagation of discontinuities of slope	484
5. Effect of velocity distribution on the celerity of short waves	486
IV. Second-order theory of wave propagation	490
1. Equation of mean flow with appreciable vertical acceleration	490
2. Height of wave as a function of x and t	491
3. Celerity of a wave-volume element	493
4. Deformation of the wave profile, assuming $gHi-\lambda U^2/2=0$	495
5. Effect of friction and slope of bed on the propagation of waves	496
6. Deformation of a straight sloping front	498
7. Change of height of an abrupt wave front	501
8. Solution of the wave equation when slope and friction are not negligible	503
9. Intumescence produced by operating locks in a canal carrying water	504
10. Effect of friction on waves when the slope of the bed vanishes	507
11. Solution of the wave equation when the slope vanishes but friction is considered	509
12. Intumescence produced by operating locks in an ordinary canal	510
13. Limitations of Boussinesq solutions	511
V. References	512

LIST OF SYMBOLS

Symbols used in only one section are omitted unless they are of general significance. Important quantities in hydraulic equations are indicated as functions of x and t. All equations are valid in any consistent set of units. The significance of barred variables is explained in section II–1.

$A(x, t)$	cross-sectional area of channel.
b	width of free surface.
exp ( )	exponential function.
e	base of natural logarithms.
$f( ), F( )$	arbitrary functions, determined by boundary conditions.
f_1	substitution variable, $(3\omega_0-5U_0)gi/3U_0(\omega_0-U_0)$.
f_2	substitution variable, $\lambda_0/4$ or $-\lambda_0/4$.
g	acceleration of gravity.
$H(x,t)$	depth of water.
H_0	undisturbed depth of water.
$h(x,t)$	increase of depth due to disturbance.
i	slope of channel bed.
k_1	substitution variable, $1-3U_0/\omega_0$.
k_2	substitution variable, $1-U_0/\omega_0$.
l, m, n	direction cosines.
p	pressure.
p_a	atmospheric pressure.
$p_{xx}, \ldots$	generalized stress components.
q	discharge per unit width of channel.
$R_{xx}, \ldots$	turbulent stress components.
R	hydraulic radius.
$S_{xx}, \ldots$	viscous stress components.
t	time.
$U(x,t)$	mean velocity in channel cross section.
U_0	undisturbed mean velocity.
$u(x,t)$	increase in mean velocity due to disturbance (sections III–3, ff.).
u	x-component of velocity (mostly before section III–3).
u'	velocity fluctuation due to turbulence.
v	y-component of velocity.
v'	velocity fluctuation due to turbulence.
w	z-component of velocity.
w'	velocity fluctuation due to turbulence.
x	Cartesian coordinate, specifically, parallel to channel in bottom plane.
y	Cartesian coordinate, specifically, lateral to channel in a horizontal plane.
z	Cartesian coordinate, specifically, drawn upward with origin at bottom of channel.
α	Boussinesq coefficient of velocity distribution.
ϵ	eddy viscosity.
λ	coefficient of channel friction.
λ_0	coefficient of channel friction, $H=H_0$.
μ	viscosity.
ρ	density.
σ	partial volume of wave per unit width.
σ'	partial volume of wave per unit width.
τ_0	mean shear per unit area on channel wall.
$\Phi ( )$	arbitrary function.
χ	wetted perimeter.
$\Psi ( ), \psi ( )$	arbitrary functions.
ω	velocity of a wave-volume element.
ω_0	velocity of a short wave, moving without change of form.

I. INTRODUCTION

This paper is the second of a series dealing with the motion of flood waves and other waves of translation in open channels. The purpose of the series is explained in the introduction to the first paper [1].[1]

[1] Figures in brackets indicate the literature references at the end of this paper.

Many of the significant properties of translation waves may be obtained by assuming that the motion of fluid particles due to the wave disturbance is irrotational [1]. Experimental observation of these properties indicates that they are in good agreement with theoretical predictions, provided that the waves are moving in still water. If, on the other hand, the disturbances are produced in a liquid which is initially in motion, as in actual currents in an open channel, some disparity will be seen between observation and theory. Bazin's experiments on the velocity of propagation of a solitary wave in still water or in a running current demonstrate these points [2].

The divergence between observation and theory, when the wave is moving in a current, can be explained in two ways. First, irrotational or potential theory supposes that the original undisturbed motion is such that all the particles in a cross section move with the same constant velocity, U_0, which may of course be zero. This condition is not fulfilled for flow in actual channels, and it thus becomes necessary to investigate the effect of the distribution of velocity in a cross section on the velocity of propagation of waves. An analysis of this effect has been carried through in great detail by Boussinesq [3]. With a view to simplifying the presentation and the solution of the problem, the authors give a new derivation (section III–5). Although the results arrived at here are different in form from those of Boussinesq, it is believed that the difference has a qualitative rather than quantitative importance.

This difference is due to two distinct forms of the equation of motion of unsteady flow in a channel, one adopted by Boussinesq and the other by the authors. The present method applies the theory of Reynolds stresses to the problem of the unsteady mean flow in a channel, without assuming any specific relation between the stresses and the velocity rates existing at points within the channel cross section. The effect of these stresses is evaluated in terms of the total friction at the wall, which is the important concept for mean flow in open channels and is usually available from observations on uniform flow. Boussinesq's method on the other hand is an extension of his own theory of turbulent flow, and specific relations between the turbulent stresses and the space-rates of the local velocities are assumed and introduced into the derivations. As the concept of Reynolds stresses is the starting point of the present analysis, the theory of these stresses is given in considerable detail (section II–1). The equation of motion of a perfect fluid is the point of departure in interpreting the relation between the stresses and velocity fluctuations. This novel procedure simplifies the presentation considerably. It is hoped that the equation of motion for gradually varied unsteady flow in prismatic channels derived in this paper, eq 47, is sufficiently rigorous to merit the attention of river engineers.

In the second place, the irrotational theory of translation waves ignores the effect of turbulence, which is one of the forces controlling the motion of the waves. Consider a short intumescence moving in a current. In the initial stages of motion the behavior of the wave is not affected by turbulence, since the wave is assumed to be short. When the wave has traveled a considerable distance the cumulative effect of friction becomes appreciable, particularly at the rear of the wave. In fact, experience shows that the front of the wave will travel with a velocity characteristic of irrotational waves, whereas at

the other end of the wave, the volume elements will move with a smaller velocity, the exact law of which is not as yet clearly understood. The wave thus flattens out considerably at the posterior end, with a consequent elongation. The tendency of short waves to deform in this manner is clearly demonstrated in Horton's experiments [4].

When the motion of the waves is controlled principally by friction, as in the quasipermanent regimes of rivers, the corresponding theory of translation waves is simple. But when it is supposed that the friction and inertia effects are of like magnitude, analysis is confronted with a difficult task. The change of shape of a short intumescence during the entire journey of the wave in a current would be accurately described if a complete solution were available, which is not the case. However, some progress in this direction is possible if it is assumed that the effect of turbulence is small, requiring only a secondary correction. Such a theory has been worked out by Boussinesq, who assumed that the velocity of the wave-volume elements differs little from the theoretical velocity of waves without friction [3]. The main purpose of this paper is to consider this theory and the corresponding solutions for waves of negligible curvature. In giving Boussinesq's solution, slight changes have been made, since it was desired to adopt Manning's law of friction in open channels [5]. Favre has employed the Boussinesq integrals to describe the motion of waves occurring during the operation of locks [6]. Because of the engineering significance of the problem we have also reproduced these applications (section IV–9 and IV–12).

The applications of the theory are presented in sections III and IV, which have been entitled first-order and second-order theories of wave propagation. The first-order theory neglects the vertical acceleration of the water particles and assumes that the combined effect of friction and velocity is small. It is found that this assumption requires that the waves be short. The second-order theory considers the effects of vertical acceleration but neglects the variations of the horizontal velocity components. As in Boussinesq's investigations, the concept of the velocity of a wave-volume element plays a very basic role. Equation 116 is the general expression for this velocity. Using this same formula, the authors have been able to study the gradual deformation of a straight sloping front and also to compute the reduction of height of an abrupt wave front.

II. FUNDAMENTAL PRINCIPLES

1. REYNOLDS EQUATIONS OF MEAN MOTION

In the Reynolds theory of turbulence [7; 8, p. 638; 9, p. 364; 10, p. 191] the velocity components u, v, w, in the directions x, y, z, respectively, are regarded as fluctuating functions of the variables x, y, z, t. The fluctuations are frequent and rapid, and the periodicity of the changes is irregular. Denoting the mean values of u, v, w by $\overline{u}$, $\overline{v}$, $\overline{w}$, and the mean value of the pressure, p, by $\overline{p}$, we have for the instantaneous values

$$\left.\begin{aligned} u&=\overline{u}+u',\\ v&=\overline{v}+v',\\ w&=\overline{w}+w',\end{aligned}\right\} \tag{1}$$

and

$$p=\overline{p}+p',$$

where u', v', w', and p' are the fluctuations whose mean values $\overline{u'}$, $\overline{v'}$, $\overline{w'}$, $\overline{p'}$ are equal to zero. The mean values may be temporal; that is, taken at a given point (x, y, z) over an interval of time of duration Δt; thus, for example,

$$\bar{u}=\frac{1}{\Delta t}\int_t^{t+\Delta t} u\,dt. \tag{2}$$

Or again the mean values may be spatial; that is, taken at a given instant t over a space of volume ΔV; thus, for example

$$\bar{u}=\frac{1}{\Delta V}\int_{\Delta V} u\,dV. \tag{3}$$

For the present it will be supposed that the averages are temporal. A difficulty arises when taking temporal means in unsteady flow. In such cases it is necessary to make the time interval Δt long enough to include a great number of fluctuations, but short enough to exclude all but negligible variations of $\bar{u}$, $\bar{v}$, $\bar{w}$, $\bar{p}$.

There are certain rules for taking the averages. Expressed symbolically [9, p. 366]

$$\left.\begin{aligned} \overline{ab} &= \bar{a}\,\bar{b}, \\ \overline{a+b} &= \bar{a}+\bar{b}, \\ \bar{\bar{a}} &= \bar{a}, \\ \overline{\frac{\partial a}{\partial s}} &= \frac{\partial}{\partial s}\overline{(a)}, \end{aligned}\right\} \tag{4}$$

and

where a and b are functions of x, y, z, t; s represents any one of the independent variables, and a bar over a quantity represents an average of the kind just described. These rules are based upon assumptions that are not exactly applicable to the flow of liquids. The errors, however, are negligible when the fluctuations within the time interval Δt are sufficiently numerous.

The specific contribution of Reynolds' analysis is the idea of interpreting the dynamic effects of the fluctuations u', v', w', as apparent tractional forces or stresses. The nature and the magnitude of these stresses can be readily obtained starting with the equations of motions of a perfect fluid. The dynamic equations in question are

$$\left.\begin{aligned} \rho\frac{du}{dt} &= -\frac{\partial p}{\partial x}+\rho X, \\ \rho\frac{dv}{dt} &= -\frac{\partial p}{\partial y}+\rho Y, \\ \rho\frac{dw}{dt} &= -\frac{\partial p}{\partial z}+\rho Z, \end{aligned}\right\} \tag{5}$$

where the operator d/dt, in terms of the local variations, is

$$\frac{d}{dt}=\frac{\partial}{\partial t}+u\frac{\partial}{\partial x}+v\frac{\partial}{\partial y}+w\frac{\partial}{\partial z}. \tag{6}$$

Together with these, there is the equation of continuity, assuming that the liquid is incompressible,

$$\frac{\partial u}{\partial x}+\frac{\partial v}{\partial y}+\frac{\partial w}{\partial z}=0. \tag{7}$$

The liquid will always be assumed to be incompressible, in this paper. In eq 5, p is the pressure, ρ the density of liquid, and X, Y, Z the components of the force of gravity per unit mass of liquid in the direction of x, y, z. These relations are valid at any instant of time independent of the fact that the quantities, u, v, w, and p are fluctuating functions of time, provided that the velocities are not discontinuous, and if discontinuities exist, they occur only occasionally during the time interval Δt.

Replacing u, v, w in eq 7 by their respective values from eq 1, averaging each term, and using the last three relations in eq 4, together with the fact that $\overline{u'}=\overline{v'}=\overline{w'}=0$, we obtain

$$\frac{\partial u}{\partial x}+\frac{\partial v}{\partial y}+\frac{\partial w}{\partial z}=0, \tag{8}$$

which states that the dilatation of the mean values of the velocity components vanish. It then follows from eq 1, 7, 8 that

$$\frac{\partial u'}{\partial x}+\frac{\partial v'}{\partial y}+\frac{\partial w'}{\partial z}=0. \tag{9}$$

The equations of motion, eq 5, are treated in a similar manner. We use 6, substitute for u, v, w their values from eq 1, multiply eq 9 by $\rho u'$, $\rho v'$, $\rho w'$, respectively, and add to the left-hand side of each equation. Each term is then averaged in accordance with eq 4, assuming ρ to be constant, that is, that the fluid is homogeneous, obtaining

$$\left.\begin{aligned}\rho\frac{d\bar{u}}{dt}&=-\frac{\partial\bar{p}}{\partial x}+\rho X+\frac{\partial R_{xx}}{\partial x}+\frac{\partial R_{yx}}{\partial y}+\frac{\partial R_{zx}}{\partial z},\\ \rho\frac{d\bar{v}}{dt}&=-\frac{\partial\bar{p}}{\partial y}+\rho Y+\frac{\partial R_{xy}}{\partial x}+\frac{\partial R_{yy}}{\partial y}+\frac{\partial R_{zy}}{\partial z},\\ \rho\frac{d\bar{w}}{dt}&=-\frac{\partial\bar{p}}{\partial z}+\rho Z+\frac{\partial R_{xz}}{\partial x}+\frac{\partial R_{yz}}{\partial y}+\frac{\partial R_{zz}}{\partial z},\end{aligned}\right\} \tag{10}$$

where, in this case,

$$\frac{d}{dt}=\frac{\partial}{\partial t}+\bar{u}\frac{\partial}{\partial x}+\bar{v}\frac{\partial}{\partial y}+\bar{w}\frac{\partial}{\partial z}, \tag{11}$$

and

$$\left.\begin{aligned}R_{xx}&=-\rho\overline{u'u'};\ R_{xy}=R_{yx}=-\rho\overline{u'v'},\\ R_{yy}&=-\rho\overline{v'v'};\ R_{xz}=R_{zx}=-\rho\overline{u'w'},\\ R_{zz}&=-\rho\overline{w'w'};\ R_{yz}=R_{zy}=-\rho\overline{v'w'}.\end{aligned}\right\} \tag{12}$$

We may refer to eq 10 as the Reynolds equations of motion for turbulent flow.

To interpret the above results we write the general equations of motion of a deformable continuum under the action of the external body forces X, Y, Z and surface tractions of an unspecified physical origin:

$$\left.\begin{aligned}\rho\frac{du}{dt}&=\rho X+\frac{\partial p_{xx}}{\partial x}+\frac{\partial p_{yx}}{\partial y}+\frac{\partial p_{zx}}{\partial z},\\ \rho\frac{dv}{dt}&=\rho Y+\frac{\partial p_{xy}}{\partial x}+\frac{\partial p_{yy}}{\partial y}+\frac{\partial p_{zy}}{\partial z},\\ \rho\frac{dw}{dt}&=\rho Z+\frac{\partial p_{xz}}{\partial x}+\frac{\partial p_{yz}}{\partial y}+\frac{\partial p_{zz}}{\partial z},\end{aligned}\right\} \tag{13}$$

where the operator d/dt is the one defined in eq 6.

It should be noted that these equations are merely Newton's law of motion as applied to any deformable continuum, and thus they apply to a wide range of phenomena. The left-hand members represent components of the rate of change of momentum per unit volume of the medium, whereas the right-hand members represent the components of the forces acting per unit volume. The nature of the medium determines the functional relation between the nine stress components, p_{xx}, p_{yx}, ... , and the other variables occurring in the equations and the intrinsic properties of the medium. Hydraulic equations established by integrating these equations over a cross section of the fluid normal to the flow are frequently referred to as *momentum equations.*

The nine stress components completely determine the forces acting on a small surface dS at the point (x, y, z). If a normal is drawn to dS away from the body of which dS forms a part of the surface, and if l, m, n are the direction cosines of the normal to dS, then the x-, y-, z-components of the surface tractions on the body at the point (x, y, z) are

$$\left.\begin{aligned}F_x&=lp_{xx}+mp_{yx}+np_{zx},\\ F_y&=lp_{xy}+mp_{yy}+np_{zy},\\ F_z&=lp_{xz}+mp_{yz}+np_{zz}.\end{aligned}\right\} \tag{14}$$

and

Comparing eq 10 and 13, we see that

$$\left.\begin{aligned}p_{xx}&=-\bar{p}+R_{xx}, & p_{xy}&=p_{yx}=R_{xy}=R_{yx};\\ p_{yy}&=-\bar{p}+R_{yy}, & p_{xz}&=p_{zx}=R_{xz}=R_{zx};\\ p_{zz}&=-\bar{p}+R_{zz}, & p_{zy}&=p_{yz}=R_{zy}=R_{yz};\end{aligned}\right\} \tag{15}$$

and thus the turbulent mean flow may be treated as ordinary streamline flow where the stresses p_{xx}, p_{ry} . . . . , are identified with the stresses R_{xx}, R_{xy} . . . . . These apparent stresses of turbulence are called Reynolds stresses, and represent mathematically the transport of momentum across a surface caused by the velocity fluctuations [10, p. 192].

If the flow instead of being turbulent is viscous in character, the stresses are of molecular origin. The stresses p_{xx}, p_{xy}, . . . are then

identified with the viscous stresses S_{xx}, S_{xy}, . . . in the following manner,

$$\left.\begin{aligned} p_{xx}&=-p+S_{xx}, & p_{xy}&=p_{yx}=S_{xy}=S_{yx};\\ p_{yy}&=-p+S_{yy}, & p_{xz}&=p_{zx}=S_{xz}=S_{zx};\\ p_{zz}&=-p+S_{zz}, & p_{yz}&=p_{zy}=S_{yz}=S_{zy}. \end{aligned}\right\} \tag{16}$$

If the liquid is incompressible, these viscous stresses become

$$\left.\begin{aligned} S_{xx}&=2\mu\frac{\partial u}{\partial x}; & S_{xy}&=S_{yx}=\mu\left(\frac{\partial v}{\partial x}+\frac{\partial u}{\partial y}\right);\\ S_{yy}&=2\mu\frac{\partial v}{\partial y}, & S_{zx}&=S_{xz}=\mu\left(\frac{\partial w}{\partial x}+\frac{\partial u}{\partial z}\right);\\ S_{zz}&=2\mu\frac{\partial w}{\partial z}, & S_{yz}&=S_{zy}=\mu\left(\frac{\partial v}{\partial z}+\frac{\partial w}{\partial y}\right); \end{aligned}\right\} \tag{17}$$

where μ is the viscosity of the liquid.

It is perfectly feasible to carry through the derivation of the Reynolds equations of motion, eq 10, using the viscous-flow interpretation of eq 13 as a starting point, and finally neglecting the viscous stresses in comparison with the Reynolds stresses, which is justifiable on the basis of experimental evidence [11, p. 186]. We have not adopted this method, since the results are identical with those obtained here by initially assuming a perfect liquid, that is, by neglecting the viscous stresses at the beginning rather than at the end, and since it is more complicated than the method used here.

Later, in sections III–1 and IV–1, we shall derive hydraulic equations for mean flow in open channels, using eq 10 as a starting point. For this purpose, it is sufficient merely to suppose that R_{xx}, R_{xy} . . . . exist, there being no necessity for determining them as functions of the mean velocity gradients, because when the Reynolds equations of motion are integrated over the cross section of the channel, the quantities R_{xx}, R_{xy}, . . . either disappear or are expressed in terms of the wall friction, τ_0, which is defined in connection with eq 45. Boussinesq, however, expressed R_{xx}, R_{xy}, . . . in terms of the velocity gradients. He simulated eq 17, merely replacing S_{xx}, S_{xy}, . . . by R_{xx}, R_{xy}, . . . ; u, v, w by $\overline{u}$, $\overline{v}$, $\overline{w}$; and μ by ϵ. The quantity ϵ was called the coefficient of internal friction by Boussinesq [3, p. 46]; present usage seems to favor the term *eddy viscosity*, since ϵ has the same dimensions as μ [11, p. 185].

When the channel is rectangular, Boussinesq assumed that ϵ is constant for every point in a given cross section, but in a channel of constant roughness, directly proportional to the product of the wall velocity and the depth of the liquid. Such assumptions form the foundation for the developments in his "Essay." The validity of his theory is thus open to question, since the assumptions concerning ϵ are widely at variance with present experimental knowledge.

Having established the basic partial differential equations governing turbulent flow in open channels, we now turn our attention to the boundary conditions. Consider first the condition to be satisfied at a fixed solid wall, which we shall suppose is covered with uniform asperities of height k. A pillbox is erected on the surface, with height h, just sufficient to clear the asperities, and radius r, large with respect to $2h$. (See fig. 1.)

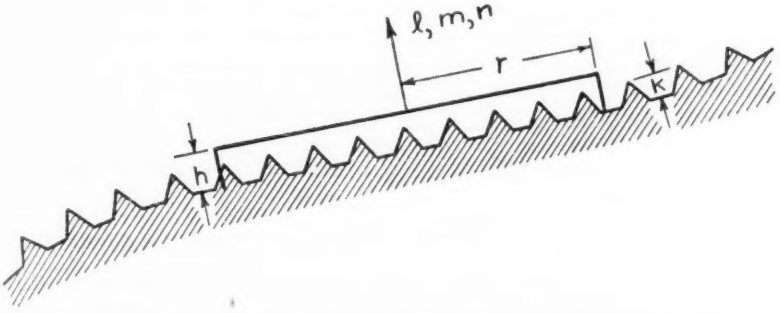

FIGURE 1.—*A pillbox enclosing the asperities on a channel wall.*

Since the liquid is incompressible, the net rate of flow across the surface of the pillbox must be zero. We neglect the discharge from the cylindrical side of the pillbox, since its area is small compared with that of the circular end. There must be at least one point on the end of the pillbox for which

$$lu+mv+nw=0,$$

where l, m, n are the direction cosines of the outward-drawn normal. Averaging the terms in this equation and assuming that $\overline{u}$, $\overline{v}$, $\overline{w}$ vary slowly in an interval of length r, we have for all points on the fixed surface

$$l\overline{u}+m\overline{v}+n\overline{w}=0, \tag{18}$$

which is the desired boundary condition for a fixed solid wall. If the wall is smooth, the argument is repeated, replacing the height of the asperities by the thickness of the laminar boundary layer.

Next we consider a boundary condition which applies to the free surface. Let $F(x,y,z,t)=0$ be the equation of the free surface. As before in the case of the velocity components and the pressure (eq 1), the surface is considered to fluctuate rapidly and irregularly about a mean value, and we write

$$F=\overline{F}+F', \tag{19}$$

where $\overline{F}$ is the mean value of F, and F' is the fluctuation whose temporal mean value $\overline{F'}$ is zero.

Since particles on the surface remain there, we have the condition

$$\frac{\partial F}{\partial t}+u_s\frac{\partial F}{\partial x}+v_s\frac{\partial F}{\partial y}+w_s\frac{\partial F}{\partial z}=0,$$

where u_s, v_s, w_s are the velocity components at the free surface. If we replace u_s, v_s, w_s by expressions obtained from eq 1 and F by its value from eq 19 and average the terms, the result is

$$\frac{\partial\overline{F}}{\partial t}+\overline{u}_s\frac{\partial\overline{F}}{\partial x}+\overline{v}_s\frac{\partial\overline{F}}{\partial y}+\overline{w}_s\frac{\partial\overline{F}}{\partial z}=0 \tag{20}$$

provided we neglect the terms $\overline{u'_s(\partial F'/\partial x)}$, ... These products

may be ignored, since either the correlation between u'_s, $\partial F'/\partial x$, etc., is zero or the term is small in comparison with those retained. On the basis of this assumption, the above equation is a boundary condition obtaining at the free surface of turbulent flow.

In order to simplify the notation from this point on, u, v, w, p, etc., will be written for $\overline{u}$, $\overline{v}$, $\overline{w}$, $\overline{p}$, etc. Any further use of the bar to indicate an average will be in the macroscopic, rather than the microscopic, sense.

2. EQUATION OF CONTINUITY FOR MEAN FLOW IN CHANNELS

Up until this point we have derived equations which are valid for turbulent flow in general. We now derive an equation which applies to any tube of flow with a cross section which varies both in space and in time. This tube is assumed not to close on itself, and since it is a mathematical representation of a flowing channel, it is drawn as such in figure 2. The cross-sectional area of the channel, normal to x, will be represented by $A=A(x,t)$, the average value of u over the cross section by $U=U(x,t)$.

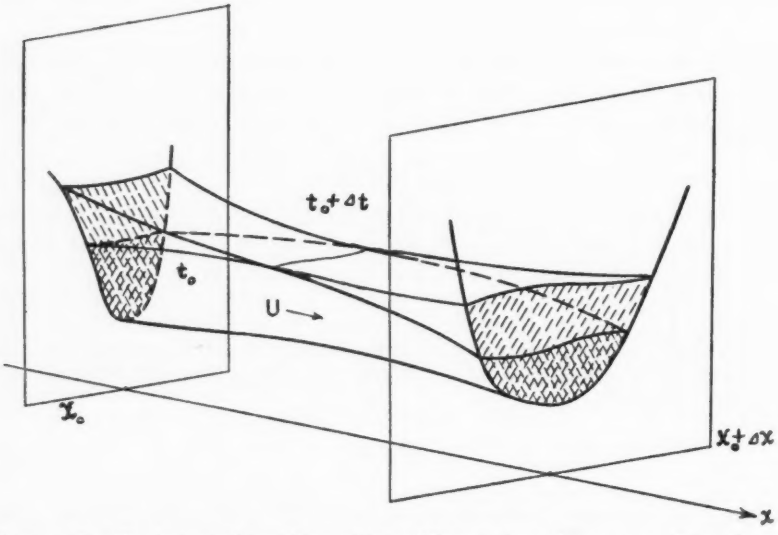

FIGURE 2.—*Surface configurations at two different times in an open channel.*

The positive sense of x is chosen so as to make U positive. The actual direction of x is arbitrary, but for convenience it should approximate the direction of the channel.

The flow into the stretch Δx during the time Δt is

$$\int_{t_0}^{t_0+\Delta t} U(x_0,t)A(x_0,t)dt,$$

while the flow out of the same stretch is

$$\int_{t_0}^{t_0+\Delta t} U(x_0+\Delta x,t)A(x_0+\Delta x,t)dt.$$

Furthermore, the volume of liquid contained within the stretch at time t_0 is

$$\int_{x_0}^{x_0+\Delta x} A(x,t_0)dx,$$

while the volume in the stretch at time $t_0+\Delta t$ is

$$\int_{x_0}^{x_0+\Delta x} A(x,t_0+\Delta t)dx.$$

Since the fluid is incompressible, net outflow plus increase of volume equals zero, or

$$\int_{t_0}^{t_0+\Delta t}[U(x_0+\Delta x,t)A(x_0+\Delta x,t)-U(x_0,t)A(x_0,t)]dt + \int_{x_0}^{x_0+\Delta x}[A(x,t_0+\Delta t)-A(x,t_0)]dx=0.$$

If we apply the theorem of the mean for integrals, divide by $\Delta x\Delta t$ and then let Δx and Δt approach zero, we obtain

$$\frac{\partial}{\partial x}(UA)+\frac{\partial A}{\partial t}=0, \tag{21}$$

which is the equation of continuity for mean flow in channels. Since no assumptions have been made regarding the shape of the channel, this equation applies to open channels in all generality.

III. FIRST-ORDER THEORY OF WAVE PROPAGATION

1. THE EQUATION OF MEAN FLOW IN PRISMATIC CHANNELS

Consider a prismatic channel and select as the origin of a right-handed system of Cartesian coordinates the lowest point of any convenient cross section (see fig. 3). Take the x-axis as the line parallel to the channel (not necessarily horizontal), with positive sense in the

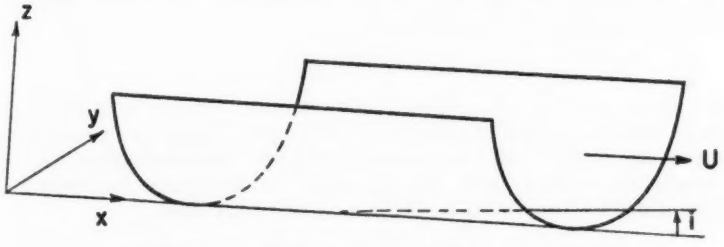

FIGURE 3.—*System of coordinates in a prismatic channel.*

direction of flow, the y-axis as the horizontal line, and the z-axis positive upward (not necessarily vertical). The channel slope, i, is the tangent of the angle θ from the positive direction of the x-axis to the horizontal, measured in the counterclockwise direction, viewed in the direction of increasing y; in other words, a positive slope is downhill. These conventions will be adhered to throughout the paper.

We assume that the angle of slope of the channel is so small that $\sin\theta$ is sensibly equal to $\tan\theta$ and $\cos\theta$ to unity, hence X and Z in eq 10 are gi and $-g$, respectively.

Again, in order to simplify the three equations of motion, eq 10, we make two distinct sets of assumptions, the first involving the terms on the left-hand side and the second involving the terms on the right-hand side. First, we assume that the second derivatives of the cross section, A, and of the mean velocity, U, and the squares and products of their first derivatives, may be neglected in comparison with the first derivatives. Such a flow is referred to by Boussinesq as *gradually varied* [3, p. 242]. In general, this requires that the sides of the channel be not much flatter than a 1:1 slope, that the slope of the wave profile be small compared to unity, and that the curvature of the wave profile be small compared to $(1/U)(\partial U/\partial x)$ or $(1/U^2)(\partial U/\partial t)$. As a result of these restrictions, dv/dt and dw/dt are small with respect to du/dt, and the left-hand sides of the last two of eq 10 vanish.

Secondly, we make certain assumptions concerning the Reynolds stresses: (1) $\overline{u'u'}=\overline{v'v'}=\overline{w'w'}$ hence $R_{xx}=R_{yy}=R_{zz}$; (2) since u is the predominant velocity component, the derivative of the correlation between the fluctuations v', w' may be neglected in comparison with the derivatives of the correlations between u', v', and u', w', which is to say, that the derivatives of R_{xy} may be neglected; (3) since the flow is gradually varied, the x-derivatives of R_{xy} and R_{xz} may be neglected.

On the basis of these two sets of assumptions, then, eq 10 reduce to

$$\frac{\partial u}{\partial t}+u\frac{\partial u}{\partial x}+v\frac{\partial u}{\partial y}+w\frac{\partial u}{\partial z}=gi-\frac{1}{\rho}\frac{\partial}{\partial x}(p-R_{xx})+\frac{1}{\rho}\frac{\partial}{\partial y}R_{yx}+\frac{1}{\rho}\frac{\partial}{\partial z}R_{zx}, \tag{22}$$

$$0=\frac{\partial}{\partial y}(p-R_{xx}), \tag{23}$$

and

$$0=\frac{1}{\rho}\frac{\partial}{\partial z}(p-R_{xx})+g. \tag{24}$$

The simultaneous solution of eq 23 and 24, with the dynamical boundary condition $p=p_a$ at $z=H$, is

$$p-R_{xx}=p_a+\rho g(H-z),$$

where H, a function of x and t only, is the z-coordinate of the free surface, and p_a is the atmospheric pressure. These symbols will be consistently used to refer to these quantities. According to the above, in gradually varied flow the pressure is hydrostatic everywhere. Differentiating the above equation, it is found that

$$\frac{\partial(p-R_{xx})}{\partial x}=\rho g\frac{\partial H}{\partial x}. \tag{25}$$

Each term in eq 22 is to be integrated over the cross section A at x. In this way, the resulting equation of motion will involve only the mean flow, U, the cross-sectional area, A, and certain other quantities to be given later. We thus eliminate the variables y and z from consideration, since all of the quantities occurring in the final result will

be functions of x and t only. Such an equation is called a hydraulic equation, and bears the same relation to circuit equations in electricity as the general equations 10 do to the electromagnetic field equations.

Let us first evaluate the integrals arising from the terms in the left-hand side. The mean flow, U, in a cross section, is implicitly defined by

$$UA = \int_A u dA. \tag{26}$$

We write the above as a double integral

$$UA = \int_0^H dz \int_{-y_1}^{y_2} u dy,$$

where y_2 and $-y_1$ are the y-coordinates of the two points on the wetted perimeter having the common distance z from the x, y-plane (see fig. 4). Obviously, y_2 and $-y_1$ are functions of z only, for a given prismatic channel configuration. Differentiating both sides of the above equation with respect to t, we obtain

$$\frac{\partial (UA)}{\partial t} = \int_A \frac{\partial u}{\partial t} dA + \frac{\partial H}{\partial t} \int_{-b_1}^{b_2} u_s dy,$$

where b_2 and $-b_1$ are the y-coordinates of the two points on the wetted perimeter at the distance H from the x, y-plane.

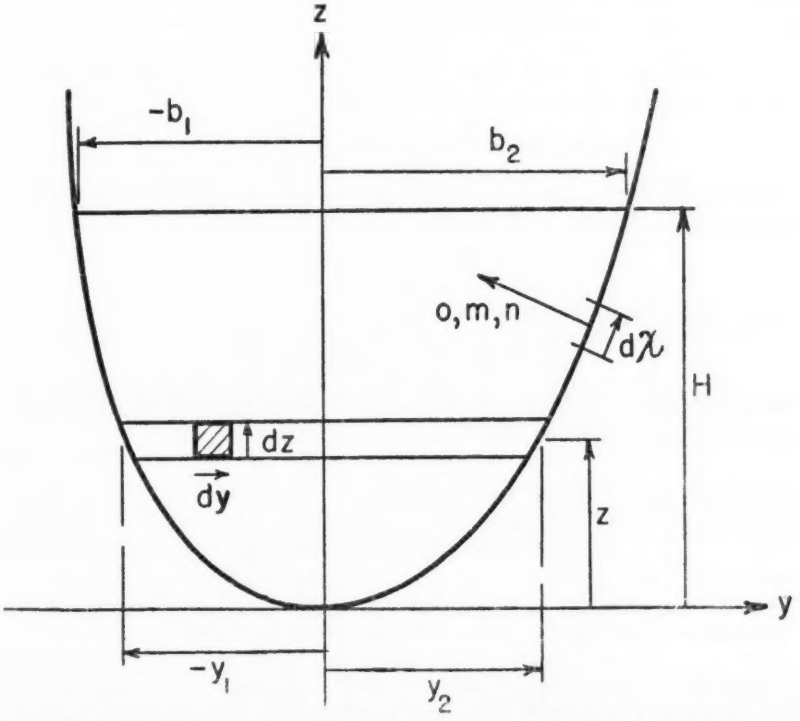

FIGURE 4.—*Double integration with respect to y and z; cross section, looking upstream.*

We now define $\overline{u_s}$ to be the mean value of the surface velocities, u_s, over the width $b=b_2+b_1$ of the free surface:

$$\overline{u_s}b=\int_{-b_1}^{b_2} u_s dy, \tag{27}$$

and the next to the last equation becomes

$$\frac{\partial}{\partial t}(UA)=\int_A \frac{\partial u}{\partial t}dA+\overline{u_s}\frac{\partial A}{\partial t}, \tag{28}$$

since $b(\partial H/\partial t)=\partial A/\partial t$. Introducing the velocity coefficient α_1, implicitly defined by

$$\alpha_1 U=\overline{u_s}-U, \tag{29}$$

eq 28 may be written

$$\int_A \frac{\partial u}{\partial t}dA=A\frac{\partial U}{\partial t}-\alpha_1 U\frac{\partial A}{\partial t}. \tag{30}$$

We now turn our attention to the second term on the left of eq 22. We define another coefficient of velocity distribution α, as the ratio of the mean of the square of velocity to the square of its mean, both means being taken over the cross section, thus

$$\alpha U^2 A=\int_A u^2 dA. \tag{31}$$

This coefficient is the only one which appears in the final equation, and was originally introduced by Boussinesq. It also plays an important role in the equation of steady flow in open channels [12] and must not be confused with the so-called Coriolis coefficient, which is frequently denoted by α. Assuming that α does not depend on x, and differentiating both sides with respect to x, in the same manner as was done in obtaining eq 28, we have

$$\alpha\frac{\partial}{\partial x}(U^2A)=\int_A \frac{\partial(u^2)}{\partial x}dA+\frac{\partial H}{\partial x}\int_{-b_1}^{b_2} u_s^2 dy.$$

Defining $\overline{u_s^2}$ to be the mean value of the squares of the surface velocities over the width, b, of the free surface,

$$\overline{u_s^2}b=\int_{-b_1}^{b_2} u_s^2 dy, \tag{32}$$

then the previous equation becomes

$$\alpha\frac{\partial}{\partial x}(U^2A)=\int_A \frac{\partial(u^2)}{\partial x}dA+\overline{u_s^2}\frac{\partial A}{\partial x},$$

since $b(\partial H/\partial x)=\partial A/\partial x$. Introducing a third coefficient of velocity distribution α_2, defined by

$$\alpha_2 2U^2=\overline{u_s^2}-\alpha U^2, \tag{33}$$

we obtain from the last two relations,

$$\int_A u\frac{\partial u}{\partial x}dA=\alpha UA\frac{\partial U}{\partial x}-\alpha_2 U^2\frac{\partial A}{\partial x}. \tag{34}$$

Next consider the integrals of the third and fourth terms of the left-hand side of eq 22. For the third term we write

$$\int_A v\frac{\partial u}{\partial y}dA=\int_0^H dz\int_{-y_1}^{y_2} v\frac{\partial u}{\partial y}dy,$$

where the notation is the same as that used in the above two integrals (see fig. 4). The integral with respect to y is integrated by parts, obtaining

$$\int_A v\frac{\partial u}{\partial y}dA=\int_0^H [(u_0v_0)_2-(u_0v_0)_1]dz-\int_A u\frac{\partial v}{\partial y}dA, \tag{35}$$

where v_0 and u_0 are the velocity components at the wetted perimeter and the subscripts 1 and 2 indicate the two sides of the channel, that is, the points $(-y_1,z)$ and (y_2,z), respectively.

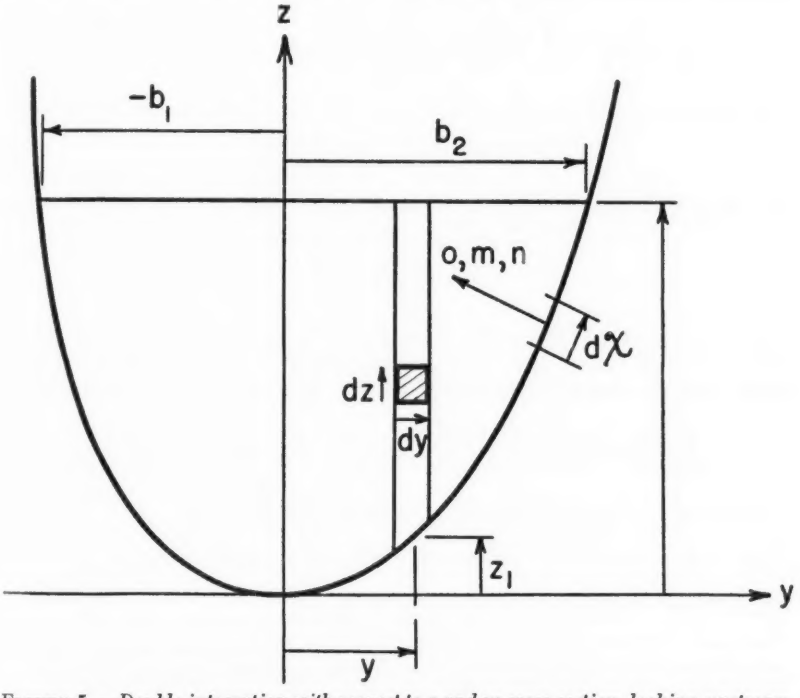

FIGURE 5.—*Double integration with respect to z and y; cross section, looking upstream.*

Again, for the fourth term

$$\int_A w\frac{\partial u}{\partial z}dA=\int_{-b_1}^{b_2}dy\int_{z_1}^H w\frac{\partial u}{\partial z}dz,$$

where z_1 is the z-coordinate of a point on the wetted perimeter at the distance y from the x,z-plane (see fig. 5). This time the integral with respect to z is integrated by parts, obtaining

$$\int_A w\frac{\partial u}{\partial z}dA=\int_{-b_1}^{b_2}(w_2u_2-w_0u_0)dy-\int u\frac{\partial w}{\partial z}dA, \tag{36}$$

where w_0, u_0 are now evaluated at the point (y,z_1).

If $d\chi$ denotes an elementary arc of the wetted perimeter, χ, measured in the counterclockwise direction, and the direction cosines of the inward-drawn normal are 0, m, n (figs. 4 and 5) then $dy=nd\chi$ and $dz=-md\chi$, and eq 35 and 36 become

$$\int_A v\frac{\partial u}{\partial y}dA=-\int_\chi u_0 v_0 m d\chi-\int_A u\frac{\partial v}{\partial y}dA, \tag{37}$$

and

$$\int_A w\frac{\partial u}{\partial t}dA=\int_{-b_1}^{b_2} w_s u_s dy-\int_\chi w_0 u_0 n d\chi-\int_A u\frac{\partial w}{\partial z}dA. \tag{38}$$

We add these two equations together, noting that as a result of eq 18 the integrals with respect to χ vanish, and combine the integrals in the extreme right by means of eq 8 and 34 obtaining

$$\int_A r\frac{\partial u}{\partial y}dA+\int_A w\frac{\partial u}{\partial z}dA=\int_{-b_1}^{b_2} w_s u_s dy+\alpha UA\frac{\partial U}{\partial x}-\alpha_2 U^2\frac{\partial A}{\partial x}. \tag{39}$$

Furthermore, since the equation of the free surface is

$$F(x,y,z,t)=z-H(x,t)=0,$$

and since $\partial A/\partial t=b(\partial H/\partial t)$ and $\partial A/\partial x=b(\partial H/\partial x)$, the surface boundary condition, eq 20, becomes

$$bw_s=\frac{\partial A}{\partial t}+u_s\frac{\partial A}{\partial x}.$$

Replacing w_s in eq 39 by its value from the above equation, recalling that A is not a function of y, evaluating the integrals by means of eq 26 and 32 and eliminating $\partial U/\partial x$ by means of eq 21, we have

$$\int_A v\frac{\partial u}{\partial y}dA+\int_A w\frac{\partial u}{\partial z}=\overline{(u_s}-\alpha U)\frac{\partial A}{\partial t}+\overline{(u_s^2}-\alpha U^2-\alpha_2 U^2)\frac{\partial A}{\partial x}.$$

Introducing a final coefficient of velocity distribution,

$$U\alpha_3=\overline{u_s}-\alpha U, \tag{40}$$

the previous equation becomes, using eq 33,

$$\int_A r\frac{\partial u}{\partial y}dA+\int_A w\frac{\partial u}{\partial z}=\alpha_3 U\frac{\partial A}{\partial t}+\alpha_2 U^2\frac{\partial A}{\partial x}. \tag{41}$$

We have now succeeded in evaluating all the terms on the left of eq 22 in terms of functions of x and t only, and proceed to the terms on the right. In view of eq 25, the first two terms become merely

$$gi\int_A dA-\frac{1}{\rho}\int_A\frac{\partial}{\partial x}(p-R_{xx})\,dA=giA-gA\frac{\partial H}{\partial x}, \tag{42}$$

since H is not a function of y or z.

The integral of the last two terms in eq 22 is transformed by Green's theorem into a line integral around the periphery of the cross section:

$$-\frac{1}{\rho}\int_A\left[\frac{\partial}{\partial y}R_{yx}+\frac{\partial}{\partial z}R_{zx}\right]dA=\frac{1}{\rho}\oint R_{yx}dz-R_{zx}dy.$$

Expressing the line integral in terms of χ as was done for eq 37 and 38,

$$\frac{1}{\rho}\int_A\left[\frac{\partial}{\partial y}R_{yx}+\frac{\partial}{\partial z}R_{zx}\right]dA=-\frac{1}{\rho}\oint[mR_{yx}+nR_{zx}]d\chi.$$

Comparison with eq 14 and 15 shows that the integrand of the line integral is the x-component of the force which the fluid exerts on the channel walls and the free surface. If we denote this shearing force by τ, and assume that the shear on the free surface is zero, and define τ_0 to be the mean shear of the fluid on the channel walls and bottom

$$\tau_0=\frac{1}{\chi}\int_\chi \tau d\chi, \tag{43}$$

then we have

$$\frac{1}{\rho}\int_A\left[\frac{\partial}{\partial y}R_{yx}+\frac{\partial}{\partial z}R_{zx}\right]dA=-\frac{\tau_0\chi}{\rho}. \tag{44}$$

Our choice of axes makes τ_0 positive, since τ_0 has the same direction as U. We now define λ the channel coefficient of friction,

$$\tau_0=\lambda\frac{\rho U^2}{2}, \tag{45}$$

and eq 44 becomes

$$\frac{1}{\rho}\int\left[\frac{\partial}{\partial y}R_{yx}+\frac{\partial}{\partial z}R_{zx}\right]dA=-\frac{\lambda U^2\chi}{2}. \tag{46}$$

Collecting the results of eq 30, 34, 41, 42, 46, and dividing them by A, the desired integral of eq 22 is

$$g\frac{\partial H}{\partial x}+\frac{\partial U}{\partial t}+\alpha U\frac{\partial U}{\partial x}+(1-\alpha)\frac{U}{A}\frac{\partial A}{\partial t}=gi-\frac{\lambda U^2}{2R}, \tag{47}$$

where $R=A/\chi$ is the hydraulic radius of the channel. This is the desired hydraulic equation of motion for gradually varied unsteady flow in prismatic channels. It will be noted that only one coefficient of velocity distribution enters into the final equation, the one related to the distribution of the squares of velocities in a cross section.

This equation was derived on the basis of the assumption that the flow was turbulent, which is the case usually met with in practice. Nevertheless, the equation also applies to viscous laminar flow, since the dynamical equations of motion, eq 13, are the same for both types of flow, except that in laminar flow the quantities p_{xx}, . . ., are replaced by S_{xx}, . . . , rather than by R_{xx}, ... It is tacitly assumed that the flow pattern is such that the assumptions made concerning the Reynolds stresses in deriving eq 22, 23, 24 are also true for the viscous stresses. Finally, in laminar flow α and λ become quantities that may be calculated rather than ones that must be experimentally determined.

2. COEFFICIENT OF RESISTANCE AS A FUNCTION OF H

If it is assumed that the coefficient λ defined by eq 45 is a function of H only, and is therefore independent of $\partial U/\partial t$ and $\partial U/\partial x$, then λ can

be evaluated from the ordinary parameters of uniform flow. Since, when the flow is uniform, U and H are constants, we have from eq 47

$$gi=\frac{\lambda U_0^2}{2R_0},$$

or

$$\frac{U_0}{\sqrt{giR_0}}=\sqrt{\frac{2}{\lambda}}, \tag{48}$$

where U_o and R_o, respectively, are the mean velocity and hydraulic radius, for uniform flow.

We assume further that the propagation of the waves is restricted to that type of turbulent flow in which the friction is determined by the surface asperities independently of the Reynolds number. The resistance law is then represented adequately by Manning's formula in the following form [5, eq 61, 80]:

$$\frac{U_0}{\sqrt{giR_0}}=8.12\left(\frac{R_0}{k_s}\right)^{1/6}, \tag{49}$$

where k_s is the equivalent sand roughness [5, p. 713] of the channel surfaces.

Equating the right-hand members of eq 48 and 49, we obtain

$$\lambda=0.0303\left(\frac{k_s}{R_0}\right)^{1/3}.$$

Differentiating with respect to H_0, the value of H for undisturbed flow, we have

$$\frac{d\lambda}{dH_0}=-\frac{\lambda}{3R_0}\frac{dR_0}{dH_0}, \tag{50}$$

since R_0 is a function of H_0. For a wide rectangular channel, $R=H_0$ and

$$\frac{d\lambda}{dH_0}=-\frac{\lambda}{3H_0}. \tag{51}$$

3. VELOCITY OF PROPAGATION OF SHORT WAVES WITH NEGLIGIBLE CURVATURE

Assuming an initial condition of uniform flow in a very wide rectangular channel, let H_0 be the depth of the liquid and U_0 be the mean velocity of flow in a cross-section. If the flow is disturbed, this can be expressed by writing:

$$\left.\begin{aligned} H(x,\,t)&=H_0+h(x,\,t),\\ \text{and}\qquad U(x,\,t)&=U_0+u(x,\,t),\end{aligned}\right\} \tag{52}$$

for the depth and for the mean velocity. The quantity u will, in general, henceforth signify the variation from U_0, the undisturbed value of U, and h the variation from H_0, the undisturbed value of H.

We replace H and U in eq 47 by their values from eq 52. Since the

channel is rectangular, A is a linear function of H; since it is wide, $R=H$; and H_0 and U_0 are constants, hence eq 47 and 21 become

$$g\frac{\partial h}{\partial x}+\frac{\partial u}{\partial t}+\alpha(U_0+u)\frac{\partial u}{\partial x}+(1-\alpha)\frac{U_0+u}{H_0+h}\frac{\partial h}{\partial t}=gi-\frac{\lambda(U_0+u)^2}{2(H_0+h)}, \quad (53)$$

$$\frac{\partial h}{\partial t}+(H_0+h)\frac{\partial u}{\partial x}+(U_0+u)\frac{\partial h}{\partial x}=0. \quad (54)$$

We now introduce two restrictions of a different kind. First, we assume that α is very nearly equal to unity and hence the term containing $1-\alpha$ may be neglected. Secondly, we assume that

$$(I) \qquad u\frac{\partial u}{\partial x}\ll\frac{\partial u}{\partial t}, \quad (55)$$

$$(II) \qquad gi-\frac{\lambda U^2}{2H}\ll\frac{\partial u}{\partial t}, \quad (56)$$

$$(III) \qquad u\frac{\partial h}{\partial x}+h\frac{\partial u}{\partial x}\ll\frac{\partial h}{\partial t}. \quad (57)$$

On this basis eq 53 and 54 reduce to

$$g\frac{\partial h}{\partial x}+\frac{\partial u}{\partial t}+U_0\frac{\partial u}{\partial x}=0, \quad (58)$$

$$\frac{\partial h}{\partial t}+H_0\frac{\partial u}{\partial x}+U_0\frac{\partial h}{\partial x}=0. \quad (59)$$

We differentiate eq 58 with respect to x and eliminate the terms containing u by means of eq 59. This gives

$$\frac{\partial^2 h}{\partial t^2}+2U_0\frac{\partial^2 h}{\partial x\partial t}+(U_0^2-gH_0)\frac{\partial^2 h}{\partial x^2}=0. \quad (60)$$

A particular solution of this is

$$h=F(x-\omega_0 t), \quad (61)$$

where F is an arbitrary function, provided ω_0 is a root of

$$\omega_0^2-2U_0\omega_0+U_0^2-gH_0=0.$$

The two roots are

$$\omega_0=U_0\pm\sqrt{gH_0}, \quad (62)$$

and it is evident upon inspecting eq 61 that the wave is propagated without change of form with the celerity, or velocity of propagation, ω_0 in the positive x-direction, since at time $t+(\Delta x/\omega_0)$, the wave profile is displaced by Δx from its position at time t. When an observer is moving with the current, that is, moving with the velocity U_0, a wave may be moving either downstream or upstream with respect to the observer. In the first case, $U_0<\omega_0$, and the wave is *descending;* in the second case, $U_0>\omega_0$, and the wave is *ascending.* Accordingly, the larger root of ω_0 gives the celerity of a descending wave and the smaller root the celerity of an ascending wave. In all formulas containing an ambiguous sign the upper sign will pertain to descending waves and the lower sign to ascending waves.

It is now a simple matter to determine the function u. From eq 61, we have

$$\frac{\partial h}{\partial t}=-\omega_0\frac{\partial h}{\partial x}. \tag{63}$$

Substituting this value of $\partial h/\partial t$ in eq 59, it becomes

$$\frac{\partial u}{\partial x}+\frac{U_0-\omega_0}{H_0}\frac{\partial h}{\partial x}=0,$$

whose integral is

$$u+\frac{U_0-\omega_0}{H_0}h+f(t)=0.$$

Since for any time t, at $h=0$, $u=0$, then since the liquid is undisturbed at infinity $f(t)\equiv 0$, and

$$u=(\omega_0-U_0)\frac{h}{H_0}; \tag{64}$$

or in view of eq 62

$$u=\pm\sqrt{gH_0}\frac{h}{H_0}, \tag{65}$$

which states that the excess of the mean velocity of the particles in a cross section under the wave is proportional to the wave height h.

It will be noted that the above equation for the celerity of waves, eq 62, is the same as that developed for the motion of irrotational waves in still water [1, eq 56], except that a constant velocity of flow, U_0, is superposed on the wave velocities relative to the water, $\sqrt{gH_0}$. This would appear to indicate that the friction due to turbulence which is inherent in the undisturbed flow, U_0, has no effect on the propagation of waves. In general, the effect of turbulence cannot be neglected, but in this case the assumptions made in deriving eq 62 restrict the size of the wave in such a way that the effect of turbulence is negligible.

The physical significance of these mathematical assumptions will now be investigated. Consider first

$$\text{(III)}\qquad u\frac{\partial h}{\partial x}+h\frac{\partial u}{\partial x}\ll\frac{\partial h}{\partial t}.$$

Replacing u by its value from eq 64, and $\partial h/\partial t$ by its value from eq 63, we have

$$\frac{h}{H_0}\ll\frac{1}{2}\left(\frac{\omega_0}{U_0-\omega_0}\right). \tag{66}$$

Consider secondly

$$\text{(I)}\qquad u\frac{\partial u}{\partial x}\ll\frac{\partial u}{\partial t}.$$

Using the same relations as before, we have

$$\frac{h}{H_0}\ll\frac{\omega_0}{U_0-\omega_0}.$$

Obviously, the first condition is sufficient for the second.

Both of these restrictions have no bearing on the fact that the undisturbed flow is controlled by friction. They are necessary but are not sufficient conditions for a wave to move without change of form. A more significant restriction arises from the assumption that the right-hand member of eq 53 is negligible:

$$\text{(II)} \qquad gi-\frac{\lambda(U_0+u)^2}{2(H_0+h)}\ll\frac{\partial u}{\partial t}.$$

Expressing the left-hand side in terms of u/U_0 and h/H_0, and replacing λ by its value from eq 48, we obtain, since $R_0=H_0$,

$$\frac{gi\frac{h}{H_0}\left(1-2\frac{uH_0}{U_0h}-\left(\frac{u}{U_0}\right)^2\frac{H_0}{h}\right)}{1+\frac{h}{H_0}}\ll\frac{\partial u}{\partial t}.$$

Eliminating u via eq 64, and transforming the right-hand side by means of eq 63, we have

$$\frac{giH_0\left(3-\frac{2\omega_0}{U_0}-\left(\frac{\omega_0}{U_0}-1\right)^2\frac{h}{H_0}\right)}{-\omega_0(\omega_0-U_0)\left(1+\frac{h}{H_0}\right)}\left(\frac{h}{H_0}\right)\ll\frac{\partial h}{\partial x}.$$

In contrast to conditions (I) and (II), where we obtained an inequality comparing h/H_0 with a constant term which is determined by the characteristics of the channel, we find in this case that both sides of the inequality are functions of h. We are also confronted with the fact that $\partial h/\partial x$ generally vanishes at the apex of the wave profile, and hence the inequality cannot be satisfied at that point even if the left-hand member also vanishes.

In order to arrive at a workable criterion for determining whether the theory is applicable, we integrate both sides of the inequality with respect to x, thus obtaining an average condition:

$$\frac{igH_0}{-\omega_0(\omega_0-U_0)}\int\left|\frac{3-2\frac{\omega_0}{U_0}-\left(\frac{\omega_0}{U_0}-1\right)^2\frac{h}{H_0}}{1+\frac{h}{H_0}}\left(\frac{h}{H_0}\right)\right|dx\ll\int\left|\frac{\partial h}{\partial x}\right|dx. \qquad (67)$$

It is not feasible to integrate the left-hand side of this inequality unless the function $h(x,t)$ is given. It is therefore necessary to assume that

$$\text{(IV)} \qquad \left(\frac{\omega_0}{U_0}-1\right)^2\frac{h}{H_0}\ll 3-\frac{2\omega_0}{U_0}, \qquad (68)$$

and

$$\text{(V)} \qquad \frac{h}{H_0}\ll 1, \qquad (69)$$

and eq 67 reduces to

$$B\int\left|\frac{h}{H_0}\right|dx\ll\int\left|\frac{\partial h}{\partial x}\right|dx \qquad (70)$$

where

$$B=igH_0\frac{2\omega_0-3U_0}{\omega_0U_0(\omega_0-U_0)}.$$

If the wave profile is such that (IV) and (V) are not both satisfied, then eq 70 does not apply, and the integral on the left of eq 67 must be evaluated. Assuming that the wave profile has a unique maximum height h_m, that $\partial h/\partial x$ is everywhere finite, that L is the length of the wave, and that h is always positive, then eq 70 becomes

$$\frac{L}{H_0}\ll\frac{2}{jB}, \tag{71}$$

where j is a fraction such that the volume of the wave per unit width of channel above the undisturbed surface is jh_mL. This last inequality is the desired average condition, one which restricts the length of the wave. Waves fulfilling this condition will be referred to as *short waves*.

In addition to this restriction on the length of the wave, we still have the three conditions on the maximum height of the wave, expressed by eq 66, 68 and 69; the first being derived from the original restriction (III), and the other two from the approximations used in obtaining eq 71. Each of the first two restrictions states that the maximum height of the wave must be small with respect to a constant determined by the channel parameters. For convenience we shall express these constants in terms of $U_0/\sqrt{gH_0}$.

For descending waves, $\omega_0=U_0+\sqrt{gH_0}$, and eq 66, 68, 69 become

$$\text{(IIIa)}\qquad \frac{h}{H_0}\ll-\frac{1}{2}\left(\frac{U_0}{\sqrt{gH_0}}+1\right),$$

$$\text{(IVa)}\qquad \frac{h}{H_0}\ll\frac{U_0}{\sqrt{gH_0}}\left(\frac{U_0}{\sqrt{gH_0}}-2\right),$$

and

$$\text{(V)}\qquad \frac{h}{H_0}\ll1.$$

For ascending waves, $\omega_0=U_0-\sqrt{gH_0}$, and the same three equations become

$$\text{(IIIb)}\qquad \frac{h}{H_0}\ll\frac{1}{2}\left(\frac{U_0}{\sqrt{gH_0}}-1\right)$$

$$\text{(IVb)}\qquad \frac{h}{H_0}\ll\frac{U_0}{gH_0}\left(\frac{U_0}{\sqrt{gH_0}}+2\right)$$

and

$$\text{(V)}\qquad \frac{h}{H_0}\ll1.$$

These relations are made more intelligible by means of figures 6 and 7. The quantity h/H_0 must be small with respect to all of the quantities plotted in the figure, that is, small with respect to the

least of them. It will be noted that the theory breaks down completely for ascending waves in water of critical depth, that is, it does not apply to the case of the hydraulic jump. The fact that it breaks

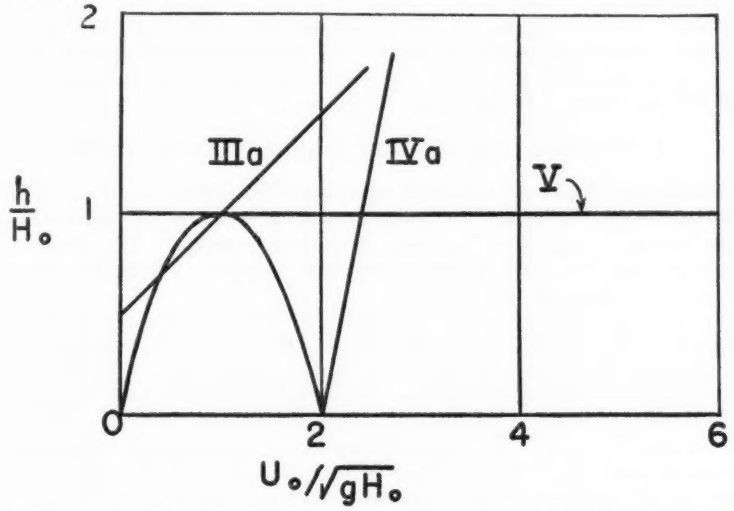

FIGURE 6.—*Limitations on height of short descending waves moving without change of form.*

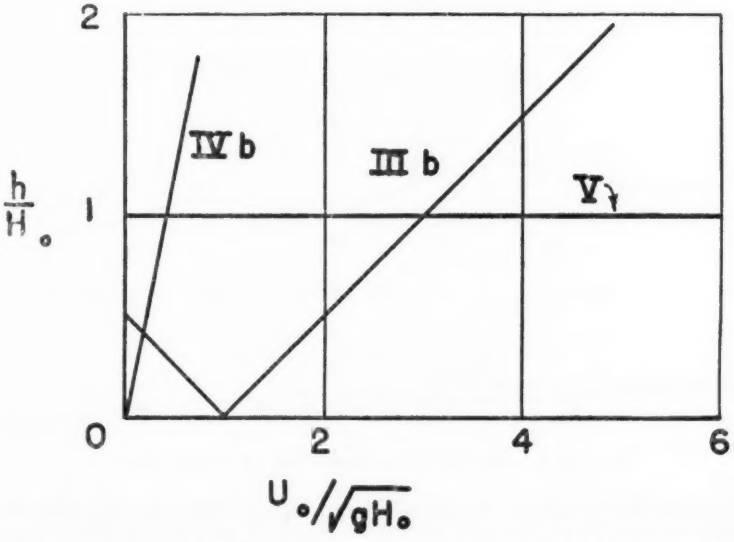

FIGURE 7.—*Limitations on height of short ascending waves moving without change of form.*

down for $U_0/\sqrt{gH_0}=2$ when the wave is descending is due merely to the approximation used in deriving eq 71, and is not inherent in the theory.

Our three original assumptions thus indicate that if a wave is short and of small height, and moving in a wide rectangular channel where the undisturbed current is controlled by friction, the waves move without change of form, and their velocity is constant. It was also assumed in deriving eq 47 that the surface curvature is negligible, and this restriction is still in force. The simple theory thus gradually loses its applicability as the waves become larger and larger. This case will be treated in the later sections.

4. PROPAGATION OF DISCONTINUITIES OF SLOPE

One of the simplest types of wave profiles which we can imagine superposed on the initial uniform flow in a wide rectangular channel is one which is polygonal in form, such as a triangle. We shall investigate the motion at a vertex of such a polygon, where the slope of the wave is discontinuous.

We assume that at $t=t_0$, the discontinuity of the slope $\partial h/\partial x$ is located at the point $x=x_0$, and the water surface is represented by two straight lines (see fig. 8). The mean velocity, U, and the depth, H, will each be described by two distinct functions; downstream from x_0, we write $U=U_1$ and $H=H_1$, and upstream from x_0, we write $U=U_2$ and $H=H_2$. We assume that both H_1 and H_2 have negligible curvature, and that the channel is rectangular. Under these conditions, eq 47 applies to each pair of functions, and we write, putting α equal to unity:

$$g\frac{\partial H_1}{\partial x}+\frac{\partial U_1}{\partial t}+U_1\frac{\partial U_1}{\partial x}=gi-\frac{\lambda U_1^2}{2H_1}, \tag{72}$$

$$g\frac{\partial H_2}{\partial x}+\frac{\partial U_2}{\partial t}+U_2\frac{\partial U_2}{\partial x}=gi-\frac{\lambda U_2^2}{2H_2}. \tag{73}$$

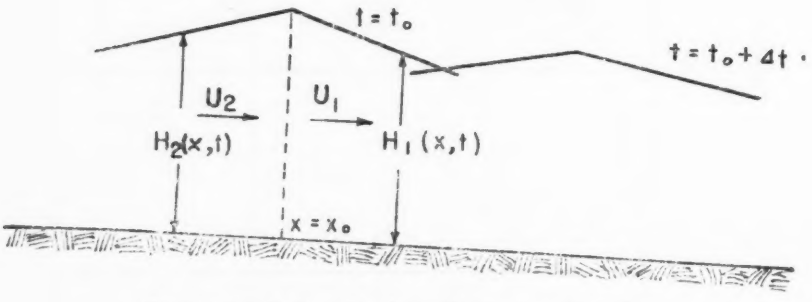

FIGURE 8.—*Motion of a discontinuity in surface slope.*

In a similar manner, we obtain from eq 21, since A is proportional to H,

$$\frac{\partial H_1}{\partial t}+U_1\frac{\partial H_1}{\partial x}+H_1\frac{\partial U_1}{\partial x}=0, \tag{74}$$

$$\frac{\partial H_2}{\partial t}+U_2\frac{\partial H_2}{\partial x}+H_2\frac{\partial U_2}{\partial x}=0. \tag{75}$$

Following Hadamard [13, p. 83], we introduce the following notation for the change in value of a derivative as the discontinuity is traversed:

$$\frac{\partial H_2}{\partial x}-\frac{\partial H_1}{\partial x}=\left[\frac{\partial H}{\partial x}\right],\quad \frac{\partial U_2}{\partial x}-\frac{\partial U_1}{\partial x}=\left[\frac{\partial U}{\partial x}\right].$$

Subtracting eq 73 from eq 72 and eq 75 from eq 74, we have, since H, U, and λ are continuous,

$$g\left[\frac{\partial H}{\partial x}\right]+\left[\frac{\partial U}{\partial t}\right]+U\left[\frac{\partial U}{\partial x}\right]=0, \tag{76}$$

$$\left[\frac{\partial H}{\partial t}\right]+U\left[\frac{\partial H}{\partial x}\right]+H\left[\frac{\partial U}{\partial x}\right]=0, \tag{77}$$

where H and U are evaluated at $x=x_0$, $t=t_0$. Since four discontinuities are involved, we need two more relations.

In figure 8 the displacement of the discontinuity during the time interval Δt is indicated. If ΔU_1 and ΔU_2 are the changes in the mean velocities, then

$$\Delta U_1=\frac{\partial U_1}{\partial x}\Delta x+\frac{\partial U_1}{\partial t}\Delta t, \tag{78}$$

$$\Delta U_2=\frac{\partial U_2}{\partial x}\Delta x+\frac{\partial U_2}{\partial t}\Delta t, \tag{79}$$

Similarly, if ΔH_1 and ΔH_2 are the changes in the height, then

$$\Delta H_1=\frac{\partial H_1}{\partial x}\Delta x+\frac{\partial H_1}{\partial t}\Delta t, \tag{80}$$

$$\Delta H_2=\frac{\partial H_2}{\partial x}\Delta x+\frac{\partial H_2}{\partial t}\Delta t. \tag{81}$$

Subtracting eq 79 from 78 and 81 from 80,

$$0=\left[\frac{\partial U}{\partial x}\right]\Delta x+\left[\frac{\partial U}{\partial t}\right]\Delta t,$$

$$0=\left[\frac{\partial H}{\partial x}\right]\Delta x+\left[\frac{\partial H}{\partial t}\right]\Delta t,$$

since U and H are continuous. We denote the velocity of propagation of the discontinuity, $\Delta x/\Delta t$, by Ω. Thus the last two equations become

$$\Omega\left[\frac{\partial U}{\partial x}\right]+\left[\frac{\partial U}{\partial t}\right]=0, \tag{82}$$

$$\Omega\left[\frac{\partial H}{\partial x}\right]+\left[\frac{\partial H}{\partial t}\right]=0. \tag{83}$$

We now have a system of four homogeneous linear equations, eq 76, 77, 82, 83, in the four unknown discontinuities. Since the discontinuities do not vanish, the determinant of the coefficients must vanish, and this relation gives

$$\Omega - U = \pm\sqrt{gH}. \tag{84}$$

The velocity at the front of a descending wave, as shown in figure 9, will now be considered. In this case, Ω is positive, and we see from eq 83 that $[\partial H/\partial x]$ and $[\partial H/\partial t]$ have opposite signs, and since in front of the wave, $\partial H_1/\partial t=0$, $\partial H_1/\partial x=0$, then behind the front of the wave, $\partial H_2/\partial t>0$, $\partial H_2/\partial x<0$. Now, $U=U_0$ and $H=H_0$ at the discontinuity, and the velocity of the wave front is

$$\Omega = U_0+\sqrt{gH_0}; \tag{85}$$

the positive sign is selected, since $\Omega>0$, regardless of the magnitude of U_0 and H_0. We thus see from eq 62 that at the front of such a wave $\Omega=\omega_0$. This analysis fails to give any information concerning the change in the magnitude of the discontinuity. Such information may be obtained by using Boussinesq's equation for the velocity of propagation of a wave-volume element. A typical case is discussed in section IV–6, page 498.

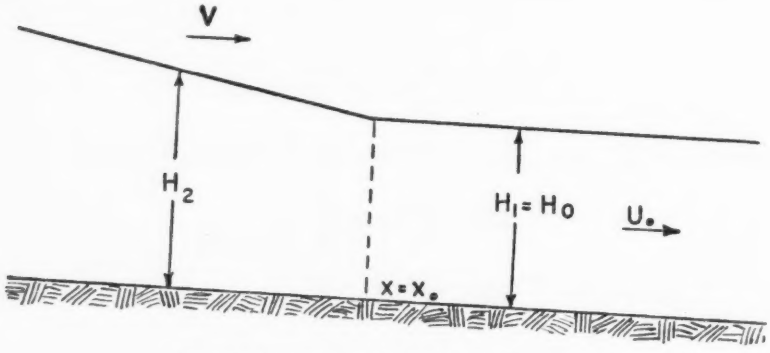

FIGURE 9.—*The front of a descending wave.*

5. EFFECT OF VELOCITY DISTRIBUTION ON THE CELERITY OF SHORT WAVES

In the derivation of the celerity of short waves, given in section III–3, page 478, it was assumed that $1-\alpha$ is a small fraction that may be neglected. This is generally true in practice, but we now drop this restriction and thereby consider the effect of the velocity distribution on the celerity of short waves. Retaining α and using the assumptions of section III–3, eq 55, 56, 69, the equation of motion, eq 53 now becomes

$$g\frac{\partial h}{\partial x}+\frac{\partial u}{\partial t}+\alpha U_0\frac{\partial u}{\partial x}+(1-\alpha)\frac{U_0+u}{H_0}\frac{\partial h}{\partial t}=0. \tag{86}$$

Even though $1-\alpha$ is not negligible, it is still true that in practice

α is of the same order of magnitude as unity. From eq 69 we have therefore

$$(1-\alpha)\frac{\omega_0-U_0}{H_0}\frac{\partial h}{\partial t}\frac{h}{H_0}\ll\frac{\omega_0-U_0}{H_0}\frac{\partial h}{\partial t}.$$

Using the relation between h and u obtained in the previous analysis, eq 64, this inequality reduces to

$$(1-\alpha)\frac{u}{H_0}\frac{\partial h}{\partial t}\ll\frac{\partial u}{\partial t},$$

and eq 86 thus becomes

$$g\frac{\partial h}{\partial x}+\frac{\partial u}{\partial t}+\alpha U_0\frac{\partial u}{\partial x}+(1-\alpha)\frac{U_0}{H_0}\frac{\partial h}{\partial t}=0.$$

Differentiating with respect to x, assuming that α does not vary with x, and eliminating the terms containing u by means of eq 59, we find

$$\frac{\partial^2 h}{\partial t^2}+2\alpha U_0\frac{\partial^2 h}{\partial x\partial t}+(\alpha U_0^2-gH_0)\frac{\partial^2 h}{\partial x^2}=0.$$

A particular solution of this is, as before,

$$h=F(x-\omega_0 t),$$

where F is an arbitrary function, provided ω_0 is one of the roots of

$$\omega_0^2-2\alpha U_0\omega_0+(\alpha U_0^2-gH_0)=0.$$

The two roots are

$$\omega_0=(1+\eta)U_0\pm\sqrt{gH_0+(\eta+\eta^2)U_0^2}, \tag{87}$$

where $\eta=\alpha-1$. (88)

This is the formula giving the celerity of short waves when the effect of the velocity distribution is considered. It will be seen that η is the excess over unity of the ratio of the mean of the velocities squared, taken over the different points of a section, to the square of the mean velocity. A corresponding expression is given by Boussinesq [3, p. 285, eq 265], which differs from the above only in the values of the coefficients.

It is preferable that the value of η for a given case be ascertained by observation. If this is not feasible, a value may be obtained by considering the relation which exists between η and U_0 and u_m, the latter being the maximum velocity occurring at the surface of a wide channel. A relation of this kind can be derived if it is assumed that in a channel of great width the "velocity defect," that is, the difference between the maximum velocity u_m and the velocity u at a point whose height above the bottom is z, depends only on the so-called "shear velocity" [5, p. 709] and the relative depth of the water, and is independent of the character of the asperities on the channel bottom. Mathematically speaking,

$$u_m-u=u_* f(\zeta), \tag{89}$$

where $\zeta=z/H_0$, and u_* is the shear velocity,

$$u_*=\sqrt{igH_0}. \tag{90}$$

Multiplying both sides of eq 89 by $d\zeta$, integrating from $z=0$ to $z=H_0$ that is, from 0 to 1, putting

$$\int_0^1 f(\zeta)d\zeta=N_1,$$

and recalling that the mean value of u is U_0, we obtain

$$u_m-U_0=N_1u_*. \tag{91}$$

Squaring both sides of eq 89, we obtain in a similar manner, using eq 88, 31, 26,

$$u_m{}^2-2u_mU_0+(1+\eta)U_0{}^2=N_2u_*{}^2, \tag{92}$$

where

$\int_0^1 f(\zeta)^2d\zeta=N_2$. Eliminating the shear velocity, u_*, between eq 91 and 92, and solving for η, we obtain

$$\eta=\left(\frac{N_2}{N_1{}^2}-1\right)\left(\frac{u_m}{U_0}-1\right)^2, \tag{93}$$

which is the desired relation expressing η in terms of u_m and U_0.

To determine the numerical values of N_1 and N_2 we make use of some of Nikuradse's experimental results concerning the velocity distribution in sand-coated circular pipes [14, p. 18–19]. The data in table 1 were obtained by selecting three determinations of the velocity distribution for each of six relative roughnesses. In Nikuradse's paper the data for each relative roughness are given in a separate table, and the three determinations on the extreme right of each table were selected, except in Zahlentafel (table) 13, where the first one and the last two were chosen. In each case, velocity-defect ratios were computed for each value of y/r, which corresponds to z/H_0 in our notation, and the mean of these 18 determinations was entered in table 1. Plotting curves for $f(\zeta)$ and $[f(\zeta)]^2$ from these data and integrating numerically, it is found that in circular pipes, $N_1=2.52$ and $N_2=12.29$. Since the "velocity defect" relation is the same both for circular pipes and for open channels of great width these values of N_1 and N_2 may be substituted in eq 93, which becomes

$$\eta=0.94\left(\frac{u_m}{U_0}-1\right)^2. \tag{94}$$

An expression for η in terms of λ may also be derived. Eliminating u_m between eq 91 and 92, we have

$$\eta=(N_2-N_1{}^2)\frac{u_*{}^2}{U_0{}^2}.$$

Eliminating u_* and U_0 via eq 90 and 48:

$$\eta=(N_2-N_1{}^2)\frac{\lambda}{2},$$

which becomes, when we replace N_2 and N_1 by their numerical values

$$\eta = 2.97\lambda. \tag{95}$$

TABLE 1.—*Velocity defect as a function of distance from channel bottom.*

$\frac{z}{H_0}$	$\frac{u_m-u}{u_*}$	$\frac{z}{H_0}$	$\frac{u_m-u}{u_*}$
0.00	12.78	0.50	1.75
.02	9.52	.60	1.23
.04	8.09	.70	0.81
.07	6.84	.80	.45
.10	5.99	.90	.189
.15	5.03	.96	.067
.20	4.29	.98	.030
.30	3.21	1.00	.000
.40	2.37		

It will be recalled that in deriving eq 62 of section I–3 it was assumed that α is nearly unity, that is, that η is small, and that this restriction was removed in deriving eq 87. By comparing these two equations we can establish an approximate relation which will show how small η must be in order that eq 62 may be used.

Equation 87 may be approximated by

$$\omega_0 = (1+\eta)U_0 \pm \sqrt{gH_0}\left(1+\frac{\eta+\eta^2}{2}\frac{U_0^2}{gH_0}\right),$$

and this reduces to eq 62 if

$$\eta U_0 \pm \frac{\eta+\eta^2}{2}\frac{U_0^2}{\sqrt{gH_0}} \ll U_0 \pm \sqrt{gH_0}.$$

Dividing by U_0, neglecting η^2 with respect to η, using eq 48, this becomes

$$\eta\left[1+\frac{1}{2}\sqrt{\frac{2i}{\lambda}}\right] \ll 1+\sqrt{\frac{\lambda}{2i}}, \tag{96}$$

or, replacing η by its value from eq 95,

$$2.97\lambda\left[1+\frac{1}{2}\sqrt{\frac{2i}{\lambda}}\right] \ll 1+\sqrt{\frac{\lambda}{2i}}. \tag{97}$$

Bazin's inexhaustible store of experimental data furnishes an example [15] of the improvement obtained by using eq 87 instead of eq 62. The observed values, together with the results of the two formulas, eq 62 and eq 87 are shown in table 2. These experiments were conducted in the discharge channel of the Grosbois reservoir. This channel was constructed of masonry, with the steep slopes of 0.101 in the upper part and 0.037 in the lower part. Before entering the channel, the water drawn from the reservoir flowed over an apron 11.20 m wide just below the gates, and which narrowed down to 1.80 m (the width of the channel). The axis of the apron described an arc of 90°, with a radius of 40.50 m, in order to join with the channel. As a result of the narrowing of the cross section and the change of direction of the apron, the flowing water was subjected to various reflections at the walls and these complex movements set up waves which passed rapidly down the channel at fairly regular intervals of about 2

sec (31 per minute). These waves were rather small in height, but their transit was easily observed owing to the slight noise which accompanied them.

The observed values of ω_0 given in the table 2 are the averages of six individual observations, the $\pm$ term representing the standard deviation. The values of η are computed from eq 94. The table shows that the values of ω_0 computed by the simple formula, eq 62, are considerably in error, whereas the values of ω_0 obtained from eq 87 compare reasonably well with the experimental values.

TABLE 2.—*Experimental and calculated values of ω_0 for torrential flow*

Experimental data (g=9.81 m/sec²)				
i	H_0	U_0	u_m	ω_0
	m	*m/sec*	*m/sec*	*m/sec*
0.101	0.110	3.785	5.51	6.25 ±.07
.037	.150	2.744	3.49	4.32 ±.08
.037	.235	3.481	4.55	5.75 ±.06

Computed values eq 62		Computed values eq 87		
ω_0	Error	η	ω_0	Error
m/sec	%		*m/sec*	%
4.82	−22.9	0.195	6.63	+6.1
3.96	−8.3	.070	4.36	+0.9
5.00	−13.0	.089	5.65	−1.7

IV. SECOND-ORDER THEORY OF WAVE PROPAGATION

1. EQUATION OF MEAN FLOW WITH APPRECIABLE VERTICAL ACCELERATION

Assuming that the liquid is flowing in a wide rectangular channel (v=0, and R_{yx}=0), that the variation with z of the x-component, u, of the local velocity is negligible, or $u=U(x, t)$ and that the assumptions made in section III–1 regarding the Reynolds stresses and the orientation of the axes still hold, then the Reynolds equations for turbulent flow, eq 10 become

$$\frac{\partial U}{\partial t}+U\frac{\partial U}{\partial x}=gi-\frac{1}{\rho}\frac{\partial(p-R_{xx})}{\partial x}+\frac{1}{\rho}\frac{\partial R_{xz}}{\partial z}, \tag{98}$$

$$0=\frac{\partial(p-R_{zz})}{\partial y},$$

and

$$\frac{\partial w}{\partial t}+U\frac{\partial w}{\partial x}+w\frac{\partial w}{\partial z}=-\frac{1}{\rho}\frac{\partial(p-R_{zz})}{\partial z}-g. \tag{99}$$

We shall eliminate p from the eq 98 with the aid of eq 99, and then eliminate z by integrating over the cross section.

We begin by evaluating w in terms of the other variables. Since $u=U$ and $v=0$, the condition of continuity eq 8 reduces to

$$\frac{\partial w}{\partial z}=-\frac{\partial U}{\partial x}.$$

Integrating with respect to z, we have, since $w=0$ when $z=0$,

$$w=-z\frac{\partial U}{\partial x},$$

which, using a condition of continuity of mean flow, derived from eq 21 on the basis of the assumption that A is proportional to H,

$$\frac{\partial H}{\partial t}+U\frac{\partial H}{\partial x}+H\frac{\partial U}{\partial x}=0, \tag{100}$$

reduces to

$$w=\frac{z}{H}\left(\frac{\partial H}{\partial t}+U\frac{\partial H}{\partial x}\right). \tag{101}$$

Replacing w in eq 99 by its value from eq 101 and neglecting squares and products of the first derivatives of H and U compared with the second derivative, we obtain, since H and U are functions of x and t only,

$$\frac{\partial(p-R_{zz})}{\partial z}=-\rho g-\frac{\rho z U^2}{H}\left(\frac{\partial^2 H}{\partial x^2}+\frac{2}{U}\frac{\partial^2 H}{\partial x\partial t}+\frac{1}{U^2}\frac{\partial^2 H}{\partial t^2}\right).$$

Multiplying by dz and integrating,

$$p-R_{zz}=p_a+\rho g(H-z)+\rho\frac{U^2H}{2}\left(1-\frac{z^2}{H^2}\right)\left(\frac{\partial^2 H}{\partial x^2}+\frac{2}{U}\frac{\partial^2 H}{\partial x\partial t}+\frac{1}{U^2}\frac{\partial^2 H}{\partial t^2}\right),$$

since at $z=H$, $p-R_{zz}=p_a$. We now differentiate the above equation with respect to x, again neglecting the products of the lower derivatives as compared with the higher derivatives, and the value thus obtained for $\partial(p-R_{zz})/\partial x$ is inserted in eq 98. The resulting equation is multiplied by dz and integrated from $z=0$ to $z=H$. Since $(R_{zz})_{z=0}$ equals τ_0, the shear on the channel bottom, and $(R_{zz})_{z=H}$ is zero, we get

$$\frac{\partial U}{\partial t}+U\frac{\partial U}{\partial x}+g\frac{\partial H}{\partial x}+\frac{HU^2}{3}\left(\frac{\partial^3 H}{\partial x^3}+\frac{2}{U}\frac{\partial^3 H}{\partial x^2\partial t}+\frac{1}{U^2}\frac{\partial^3 H}{\partial x\partial t^2}\right)=gi-\frac{\lambda U^2}{2H}, \tag{102}$$

upon replacing τ_0 by its value from eq 45.

This is the equation of mean flow for a wide rectangular channel where the vertical accelerations are not negligible but the horizontal velocities in a section are practically uniform.

2. HEIGHT OF WAVE AS A FUNCTION OF x AND t

Replacing $\partial U/\partial x$ in eq 102 by its value obtained by solving eq 100, and multiplying through by H, we obtain

$$H\frac{\partial U}{\partial t}-U\frac{\partial H}{\partial t}+(gH-U^2)\frac{\partial H}{\partial x}+\frac{H^2U^2}{3}\left(\frac{\partial^3 H}{\partial x^3}\right.$$

$$\left.+\frac{2}{U}\frac{\partial^3 H}{\partial x^2\partial t}+\frac{1}{U^2}\frac{\partial^3 H}{\partial x\partial t^2}\right)=gHi-\frac{\lambda}{2}U^2. \tag{103}$$

We again introduce the expressions

$$\left.\begin{aligned} H(x,\,t) &= H_0 + h(x,\,t), \\ U(x,\,t) &= U_0 + u(x,\,t). \end{aligned}\right\} \quad \text{and} \tag{52}$$

Substituting in eq 100, we have

$$\frac{\partial h}{\partial t} + H_0\frac{\partial u}{\partial x} + U_0\frac{\partial h}{\partial x} + h\frac{\partial u}{\partial x} + u\frac{\partial h}{\partial x} = 0, \tag{104}$$

while eq 103 becomes

$$H_0\frac{\partial u}{\partial t} - U_0\frac{\partial h}{\partial t} + (gH_0 - U_0^2)\frac{\partial h}{\partial x} + h\frac{\partial u}{\partial t} - u\frac{\partial h}{\partial t} + (gh - 2U_0u)\frac{\partial h}{\partial x}$$

$$+\frac{H_0^2U_0^2}{3}\left(\frac{\partial^3 h}{\partial x^3} + \frac{2}{U_0}\frac{\partial^3 h}{\partial x^2\partial t} + \frac{1}{U_0^2}\frac{\partial^3 h}{\partial x\partial t^2}\right) = gHi - \frac{\lambda}{2}U^2, \tag{105}$$

when u^2 is neglected with respect to U_0^2, and in the term containing the third derivatives, u and h are neglected in comparison with U and H. Various assumptions as to the nature of the right-hand member will be made in later sections.

The terms of small order in the left-hand members of the above equations, that is, the last two in eq 104 and the last four in eq 105, are simplified by introducing values from the first approximate solution:

$$u = \frac{\omega_0 - U_0}{H_0}h, \tag{64}$$

and

$$\frac{\partial h}{\partial t} = -\omega_0\frac{\partial h}{\partial x}. \tag{63}$$

From the latter and eq 61, we obtain the further relation

$$\frac{\partial^2 h}{\partial t^2} = \omega_0^2\frac{\partial^2 h}{\partial x^2}.$$

For the sake of brevity, we introduce the new variables

$$\left.\begin{aligned} k_1 &= 1 - \frac{3U_0}{\omega_0} \\ k_2 &= 1 - \frac{U_0}{\omega_0}, \end{aligned}\right\} \quad \text{and} \tag{106}$$

and we also make use of the equation

$$gH_0 = (\omega_0 - U_0)^2, \tag{107}$$

which is derived from eq 62. On the basis of the above relations, then eq 104 and 105 become

$$\frac{\partial h}{\partial t}+H_0\frac{\partial u}{\partial x}+U_0\frac{\partial h}{\partial x}+(\omega_0-U_0)\frac{\partial}{\partial x}\left(\frac{h^2}{H_0}\right)=0; \tag{108}$$

and

$$H_0\frac{\partial u}{\partial t}-U_0\frac{\partial h}{\partial t}+(gH_0-U_0^2)\frac{\partial h}{\partial x}+\omega_0(\omega_0-U_0)\frac{\partial}{\partial x}\left(\frac{k_1}{2}\frac{h^2}{H_0}+\frac{k_2H_0^2}{3}\frac{\partial^2 h}{\partial x^2}\right)=gHi-\frac{\lambda}{2}U^2. \tag{109}$$

We now differentiate eq 108 with respect to t. In differentiating the last term, which is of the second order, we use the relation

$$\left(\frac{\partial}{\partial t}\right)=-\omega_0\left(\frac{\partial}{\partial x}\right), \tag{110}$$

since these small terms may be treated as functions of $x-\omega_0 t$ [1, p. 73]. We next differentiate eq 109 with respect to x, and subtract this equation from the one obtained from eq 108. The result is

$$\frac{\partial^2 h}{\partial t^2}+2U_0\frac{\partial^2 h}{\partial x\partial t}-(gH_0-U_0^2)\frac{\partial^2 h}{\partial x^2}$$

$$-\omega_0(\omega_0-U_0)\frac{\partial^2}{\partial x^2}\left(\frac{2+k_1}{2}\left(\frac{h^2}{H_0}\right)+\frac{k_2H_0^2}{3}\frac{\partial^2 h}{\partial x^2}\right)=-\frac{\partial}{\partial x}\left(gHi-\frac{\lambda}{2}U^2\right), \tag{111}$$

which is the fundamental equation for determining h as a function of x and t.

This equation, which was derived from eq 102, has the same range of validity, namely, it applies to flow in wide rectangular channels where the horizontal velocities in a section are practically uniform. This equation takes account of vertical accelerations, finite wave heights, surface curvature, and friction.

3. CELERITY OF A WAVE-VOLUME ELEMENT

In order to integrate eq 111, the concept of *celerity of a wave-volume element*, an essential simplification due to Boussinesq [3, p. 451], is introduced. To define this concept, we consider the volume of the wave per unit width of channel, above the undisturbed primitive level of the liquid and between x, an arbitrary point, and ∞, for a descending wave, and between x and $-\infty$, for an ascending wave. Denoting this volume by σ, we have

$$\sigma=\int_x^{\infty} h\,dx \text{ and } \sigma=\int_{-\infty}^{x} h\,dx,$$

for descending and ascending waves, respectively. Recalling the convention of signs introduced in section III–3, the above equations become

$$\sigma=\pm\int_x^{\pm\infty} h\,dx. \tag{112}$$

Imagine a plane, normal to the channel axis at the point x, and which moves in such a way that the wave volume in front of it, σ, remains constant. This velocity is the celerity of the volume element σ, and

is denoted by $\omega=\omega(x,t)$. Differentiating eq 112 with respect to t, we have

$$0=\pm\int_x^{\pm\infty}\frac{\partial h}{\partial t}dx\mp h\omega,$$

since by definition $dx/dt=\omega$, σ remains constant, and we assume that the surface of the liquid is undisturbed at infinity, that is, h vanishes at $\pm\infty$. Differentiating the above equation with respect to x, we have, regardless of choice of sign,

$$\frac{\partial h}{\partial t}+\frac{\partial}{\partial x}(h\omega)=0, \tag{113}$$

which gives the relation obtaining between ω and h.

We now introduce the value of $\partial h/\partial t$ from eq 113 into the first two terms of eq 111, thus obtaining

$$-\frac{\partial^2}{\partial x\partial t}(h\omega)-2U_0\frac{\partial^2}{\partial x^2}(h\omega)-(gH_0-U_0^2)\frac{\partial^2 h}{\partial x^2}$$
$$-\omega_0(\omega_0-U_0)\frac{\partial^2}{\partial x^2}\left(\frac{2+k_1}{2}\frac{h^2}{H_0}+\frac{k^2H_0^2}{3}\frac{\partial^2 h}{\partial x^2}\right)=-\frac{\partial}{\partial x}\left(gHi-\frac{\lambda}{2}U^2\right).$$

This equation is immediately integrable once with respect to x. The arbitrary function of integration vanishes as a result of the previous assumption that the surface of the liquid is undisturbed at infinity. We thus have

$$\frac{\partial}{\partial t}(h\omega)+2U_0\frac{\partial}{\partial x}(h\omega)+(gH_0-U_0^2)\frac{\partial h}{\partial x}$$
$$+\omega_0(\omega_0-U_0)\frac{\partial}{\partial x}\left(\frac{2+k_1}{2}\frac{h^2}{H_0}+\frac{k_2H_0^2}{3}\frac{\partial^2 h}{\partial x^2}\right)=gHi-\frac{\lambda}{2}U^2. \tag{114}$$

We next transform eq 114 into a form which can be integrated. In this process it is necessary to operate only on the first three terms in the left-hand member. If we assume that ω/ω_0 is near to unity, we may write as an approximation

$$\omega=\omega_0(1+\delta(x,t)). \tag{115}$$

Substituting this value of ω in the terms under consideration, we obtain

$$\omega_0\frac{\partial}{\partial t}(h+h\delta)+2\omega_0U_0\frac{\partial}{\partial x}(h+h\delta)+(gH_0-U_0^2)\frac{\partial h}{\partial x}.$$

Now using eq 113 and 107 we obtain

$$-\omega_0\frac{\partial}{\partial x}(h\omega)+\omega_0\frac{\partial}{\partial t}(h\delta)+2\omega_0U_0\frac{\partial}{\partial x}(h+h\delta)+(\omega_0^2-2\omega_0U_0)\frac{\partial h}{\partial x}.$$

Applying eq 115 again to the first term and eq 110 to the second term (which can be done because $h\delta$ is a small quantity), and cancelling terms, we obtain

$$-2\omega_0^2\frac{\partial}{\partial x}(h\delta)+2\omega_0U_0\frac{\partial}{\partial x}(h\delta),$$

which can be written

$$-\omega_0(\omega_0-U_0)\frac{\partial}{\partial x}(2h\delta)\cdot$$

Hence eq 114 transforms into

$$-\omega_0(\omega_0-U_0)\frac{\partial}{\partial x}(2h\delta)+\omega_0(\omega_0-U_0)\frac{\partial}{\partial x}\left(\frac{2+k_1}{2}\left(\frac{h^2}{H_0}\right)+\frac{k_2H_0^2}{3}\frac{\partial^2h}{\partial x^2}\right)=gHi-\frac{\lambda}{2}U^2,$$

which, when integrated, gives

$$\delta=\frac{2+k_1}{4}\frac{h}{H_0}+\frac{k_2H_0^2}{6h}\frac{\partial^2h}{\partial x^2}-\frac{1}{2h\omega_0(\omega_0-U_0)}\int_{\pm\infty}^{x}\left(gHi-\frac{\lambda}{2}U^2\right)dx,$$

and hence from eq 115

$$\frac{\omega}{\omega_0}=1+\frac{2+k_1}{4}\frac{h}{H_0}+\frac{k_2H_0^2}{6h}\frac{\partial^2h}{\partial x^2}+\frac{1}{2h\omega_0(\omega_0-U_0)}\int_{x}^{\pm\infty}\left(gHi-\frac{\lambda}{2}U^2\right)dx. \quad (116)$$

This is a general expression for determining the effects of wave height, curvature of the wave profile, and friction, on the celerity of a wave-volume element. The integral containing the friction term requires further consideration before the actual wave profile can be determined as a function of time.

It remains to evaluate that part u of the velocity U under the wave in eq 52. Transforming the equation of continuity, eq 100, by means of eq 52,

$$\frac{\partial h}{\partial t}+\frac{\partial}{\partial x}(U_0+u)(H_0+h)=0.$$

The result of subtracting eq 113 from the above is

$$\frac{\partial}{\partial x}[(U_0+u)(H_0+h)-h\omega]=0.$$

Integrating, and using the boundary condition at $x=\infty$, for all times t, $h=0$, and $u=0$, we have

$$(U_0+u)(H_0+h)-h\omega=U_0H_0,$$

or

$$u=\frac{\omega-U_0}{H_0+h}h. \quad (117)$$

4. DEFORMATION OF THE WAVE PROFILE, ASSUMING $gHi-\frac{\lambda}{2}U^2=0$

A natural assumption, in proceeding from eq 116, is that the right-hand member $(gHi-\lambda U^2/2)$ is negligible. From eq 56 this implies that

the waves are short, as described in section III–3. On this basis, eq 116 becomes

$$\omega=\omega_0\left(1+\frac{2+k_1}{4}\frac{h}{H_0}+\frac{k_2H_0^2}{6h}\frac{\partial^2h}{\partial x^2}\right), \tag{118}$$

or when we introduce the values of k_1, k_2, and ω_0 from eq 106 and 62,

$$\omega-U_0=\pm\sqrt{gH_0}\left(1+\frac{3h}{4H_0}+\frac{H_0^2}{6h}\frac{\partial^2h}{\partial x^2}\right). \tag{119}$$

Comparison with an earlier paper [1, eq 112] shows that this expression is equivalent to that for the propagation of an irrotational wave relative to the mean velocity of flow, U_0. The assumption that $gHi-\lambda U^2/2$ is equal to zero is thus tantamount to assuming that the only effect of friction and slope is to superpose a constant velocity U_0 on the wave, which itself is propagated without any change of shape due to frictional damping or to the x-component of gravity.

The deformation of the wave profile, in a short time interval, is determined by using eq 119. Equation 113 can be written

$$\frac{\partial h}{\partial t}+\omega_0\frac{\partial h}{\partial x}+\frac{\partial}{\partial x}h(\omega-\omega_0)=0.$$

For small values of t, the integral of the above equation is

$$h=f(x-\omega_0t)-t\frac{\partial}{\partial x}[h(\omega-\omega_0)]. \tag{120}$$

In verifying this solution, we must use eq 110 when differentiating the second term on the right, which necessitates assuming that this term is small compared with the first term. In other words, the magnitude of the time interval in which this approximation is permissible varies inversely with $\partial[h(\omega-\omega_0)]/\partial x$. Clearly, since at $t=0$, we have $h=f(x)$, the function f represents the wave profile at the fiducial instant. Finally, using eq 119 and 62, eq 120 can be thrown into the form

$$h=f(x-\omega_0t)\mp t\sqrt{gH_0}\frac{\partial}{\partial x}\left(\frac{3h^2}{4H_0}+\frac{H_0^2}{6}\frac{\partial^2h}{\partial x^2}\right). \tag{121}$$

For a discussion of the deformation of a wave of negligible curvature, propagated without damping, the reader is referred to the earlier paper [1, p. 89]. All the formulas on the page cited are directly applicable, provided the expression $\sqrt{gH}(1+\ldots)$ is replaced by $U_0\pm\sqrt{gH_0}(1+\ldots)$, wherever it occurs. This, again, is merely equivalent to superposing the velocity of flow U_0, on the velocity of propagation of the wave-volume element.

5. EFFECT OF FRICTION AND SLOPE OF BED ON THE PROPAGATION OF WAVES

In the above solution of eq 116, the term $gHi-\lambda U^2/2$ was ignored. If the wave is short, the influence of this term is negligible, as explained in section III–3. For long waves, however, these effects become

appreciable at distances sufficiently removed from the head of the wave. The problem of determining these effects is considered separately for the two cases, (I) $i>0$ and $U_0>0$, and (II) $i=0$ and $U_0=0$. The first case will now be considered.

From eq 52, we have, after neglecting u^2 in comparison with U_0^2,

$$gHi-\frac{\lambda}{2}U^2=gH_0i-\frac{\lambda}{2}U_0^2+ghi-\lambda U_0u. \tag{122}$$

Considering the first two terms of the Taylor expansion of $\lambda=\lambda(H)$ at H_0,

$$\lambda=\lambda_0+\left(\frac{d\lambda}{dH}\right)h, \tag{123}$$

where $\lambda_0=\lambda(H_0)$, and $d\lambda/dH$ is evaluated at $H=H_0$. Replacing λ by the above value, and neglecting the small hu term, eq 122 becomes

$$gHi-\frac{\lambda}{2}U^2=gH_0i-\frac{\lambda_0}{2}U_0^2+ghi-\frac{1}{2}\frac{d\lambda}{dH}hU_0^2-\lambda_0U_0u.$$

From eq 48 we have

$$gH_0i-\frac{\lambda_0}{2}U_0^2=0, \tag{124}$$

that is, in uniform flow the effects of slope and friction are in equilibrium, and thus

$$gHi-\frac{\lambda}{2}U^2=ghi-\frac{1}{2}\frac{d\lambda}{dH}hU_0^2-\lambda_0U_0u.$$

Evaluating $d\lambda/dH$ by means of eq 51 and 124, and introducing the value of u from the first approximation, eq 64, the above equation becomes

$$gHi-\frac{\lambda}{2}U^2=-2(\omega_0-U_0)hf_1, \tag{125}$$

where

$$f_1=\frac{3\omega_0-5U_0}{3U_0(\omega_0-U_0)}gi. \tag{126}$$

Since from eq 112, $d\sigma/dx=\mp h$, eq 125 can be written

$$gHi-\frac{\lambda}{2}U^2=\pm2\omega_0(\omega_0-U_0)\frac{d}{dx}\left(\frac{\sigma f_1}{\omega_0}\right). \tag{127}$$

Substituting this in eq 116, we have

$$\omega=\omega_0\left(1+\frac{2+k_1}{4}\frac{h}{H_0}+\frac{k_2H_0^2}{6h}\frac{\partial^2h}{\partial x^2}\mp\frac{\sigma f_1}{\omega_0h}\right), \tag{128}$$

or introducing the values of k_1 and k_2 from eq 106, and using eq 62

$$\omega-U_0=\pm\left(\sqrt{gH_0}\left(1+\frac{3h}{4H_0}+\frac{H_0^2}{6h}\frac{\partial^2h}{\partial x^2}\right)-\frac{\sigma f_1}{h}\right). \tag{129}$$

This integral of eq 116 is due to Boussinesq [3, p. 451], except that the value of f_1 given above is new, being based on Manning's quadratic law of resistance developed in section III–2.

We now consider the sign of the quantity $\sigma f_1/h$. If the intumescence is everywhere positive or everywhere negative; that is, for all x, $h \geqq 0$ or $h \leqq 0$, then σ has the same sign as h, and σ/h is positive. At the head of the wave this ratio vanishes, since σ is of higher order than h, and it increases toward the rear of the wave. Since f_1 is constant for a given channel and depth of water in uniform flow, the absolute value of the term varies in the manner just described, and its sign is the same as that of f_1. Upon examining eq 126 we find that f_1 is positive if (1) $U_0 > \omega_0$ or (2) $U_0 < \omega_0$ and $3\omega_0 > 5U_0$, and negative if (3) $U_0 < \omega_0$ and $3\omega_0 < 5U_0$. Comparison with eq 62 shows that (1) applies to all descending waves, (2) to descending waves where $U_0^2 < (9/4)gH_0$, (3) to descending waves where $U_0^2 > (9/4)gH_0$. Thus, except in the last case, the combined effect of friction and slope on the damping of the wave is to cause a diminution of the absolute value of the velocity of propagation with respect to the velocity of flow of the various parts of the intumescence, the effect increasing with increasing distance from the head of the wave. The last case is of special interest. It has been shown elsewhere [16] that if $U_0^2 > (9/4)gH_0$, the waves become unstable, a phenomenon which is apparently closely related to the origin of roll waves.

6. DEFORMATION OF A STRAIGHT SLOPING FRONT

We suppose that the wave is descending (fig. 10). Denoting the slope of the front by β, $\beta = -\tan \varphi$. Since we are only considering waves whose profiles lie above the free surface, β is always positive. Denoting, at $t=0$, the position of the front of the wave by x_0, and the value of the slope by β_0, the equation of the wave profile is thus,

$$\begin{aligned} h &= \beta_0(x_0 - x), \quad && x \leqq x_0,\ t=0; \\ h &= 0, && x \geqq x_0,\ t=0. \end{aligned}$$

Equation 112 then becomes

$$\left.\begin{aligned} \sigma &= \frac{\beta_0(x_0-x)^2}{2}, \quad && x \leqq x_0,\ t=0; \\ \sigma &= 0 && x \geqq x_0,\ t=0. \end{aligned}\right\} \tag{130}$$

Introducing the equation for the velocity of propagation of a wave volume element, eq 128, we obtain from the above equations

$$\omega = \omega_0\left[1 + \left(\frac{2+k_1}{4H_0}\beta_0 - \frac{f_1}{2\omega_0}\right)(x_0 - x)\right], \quad x \leqq x_0,\ t=0.$$

If we write

$$\theta_0 = \frac{2+k_1}{4H_0}\omega_0\beta_0 - \frac{f_1}{2}, \tag{131}$$

then the last equation becomes

$$\omega - \omega_0 = \theta_0(x_0 - x), \quad x \leqq x_0,\ t=0. \tag{132}$$

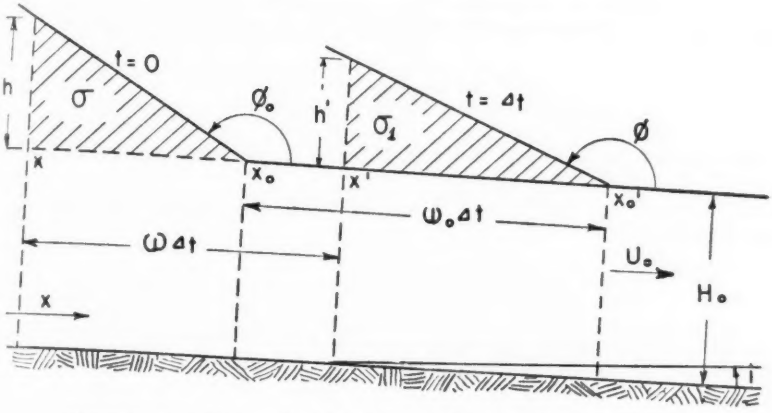

FIGURE 10.—*Deformation of the linear front of a descending wave.*

Now let the position of the front of the wave at $t=\Delta t$ be x_0' (fig. 10). The section which at time $t=0$ had the volume σ in front of it has moved from x to x', and the height has changed from h to h'. Since the wave front moves with the velocity ω_0 (section III–4), while the section at x moves with velocity ω, we have

$$x_0'-x'=(\omega_0-\omega)\Delta t+(x_0-x), \quad x<x_0,\ t=0.$$

Using eq 132, we obtain

$$x_0'-x'=(1-\theta_0\Delta t)(x_0-x), \quad x<x_0,\ t=0. \tag{133}$$

But the volume σ in front of x is equal to the volume σ_1 in front of x', and thus we have from eq 130 and 133

$$\sigma_1=\frac{\beta_0}{2}(x_0'-x')^2(1+2\theta_0\Delta t).$$

Comparison with eq 130 shows that during the time Δt the linear character of the wave front is preserved, but the slope has changed from β_0 to β',

$$\beta'=(1+2\theta_0\Delta t)\beta_0. \tag{134}$$

Putting

$$\beta'=\beta_0+\frac{d\beta}{dt}\Delta t,$$

we have from eq 134

$$\frac{d\beta}{dt}=2\theta_0\beta_0, \quad t=0, \tag{135}$$

which enables us to determine the variation of the slope. Since β_0 is positive, we find that if $\theta_0>0$, the wave is becoming steeper, if $\theta_0=0$, the slope remains constant, if $\theta_0<0$, the wave is flattening out.

It is desirable to translate these conditions into relations involving β_0, i, and λ. Using eq 106, 126, 62, and 48, eq 131 becomes

$$\theta_0=\frac{3}{4}\sqrt{\frac{g}{H_0}}(\beta_0-I), \tag{136}$$

where $I=i\left(\frac{2}{3}\sqrt{\frac{\lambda}{2i}}-\frac{4}{9}\right)$. Since g, H_0, and β_0 are positive, we thus find that if $\beta_0>I$, $\theta_0>0$; if $\beta_0=I$, $\theta_0=0$; and if $\beta_0<I$, $\theta_0<0$. Accordingly, we find that,

$\beta_0>\left(\frac{2}{3}\sqrt{\lambda/2i}-\frac{4}{9}\right)i$, the wave is becoming steeper;

$\beta_0=\left(\frac{2}{3}\sqrt{\lambda/2i}-\frac{4}{9}\right)i$, the slope remains constant;

$\beta_0<\left(\frac{2}{3}\sqrt{\lambda/2i}-\frac{4}{9}\right)i$, the wave is flattening out.

We now derive an expression for β as function of time. Since it has been demonstrated that the wave front conserves its linear character, eq 135 holds for any value of t, and we obtain, using eq 135 and 136 and discarding the subscript which refers to $t=0$,

$$\frac{d\beta}{dt}=\frac{3}{2}\sqrt{\frac{g}{H_0}}(\beta^2-I\beta). \tag{137}$$

The solution of this differential equation for the initial condition $\beta=\beta_0$ at $t=0$ is

$$\beta=\frac{\beta_0 I}{\beta_0-(\beta_0-I)\exp\frac{3}{2}\sqrt{\frac{g}{H_0}}It}. \tag{138}$$

If $I=0$, the solution of eq 137 becomes

$$\beta=\frac{\beta_0}{1-\frac{3}{2}\sqrt{\frac{g}{H_0}}\beta_0 t}, \tag{139}$$

and the slope continually increases.

We next suppose that the wave is ascending (fig. 11). Denoting the slope of the front by β, $\beta=\tan\varphi$. We again suppose that the wave profile lies above the free surface, which makes β positive. Using the same method of reasoning as in the above, we obtain corresponding to eq 135 and 136,

$$\frac{d\beta}{dt}=2\theta_0\beta_0,$$

$$\theta_0=\frac{3}{4}\sqrt{\frac{g}{H_0}}(-J+\beta_0),$$

where

$$J=\left(\frac{2}{3}\sqrt{\frac{\lambda}{2i}}+\frac{4}{9}\right)i.$$

Thus, if $\beta_0 > \left(\frac{2}{3}\sqrt{\frac{\lambda}{2i}}+\frac{4}{9}\right)i$, the wave is becoming steeper;

$\beta_0 = \left(\frac{2}{3}\sqrt{\frac{\lambda}{2i}}+\frac{4}{9}\right)i$, the slope remains constant;

$\beta_0 < \left(\frac{2}{3}\sqrt{\frac{\lambda}{2i}}+\frac{4}{9}\right)i$, the wave is flattening out.

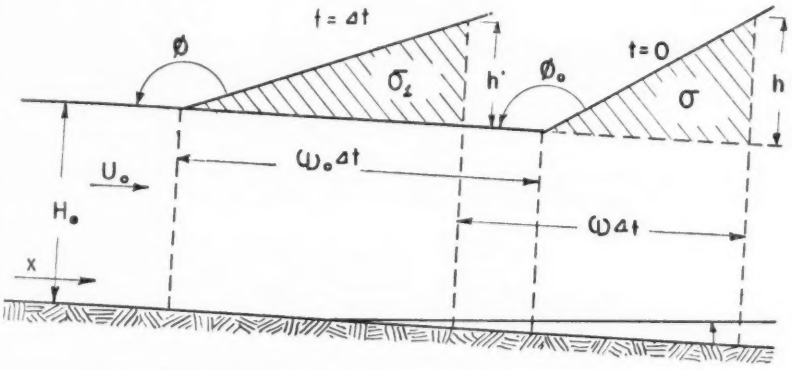

FIGURE 11.—*Deformation of the linear front of an ascending wave.*

The expression for β as function of time, becomes

$$\beta = \frac{\beta_0 J}{\beta_0 - (\beta_0 - J)\exp\frac{3}{2}\sqrt{\frac{g}{H_0}}Jt}, \tag{140}$$

and if $J=0$, which for ascending waves can only be the case if the slope, i, vanishes, the latter reduces again to

$$\beta = \frac{\beta_0}{1-\frac{3}{2}\sqrt{\frac{g}{H_0}}\beta_0 t}, \tag{141}$$

and the slope of the wave is continually increasing.

If it is desired to express β as a function of the distance $x_0'-x_0$ traversed by the wave, this is obtained by introducing $(x_0'-x_0)/\omega_0$ in place of t in the various expressions giving β as a function of t, since the head of wave is traveling with the velocity ω_0.

7. CHANGE OF HEIGHT OF AN ABRUPT WAVE FRONT

In a wave having an abrupt wave front there is a discontinuity of height at the wave front (fig. 12). If for some considerable distance behind the front, the height is constant, the change of height with time, or preferably with the displacement of the front, can be readily determined, using the Boussinesq formula for the velocity of propagation of a volume element.

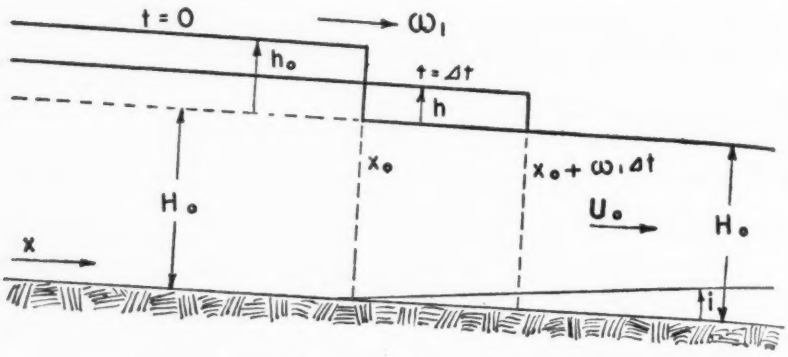

FIGURE 12.—*Deformation of an abrupt wave front*

It is thus assumed that at $t=0$, in the initial portion of the wave, h is constant, and the wave is descending, that is,

$$h=h_0, \quad x \leqq x_0, \; t=0;$$
$$h=0, \quad x \geqq x_0, \; t=0.$$

Since the wave is descending, eq 112 becomes

$$\sigma=h_0(x_0-x), \quad x \leqq x_0, \; t=0;$$

$$\sigma=0, \quad x \geqq x_0, \; t=0.$$

The velocity of propagation of a wave-volume element is thus from eq 128, 106, 62

$$\omega=\omega_0\left[1+\frac{3}{4}\frac{\sqrt{gH_0}}{\omega_0}\frac{h_0}{H_0}+\frac{(x-x_0)f_1}{\omega_0}\right], \quad x \leqq x_0, \; t=0. \tag{142}$$

From this it follows that the velocity of the wave front, ω_1, is

$$\omega_1=\omega_0\left[1+\frac{3}{4}\frac{\sqrt{gH_0}}{\omega_0}\frac{h_0}{H_0}\right], \quad t=0. \tag{143}$$

Since the height is constant behind the wave front, $\partial h/\partial x=0$, and we have

$$\frac{dh}{dt}=\frac{\partial h}{\partial t}, \quad x<x_0, \; t=0, \tag{144}$$

and from eq 113

$$\frac{\partial h}{\partial t}=-h_0\frac{\partial \omega}{\partial x}, \quad x<x_0, \; t=0. \tag{145}$$

Differentiating eq 142 with respect to x, $\partial\omega/\partial x=f_1$, and eq 145 now becomes

$$\frac{dh}{dt}=-f_1h_0, \quad x<x_0, \; t=0. \tag{146}$$

We consider two distinct values of x at $t=0$, both behind the wave front, denoting them by x_1 and x_2, and write $h_1=h(x_1)$, $h_2=h(x_2)$. After an interval of time Δt, let the height of the corresponding wave elements be h_1' and h_2'. Now

$$h_1'-h_1=\frac{dh}{dt}\Delta t=-f_1h_0\Delta t,$$

and

$$h_2'-h_2=\frac{dh}{dt}\Delta t=-f_1h_0\Delta t.$$

Since $h_1=h_2=h_0$, we see that $h_1'=h_2'$. This shows that the constancy of height of the wave front is preserved. Replacing h_0 by h in eq 143, we see that the velocity of the wave front ω_1 is

$$\omega_1=\omega_0\left[1+\frac{3}{4}\frac{\sqrt{gH_0}}{\omega_0}\frac{h}{H_0}\right],\ t=t. \tag{147}$$

Again replacing h_0 by h, eq 146 now becomes

$$\frac{dh}{dt}=-f_1h,\quad x<x_0+\int_0^t\omega_1dt. \tag{148}$$

Integrating this equation, and using the initial condition $h=h_0$ at $t=0$, we obtain h as a function of t

$$h=h_0e^{-f_1t},\quad x<x_0+\int_0^t\omega_1dt. \tag{149}$$

If it is desired to determine h as a function of the distance $x_0'-x_0$ traveled by the wave front, we write from eq 147 and 148

$$\frac{dh}{dx_0'}=\frac{-f_1h}{\omega_0}\left[1-\frac{3}{4}\frac{\sqrt{gH_0}}{\omega_0}\frac{h}{H_0}\right], \tag{150}$$

since $dx_0'/dt=\omega_1$; and $3h\sqrt{gH_0}/4\omega_0H_0$ is required to be small with respect to unity. The solution of this differential equation for the initial condition $h=h_0$, at $x_0'=x_0$ is

$$\frac{h}{h_0}=\frac{1-\frac{3}{4}\frac{\sqrt{gH_0}}{\omega_0}\frac{h}{H_0}}{1-\frac{3}{4}\frac{\sqrt{gH_0}}{\omega_0}\frac{h_0}{H_0}}\exp\left[\frac{f_1(x_0-x_0')}{\omega_0}\right]. \tag{151}$$

8. SOLUTION OF THE WAVE EQUATION WHEN SLOPE AND FRICTION ARE NOT NEGLIGIBLE

The significance of introducing ω, the celerity of a wave-volume element, lies in the fact that the integration of the wave equation, eq 111 becomes equivalent to solving

$$\frac{\partial h}{\partial t}+\frac{\partial}{\partial x}(h\omega)=0, \tag{113}$$

where ω is given by eq 116, or in this particular case by eq 128. Although the general solution is complicated, if it be assumed that $\partial^2 h/\partial x^2$ is negligible, compared to $6h/H_0^2 k_2$, the problem is considerably simplified. This assumption requires that the curvature of the wave profile be small. We thus obtain from eq 129 and eq 62:

$$\omega h = hU_0 + (\omega_0 - U_0)\left(1 + \frac{3h}{4H_0}\right)h \mp \sigma f_1, \tag{152}$$

and eq 113 becomes

$$\frac{\partial h}{\partial t} + \left[U_0 + (\omega_0 - U_0)\left(1 + \frac{3h}{2H_0}\right)\right]\frac{\partial h}{\partial x} = -hf_1, \tag{153}$$

since $\partial\sigma/\partial x = \mp \dot{h}$. The general solution of this differential equation is

$$x = \left(\omega_0 + (\omega_0 - U_0)\frac{3h}{2H_0}\,\frac{e^{tf_1} - 1}{tf_1}\right)t + \Phi(he^{tf_1}), \tag{154}$$

where Φ is an arbitrary function. This integral is due to Boussinesq [3, p. 457, eq 392] and Favre speaks of it as one of the Boussinesq integrals [6, p. 106].

In determining the arbitrary function Φ, two cases are of particular interest; (1) the channel is infinite in both directions, and (2) the channel has an entrance and is infinite in only one direction. In the first case, if for $t=0$, h is a known function of x, $-\infty < x < \infty$, then Φ can be obtained directly. Let the function be $h=\Psi(x)$, $t=0$. Putting $t=0$ in eq 154, we have $x=\Phi(h)$, $t=0$, hence in this case Φ is simply the inverse of Ψ. In the second case, Φ is determined from the boundary condition $h=\psi(t)$ at the channel entrance $x=0$, but in this case the evaluation is indirect and tedious. At $x=0$, eq 154 gives

$$\Phi(he^{f_1 t}) = -\left[\omega_0 + (\omega_0 - U_0)\frac{3h}{2H_0}\,\frac{\exp(f_1 t - 1)}{f_1 t}\right]t. \tag{155}$$

In general, the form of the equation does not permit solving explicitly for either t or h, hence it is necessary to evaluate Φ numerically. By considering values of t in the range $-\infty$ to $+\infty$, and the corresponding values of h at the entrance, using $h=\psi(t)$, the magnitude of the independent variable can be computed. Corresponding values of Φ are obtained from the right-hand member of eq 155 by inserting the same values of h and t used to evaluate he^{tf_1}.

9. INTUMESCENCES PRODUCED BY OPERATING LOCKS IN A CANAL CARRYING WATER

We now consider a practical example of case (2) above which can be treated by a simpler method. In many cases the canals leading to and from hydroelectric plants are also used for navigation, and a lock is provided to bridge the difference in head utilized by the plant. Whenever this lock is emptied, a positive wave is produced in the downstream canal, and, whenever it is filled, a negative wave is produced in the upstream canal. The former, of course, travels downstream, whereas the latter travels upstream.

Because of such design considerations as the possibility of overtopping the embankments, it is desirable to predict by computation the magnitude and deformation of these waves. Ordinarily the discharge from the lock is a continuous function of time, the exact relation being obtained from computation or model experiments. The waves produced by operating the lock are small in height and long enough so that the curvature is negligible, and thus eq 154 is applicable.

As far as this analysis is concerned, the lock constitutes a termination of the canal, and the boundary conditions of case (2) apply. The complications of this case are eliminated by a method due to Favre [6, p. 112], which is based on the fact that the distance traveled by the wave is very large compared to its length. The initial shape of the wave is computed for the initial time $t=0$, in the form $h=\Psi(x)$, assuming that the effect of friction is negligible during the short time interval required for the formation of the wave. This function is then used to determine Φ.

Let the discharge at the lock per unit width of channel be represented by the function

$$q=f(t),\ x=0. \tag{156}$$

As a result of the above, we may also write

$$t=F(q),\ x=0. \tag{157}$$

It follows from eq 154 that the form of the wave at the moment it is produced and shortly thereafter, neglecting the effect of friction during the genesis of the wave, is represented by

$$x=\left[\omega_0+(\omega_0-U_0)\frac{3h}{2H_0}\right]t+\Phi(h), \tag{158}$$

since $\underset{tf_1\to 0}{\text{Lim}}\dfrac{\exp(f_1t-1)}{tf_1}=1$. From eq 52 and 117 the mean velocity in a cross section beneath the wave is

$$U=U_0+\frac{\omega-U_0}{H_0+h}h. \tag{159}$$

Neglecting the effects of friction and curvature in eq 129, this becomes, using eq 62

$$U=U_0+(\omega_0-U_0)\left(1+\frac{3h}{4H_0}\right)\frac{h}{H_0+h}. \tag{160}$$

The discharge per unit width at $x=0$ is thus

$$q=HU=U_0(H_0+h)+(\omega-U_0)\left(1+\frac{3h}{4H_0}\right)h=f(t),\ x=0.$$

Comparing this equation with eq 157 we have

$$t=F(U_0(H_0+h)+(\omega_0-U_0)\left(1+\frac{3h}{4H_0}\right)h),\ x=0, \tag{161}$$

which expresses h as a function of t for $x=0$, and thus serves to determine the arbitrary function Φ in eq 158. Placing $x=0$ in that equation, we have

$$\Phi(h)=-\left[\omega_0+(\omega_0-U_0)\frac{3h}{2H_0}\right]t, \tag{162}$$

and from eq 161

$$\Phi(h)=-\left[\omega_0+(\omega_0-U_0)\frac{3h}{2H_0}\right]F(U_0(H_0+h)+(\omega_0-U_0)\left(1+\frac{3h}{4H_0}\right)h). \tag{163}$$

Since the function Φ in eq 158 is the same as the function Φ in eq 154, we write for the second term in the right-hand member of this equation,

$$\Phi(he^{f_1t})=-\left[\omega_0+(\omega_0-U_0)\frac{3he^{f_1t}}{2H_0}\right]F(U_0(H_0+he^{f_1t}) + (\omega_0-U_0)\left(1+\frac{3he^{f_1t}}{4H_0}\right)he^{f_1t}). \tag{164}$$

The solution of a typical problem will now be described in detail. It is desired to find the wave profile in the canal at any instant t when the discharge is given as a function of time, $Q/b=q=f(t)$, b being the width of the free surface of the canal. We shall assume that the discharge first increases and then decreases, as shown in figure 13. This will create a positive surge in the discharge canal and a negative surge in the supply canal. The origin in figure 13 is conveniently chosen to correspond to the instant of maximum discharge. The abscissa t is, of course, expressed in seconds, and the ordinate, q, in any convenient unit of discharge per unit width, such as square feet per second. In eq 154 and 164, upon which the solution depends, U_0 and ω_0 will have to be expressed in corresponding units of velocity, such as feet per second.

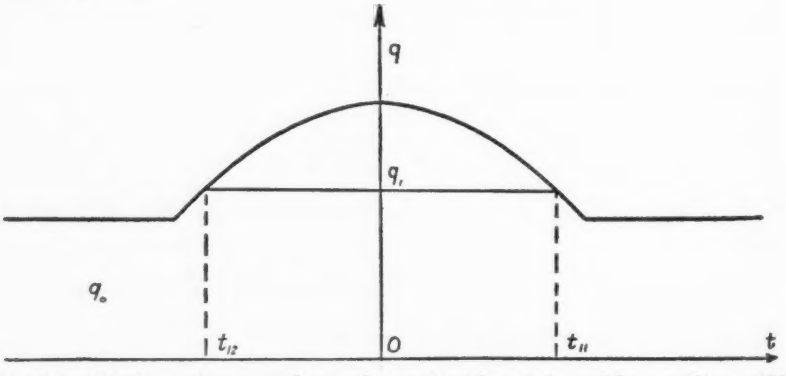

FIG. 13.—*Discharge from supply canal as a function of time: $Q/b=q=f(t)$, eq 156, or $t=F(q)$, eq 157.*

The positive surge in the discharge canal will now be considered. The quantities U_0, H_0, R_0 and i are determined from measurements of the steady flow. The coefficient of friction, λ_0, is then determined from eq 48. All the quantities needed to determine ω_0 from eq 62, and f_1 from eq 126 are thus available. Note that the positive sign in eq 62

is selected, since the wave will be moving downstream. A small positive value of h is now selected, which we shall denote as h_1. The argument of the function F in eq 164 is computed, using the value of t corresponding to the instant for which the wave profile is desired. As is seen from eq 157, this gives a corresponding value of q, which we shall call q_1. If q_1 is greater than the maximum value of q which is actually obtained, this signifies that h_1 was higher than any point of the intumescence. It will be advisable to select h_1 very small at first and then increase it until the top of the curve in figure 13 is attained. The values of t corresponding to h_1 will be denoted by t_{11} and t_{12} since, there will generally be two of these, the first positive and the second negative. This is clearly indicated in figure 13. These two values, t_{11} and t_{12}, are thus the desired values of the function F occurring in eq 164, and the two values of the double-valued function Φ can now be obtained by replacing h in the coefficient of F by the quantity h_1. Turning now to eq 154, replacing h by h_1 and t by the value corresponding to the instant for which the wave profile is desired, we obtain two values for x, corresponding to the original value h_1, which we shall denote by x_{11} and x_{12}. These are the abscissas of the points on the profile having the height h_1 (see fig. 14). The whole process is repeated for greater heights, h_2, h_3, . . . , until sufficient points are determined to establish the contour of the wave.

The process for determining the negative surge in the supply channel is exactly the same, except that in eq 62 the minus sign is chosen, since the wave is traveling upstream. The quantities h_1, ... and x_{11}, x_{12}, . . . , will be negative, as shown in figure 15.

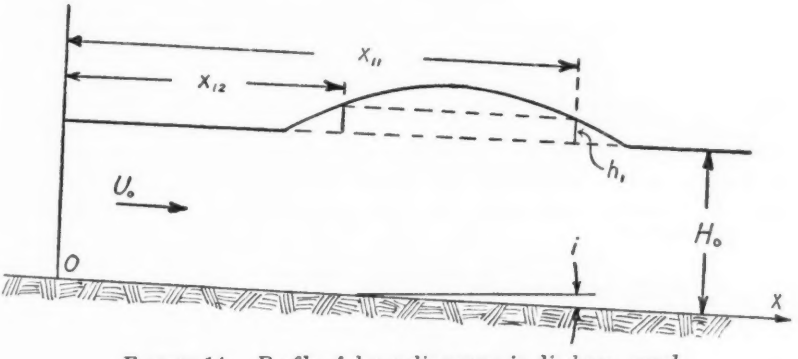

FIGURE 14.—*Profile of descending wave in discharge canal.*

10. EFFECT OF FRICTION ON WAVES WHEN THE SLOPE OF THE BED VANISHES

We now consider case (II) of section IV–5, $i=0$ and $U_0=0$. The determination of the positive sense of the x-axis on the basis of the conventions in section III–1 fails, since there is no flow. Furthermore, the terms "ascending" and "descending" waves explained in section III–3 fail to have any significance, since we have no method of distinguishing the upstream from the downstream direction. We thus are forced to make an arbitrary choice of the positive x-direction, and consider downstream to be in this direction. A descending wave thus

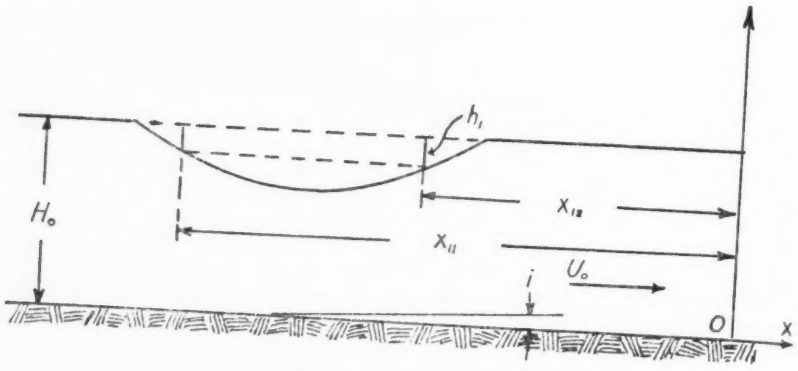

FIGURE 15.—*Profile of ascending wave in supply canal.*

becomes one for which $\omega_0>0$, and an ascending wave one for which $\omega_0<0$, that is to say, a descending wave is propagated in the positive x-direction, and an ascending wave is propagated in the opposite direction, since our hypothetical observer is stationary and the downstream direction coincides with the arbitrarily chosen positive sense of the x-axis.

Since $i=0$ and $U_0=0$, it follows immediately from eq 52 that

$$gHi-\frac{\lambda}{2}U^2=-\frac{\lambda}{2}u^2. \tag{165}$$

It has previously been tacitly assumed that U was always positive, that is, u was smaller than U_0, so that U and U_0 had the same sign. Since in this case $U_0=0$, this assumption is no longer valid. The sense of the friction is always opposite to that of the velocity, and thus if u is negative, the sign of the right-hand member of the above equation must be changed, since we wish to keep λ positive, regardless of the sign of τ_0. From the first approximation, eq 64, $u=\omega_0 h/H_0$, and thus the velocity must have the same sign as $\omega_0 h$. We introduce the new parameter

$$\left.\begin{aligned} f_2&=\frac{\lambda_0}{4}, \text{ if } \omega_0 h>0;\\ f_2&=-\frac{\lambda_0}{4}, \text{ if } \omega_0 h<0; \end{aligned}\right\} \tag{166}$$

and obtain from eq 165

$$gHi-\frac{\lambda}{2}U^2=-2\omega_0^2\left(\frac{h}{H_0}\right)^2 f_2. \tag{167}$$

The difference between $\lambda_0 u^2$ and λu^2 is a quantity of the order being neglected in this analysis. If we introduce the quantity

$$\sigma'=\pm\int_x^{\pm\infty} h^2 dx, \tag{168}$$

then since $d\sigma'/dx = \mp h^2$, we can write eq 167 in the form

$$gHi - \frac{\lambda}{2}U^2 = \pm 2\omega_0^2 f_2 \frac{d}{dx}\left(\frac{\sigma'}{H_0^2}\right). \tag{169}$$

Substituting this in eq 116, we have for the velocity of propagation of a volume element

$$\omega = \omega_0\left(1 + \frac{2+k_1}{4}\frac{h}{H_0} + \frac{k_2 H_0^2}{6h}\frac{\partial^2 h}{\partial x^2} \mp \frac{\omega_0}{\omega_0 - U_0}\frac{\sigma' f_2}{hH_0^2}\right). \tag{170}$$

Since in this case $U_0 = 0$, we see from eq 106 that $k_1 = k_2 = 1$, and thus

$$\omega = \omega_0\left(1 + \frac{3h}{4H_0} + \frac{H_0^2}{6h}\frac{\partial^2 h}{\partial x^2} \mp \frac{\sigma' f_2}{hH_0^2}\right). \tag{171}$$

Consider the sign of $\omega_0\sigma' f_2/hH_0^2$, which equals $\omega_0^2\sigma' f_2/\omega_0 h H_0^2$. Since from eq 168, σ' is always positive, it follows that the sign of the above is the same as that of $f_2/\omega_0 h$. But from eq 166 f_2 has the same sign as $\omega_0 h$, hence the original term is always positive. In accordance with the convention of choice of signs for descending and ascending waves, the choice in eq 171 is always opposite to that of the sign of ω_0. Therefore, the effect of friction on the celerity ω when $i = 0$, $U_0 = 0$, is to diminish its absolute value by an amount which increases with the distance from the head of the wave.

11. SOLUTION OF THE WAVE EQUATION WHEN THE SLOPE VANISHES BUT FRICTION IS CONSIDERED

As in section IV–3, the problem is to solve

$$\frac{\partial h}{\partial t} + \frac{\partial}{\partial x}(h\omega) = 0, \tag{113}$$

where ω is given by eq 116 or, in this particular case, by eq 171. For the reasons mentioned in the same section, we assume that $\partial^2 h/\partial x^2$ is negligible. Equations 171 and 113 thus become

$$\omega = \omega_0\left(1 + \frac{3h}{4H_0} \mp \frac{\sigma' f_2}{hH_0^2}\right), \tag{172}$$

and

$$\frac{\partial h}{\partial t} + \omega_0\left(1 + \frac{3h}{2H_0}\right)\frac{\partial h}{\partial x} = -f_2\omega_0\left(\frac{h}{H_0}\right)^2, \tag{173}$$

respectively, since $d\sigma'/dx = \mp h^2$. Assuming that the wave is everywhere positive or everywhere negative, then f_2 is constant, and the general integral of the above differential equation is

$$x = \omega_0\left[1 + \frac{3h}{2H_0}\frac{\log\left(1 - \frac{f_2\omega_0}{H_0^2}ht\right)}{-\frac{f_2\omega_0}{H_0^2}ht}\right]t + \Phi\left[\frac{h}{1 - \frac{f_2\omega_0}{H_0^2}ht}\right], \tag{174}$$

where Φ is an arbitrary function. This is Boussinesq's second integral [3, p. 454 eq 393].

Regarding the determination of this arbitrary function, we consider the same two cases as in section IV–8: (1) the channel is infinite in

both directions, and (2) the channel has an entrance which is infinite in only one direction. In the first case, if for $t=0$, h is a known function of x, $-\infty<x<\infty$, then Φ can be obtained directly. Let the function be $h=\Psi(x)$, $t=0$. Putting $t=0$ in eq 174 we have $x=\Phi(h)$, $t=0$, hence in this case Φ is simply the inverse of Ψ. In the second case, Φ is determined from the boundary condition $h=\psi(t)$ at the channel entrance $x=0$; but in this case the evaluation is indirect and tedious. At $x=0$, eq 174 gives

$$\Phi\left(\frac{h}{1-\frac{f_2\omega_0}{H_0^2}ht}\right)=-\omega_0\left[1+\frac{3h}{2H_0}\frac{\log\left(1-\frac{f_2\omega_0}{H_0^2}ht\right)}{-\frac{f_2\omega_0}{H_0^2}ht}\right]t. \tag{175}$$

In general, the form of the equation does not permit solving explicitly for either t or h, hence it is necessary to evaluate Φ numerically. By considering values of t in the range $-\infty$ to $+\infty$, and the corresponding value of h at the entrance, using $h=\psi(t)$, the magnitude of the independent variable can be computed. Corresponding values of Φ are obtained from the right-hand member of eq 175 by inserting the same values of h and t used to evaluate

$$\frac{h}{1-\frac{f_2\omega_0}{H_0^2}ht}.$$

These methods are precisely analogous to those discussed in connection with eq 155.

12. INTUMESCENCE PRODUCED BY OPERATING LOCKS IN AN ORDINARY CANAL

In contrast to canalized rivers and hydroelectric canals, such as discussed in section IV–9, ordinary canals contain still water except when disturbances are set up by the operation of the locks. The general considerations at the beginning of section IV–9 (through eq 157) also apply to this case, except that $i=0$ and $U_0=0$, and hence we must consider case (2) of eq 174.

The discharge per unit width at the lock is again represented by

$$q=f(t), \quad x=0, \tag{156}$$

or by the inverse function

$$t=F(q), \quad x=0. \tag{157}$$

Neglecting the effect of friction during the formation of the wave and shortly thereafter, we obtain from eq 174

$$x=\omega_0\left(1+\frac{3h}{2H_0}\right)t+\Phi(h), \tag{176}$$

since

$$\lim_{t\to 0}\frac{\log\left(1-\frac{f_2\omega_0}{H_0^2}ht\right)}{-\frac{f_2\omega_0}{H_0^2}ht}=1.$$

For the mean velocity in a cross section beneath the wave, eq 52, 117, 171 give

$$U=\omega_0\left(1+\frac{3h}{4H_0}\right)\frac{h}{H_0+h}, \tag{177}$$

since $U_0=0$, and friction and curvature are neglected. The discharge per unit width at $x=0$ is, therefore,

$$q=HU=\omega_0 h\left(1+\frac{3h}{4H_0}\right),\ x=0. \tag{178}$$

Substituting this value of q in eq 157, we obtain

$$t=F\left(\omega_0 h\left(1+\frac{3h}{4H_0}\right)\right),\ x=0. \tag{179}$$

But from eq 176

$$\Phi(h)=-\omega_0\left(1+\frac{3h}{2H_0}\right)t,\ x=0, \tag{180}$$

or from eq 179

$$\Phi(h)=-\omega_0\left(1+\frac{3h}{2H_0}\right)F\left(\omega_0 h\left(1+\frac{3h}{4H_0}\right)\right). \tag{181}$$

Since this function Φ in eq 176 is the same as the function Φ in eq 174, we have for the right-hand member of this equation,

$$\Phi\left(\frac{h}{1-\frac{f_2\omega_0}{H_0^2}ht}\right)=-\omega_0\left[1+\frac{3h}{2H_0\left(1-\frac{f_2\omega_0}{H_0^2}ht\right)}\right] F\left(\frac{\omega_0 h}{1-\frac{f_2\omega_0}{H_0^2}ht}\left[1+\frac{3h}{4H_0\left(1-\frac{f_2\omega_0}{H_0^2}ht\right)}\right]\right). \tag{182}$$

Equations 174 and 182 are used to determine the wave profile at any instant t, as is described in section IV–9.

13. LIMITATIONS OF BOUSSINESQ SOLUTIONS

It is necessary to emphasize the fact that the second-order theory, which is based on the concept of the velocity of propagation, ω, of a volume element, is subject to certain important restrictions. The most general expression for ω is given in eq 116. In deriving this equation, the important assumption was made that ω/ω_0 is nearly equal to unity.

We shall now turn our attention to the specialized equations derived from eq 116. These are eq 118, 128, 171. Examination shows that in each case, $\omega/\omega_0=1+$(correction terms). The restriction on the theory thus requires that these terms shall be small compared to unity. The first term, which is common to all equations, is $(2+k_1)h/4H_0$. This merely requires that $h\ll 4H_0/(2+k_1)$. The second term, which expresses the effect of curvature, requires that $(\partial^2 h/\partial x^2)/h \ll 6/H_0^2 k_2$. We see from this, that $(\partial^2 h/\partial x^2)$ must vanish to a higher order than h.

The third term, which appears only in eq 128 and 171, expresses the effect of friction. These two equations are applicable only when

$\sigma f_1/\omega_0 h$ or $\sigma' f_2/hH_0^2$, respectively, is small. But σ and σ' can be made as large as we please merely by considering longer and longer intumescences, and if the intumescence has a finite volume, h approaches zero at the tail whereas σ and σ' remain finite. This shows that the term under consideration may be large, or even infinite. In view of this fact, it may be expected that these solutions will give correct values only in the frontal portion of the wave where σ/h and σ'/h are small. It should be noted that this remark applies with equal force to the Boussinesq integrals, eq 154 and 174.

V. REFERENCES

[1] G. H. Keulegan and G. W. Patterson, *Mathematical theory of irrotational translation waves*, J. Research NBS **24,** 47 (1940) RP1272.
[2] H. Bazin, *Recherches experimentales sur la propagation des ondes*, Mém. divers Savants a L'Acad. des Sci. **19,** 495 (1865).
[3] J. Boussinesq, *Essai sur la théorie des eaux courantes.* Mém. divers Savants a L'Acad. des Sci. **23,** 1, (1877).
[4] R. E. Horton, Channel Waves Subject Chiefly to Momentum Control, U. S. Department of Agriculture, Soil Conservation Service Technical Publication 16, (mimeographed, 1938).
[5] G. H. Keulegan, *Laws of turbulent flow in open channels.* J. Research NBS **21,** 707 (1938) RP1151.
[6] H. Favre, Étude Théorique et Expérimentale des Ondes de Translation dans les Canaux Découverts (Dunod, Paris, 1935).
[7] O. Reynolds, *On the dynamical theory of incompressible viscous fluids and the determination of the criterion.* Phil. Trans. [A] **186,** 123 (1895).
[8] H. Lamb, Hydrodynamics, [ed. 5] (Cambridge University Press, Cambridge, England, 1924).
[9] H. L. Dryden, F. D. Murnaghan, H. Bateman, *Report of the committee on hydrodynamics,* Bul. National Research Council, No. 84 (1922).
[10] S. Goldstein, ed., Modern Developments in Fluid Dynamics, **1,** (Oxford University Press, Oxford, England, 1938).
[11] H. Rouse, Fluid Mechanics for Hydraulic Engineers (McGraw-Hill Book Co., Inc., New York, N. Y., 1938).
[12] G. H. Keulegan, *Equation of motion for the steady mean flow of water in open channels,* J. Research NBS **29,** 97 (1942) RP1488.
[13] J. Hadamard, Leçons sur la Propagation des Ondes et les Équations de l'Hydrodynamique (Librarie Scientifique A. Hermann, Paris, 1903).
[14] J. Nikuradse, Strömungsgesetze in rauhen Rohren (Verein Deutscher Ingenieure, Forschungsheft 361, 1933).
[15] H. Bazin, *Experiences sur la propagation des ondes le long d'un cours d'eaux torrenteux . . .,* Compt. rend. **100,** 1492 (1885).
[16] G. H. Keulegan and G. W. Patterson, *A criterion for instability of flow in steep channels,* Trans. Am. Geophys. Union, part II, 594, (1940).

WASHINGTON, March 1, 1943.

INDEX TO VOLUME 30

A

Page

Abbe-type refractometer, use, RP1535 311
Acetate, cellulose, mechanical properties, RP1513 1
Acetic acid, dissociation constant, RP1537 347
Acree, S. F., Roger G. Bates, pH values of certain phosphate-chloride mixtures, and the second dissociation constant of phosphoric acid from 0° to 60° C, RP1524 129
——, *Roger G. Bates, Gerda L. Siegel*, Dissociation constants and pH-titration curves at constant ionic strength from electrometric titrations in cells without liquid junction: Titrations of formic acid and acetic acid, RP1537 347
Alkali-treated wool, nature of reaction, RP1516 47
Alloys, copper, thermal expansion, RP1518 75
Alumina in the system CaO–Al_2O_3–H_2O, RP1539 367

B

Bates, Roger G., S. F. Acree, pH values of certain phosphate-chloride mixtures, and the second dissociation constant of phosphoric acid from 0° to 60° C, RP1524 129
——, *Gerda L. Siegel, S. F. Acree*, Dissociation constants and pH-titration curves at constant ionic strength from electrometric titrations in cells without liquid junction: Titrations of formic acid and acetic acid, RP1537 347
Beater practice in manufacture of offset papers, RP1532 267
Bishop, Dana L., Function of carbon dioxide in producing efflorescence on plaster and cement products, RP1538 361
Blaine, Raymond L., Edwin S. Newman, Charles H. Jumper, George L. Kalousek, Effects of added materials on some properties of hydrating portland cement clinkers, RP1533 281
Blair, Mary Grace, Peter Hidnert, Thermal expansivity and density of indium, RP1541 427
Blankets, properties:
RP1528 203
RP1529 209
Blanket-sheet combination for outdoor use, RP1529 209
Bronzes, thermal expansion, RP1518 75
Buffers of phosphate and chloride, pH values, RP1524 129

C

Calcium aluminate hydrates, occurrence in system CaO–Al_2O_3–H_2O, RP1539 367
Carbohydrases, classification of, RP1531 257
Carbohydrates, enzymes hydrolyzing, RP1531 257
Carbon dioxide, function in producing efflorescence in plastic and cement products, RP1538 361
Carius combustion tube, bursting pressures, RP1521 107
Carson, F. T., Vernon Worthington, Measuring the degree of curl of paper, RP1522 113
Cellulose acetate, mechanical properties, RP1513 1
Cement and plaster products, efflorescence on, RP1538 361
Cement, portland, clinker pastes, composition and physical properties:
RP1530 215
RP1533 281
Channel slope and turbulence, effect on translation waves, RP1544 461
Clarke W. F., Lansing S. Wells, H. F. Mc Murdie, Study of the system CaO–Al_2O_3–H_2O at temperatures of 21° and 90° C., RP1539 367
Classification of carbohydrases, RP1531 257
Coblentz, W. W., R. Stair, Measurements of ultraviolet solar radiation in Washington, 1936 to 1942, RP1542 434
Columns, steel, compressive properties of cover plates for:
RP1514 15
RP1527 177
RP1540 411
Combustion tubes, glass, bursting pressures, RP1521 107
Copper-base alloys, thermal expansion, RP1518 75
Corliss, Charles H., Bourdon F. Scribner, An improved electrode holder for spectrographic analysis, RP1515 41
Counter, miniature Geiger-Müller, RP1525 157
Cover plates for steel columns, perforated:
RP1514 15
RP1527 177
RP1540 411
Curl of paper, RP1522 113
Curtiss, Leon F., Miniature Geiger-Müller counter, RP1525 157

D

Density of indium, RP1541 427
Density of titanium, RP1520 101
Dissociation constants of formic and acetic acids from electrometric titrations, RP1537 347
Dissociation constant of phosphoric acid, second, RP1524 129

E

Efflorescence on plastic and cement products, RP1538 361
Elastic constants of steel columns:
RP1514 15
RP1527 177
RP1540 411
Electrode holder for spectrographic analysis, RP1515 41
Electrometric titrations in cells without liquid junction, RP1537 347
Elements, hydrolytic behavior, RP1519 89
Expansion, thermal, of indium, RP1541 427
Expansion, thermal, of some bronzes, RP1518 75
Expansion, thermal, of titanium, RP1520 101

F

Fire-clay mortars, heat-setting, RP1534 303
Formic acid, dissociation constant, RP1537 347
Fugitt, Charles H., Jacinto Steinhardt, Milton Harris, Combination of wool protein with weak acids, RP1523 123
Fungi, enzymes from, RP1526 159

G

Geiger-Müller counter, hypodermic needle type, RP1525 157
Gibbsite, occurrence of in the system CaO–Al_2O_3–H_2O, RP1539 367
Gilchrist, Raleigh, Analytical separations by means of controlled hydrolytic precipitation, RP1519 89
Glass tubes, bursting pressures, RP1521 107
Gordon, Charles L., Modification of the Carius combustion tube to minimize losses by explosion: Pressures attained on heating nitric acid to 300° C., RP1521 107
Greenspan, Martin, Ambrose H. Stang, Perforated cover plates for steel columns: Compressive properties of plates having ovaloid perforations and a width-to-thickness ratio of 53, RP1514 15
——, ——, Perforated cover plates for steel columns: Compressive properties of plates having circular perforations and a width-to-thickness ratio of 53, RP1527 177
——, ——, Perforated cover for steel columns: Compressive properties of plates having a net-to-gross cross-sectional-area ratio of 0.33, RP1540 411

H

Harris, Milton, Arnold M. Sookne, Mechanical properties of cellulose acetate as related to molecular chain length, RP1513 1

Page

Harris' Milton, Louis R. Mizell, Nature of the reaction of wool with alkali, RP1516 47
——, *Jacinto Steinhardt, Charles H. Fugitt*, Combination of wool protein with weak acids, RP1523 123
Heindl, Raymond A., William L. Pendergast, Some properties of heat-setting refractory mortars, RP1534 303
Hidnert, Peter, Thermal expansion of some bronzes, RP1518 75
——, Thermal expansion of titanium, RP1520 .. 101
——, *MaryGrace Blair*, Thermal expansivity and density of indium, RP1541 427
Hydrolytic precipitation, analytical separations by, RP1519 89
Hydroxides, precipitation, RP1519 89

I

Index of refraction, measurement, RP1535 311
Indium, thermal expansivity and density, RP1541 427
Enzymatic hydrolysis of sucrose and inulin, RP1526 159
Inulin, hydrolysis by enzymes, RP1526 159
Invertases, action on inulin, RP1526 159
Ionization constant of phosphoric acid, second, RP1524 129

J

Jumper, C. H., George L. Kalousek, J. J. Tregoning, Composition and physical properties of aqueous extracts from portland cement clinker pastes containing added materials, RP1530 215
——, *Edwin S. Newman, Raymond L. Blaine, George L. Kalousek*, Effects of added materials on some properties of hydrating portland cement clinkers, RP1533 281

K

Kalousek, George L., C. H. Jumper, J. J. Tregoning, Composition and physical properties of aqueous extracts from portland cement clinker pastes containing added materials, RP1530 215
——, *Edwin S. Newman, Raymond L. Blaine, Charles H. Jumper*, Effects of added materials on some properties of hydrating portland cement clinkers, RP1533 281
Keulegan, Garbis H., George W. Patterson, Effect of turbulence and channel slope on translation waves, RP1544 461

L

Lamp, tungsten-in-quartz, applications in photoelectric radiometry, RP1543 449
Laundering, effect on blankets:
RP1528 203
RP1529 209
Launer, Herbert F., William K. Wilson, Photochemical stability of papers, RP1517 55
Levulose, preparation by enzymic hydrolysis, RP1526 159
Light stability of papers, RP1517 55
Lime, aluminate hydrates of, and hydrate of, in the system CaO–Al_2O_3–H_2O, RP1539 367

M

McMurdie, H. F., Lansing S. Wells, W. F. Clarke, Study of the system CaO–Al_2O_3–H_2O at temperatures of 21° and 90° C, RP1539 367
Mizell, Louis R., Milton Harris, Nature of the reaction of wool with alkali, RP1516 47
——, *Herbert F. Schiefer, F. T. Mosedale*, Part-wool blankets for use in barracks, RP1528 203
Molecular chain length as related to the mechanical properties of cellulose, RP1513 1
Mortars, refractory, heat-setting, RP1534 303
Mosedale, F. T., Herbert F. Schiefer, Louis R. Mizell, Part-wool blankets for use in barracks, RP1528 203

N

Page

Newman, Edwin S., Raymond L. Blaine, Charles H. Jumper, George L. Kalousek, Effects of added materials on some properties of hydrating portland cement clinkers, RP1533 281
Nitric acid, pressure of, RP1521 107

O

Offset papers, beater practice in manufacture, RP1532 267
O'Leary, Martin, J., Charles G. Weber, Merle B. Shaw, Further experimental study of beater practice in the manufacture of offset papers, RP1532 267

P

Paper, curl of RP1522 113
Papers, offset, beater practice in manufacture, RP1532 267
Papers, photochemical stability, RP1517 55
Patterson, George W., Garbis H. Keulegan, Effect of turbulence and channel slope on translation waves, RP1544 461
Pendergast, William L., Raymond A. Heindl, Some properties of heat-setting refractory mortars, RP1534 303
Perforated cover plates for steel columns:
RP1514 15
RP1527 177
RP1540 411
pH standards composed of phosphate salts, values of, RP1524 129
pH titration curves of formic and acetic acids, RP1537 347
Phase equilibria in the system CaO–Al_2O_3–H_2O, RP1539 367
Phosphate-chloride mixtures, pH values, RP-1524 129
Phosphoric acids, second dissociation constant, RP1524 129
Photochemical stability of papers, RP1517 55
Pigman, William Ward, Occurence of sucrose and inulin-hydrolyzing enzymes in commercial enzyme preparations, RP1526 159
——, Classification of carbohydrases, RP1531 ... 257
Plaster and cement products, efflorescence on, RP1538 361
Poisson's ratio (steel):
RP1514 15
RP1527 177
RP1540 411
Portland cement clinker, nature of prismatic dark interstitial material in, RP1536 329
Portland cement clinker pastes, composition and physical properties:
RP1530 215
RP1533 281
Prismatic dark interstitial material in portland cement clinker, nature, RP1536 329
Proteins, combination of wool with weak acids, RP1523 123

R

Radiation, ultraviolet solar, RP1542 434
Radiometry, photoelectric, applications of tungsten-in-quartz lamp in, RP1543 449
Refractive index, measurement, RP1535 311
Refractometry, sources of error in, RP1535 311

S

Schiefer, Herbert F., Louis R. Mizell, F. T. Mosedale, Part-wool blankets for use in barracks, RP1528 203
——, Advantages of a blanket-and-sheet combination for outdoor use, RP1529 209
Scribner, Bourdon, F., Charles H. Corliss, An improved electrode holder for spectrographic analysis, RP1515 41
Shaw, Merle B., Charles G. Weber, Martin J. O'Leary, Further experimental study of beater practice in the manufacture of offset papers, RP1532 267
Sheet-blanket combination for outdoor use, RP1529 209

Page

Siegel, Gerda L., Roger G. Bates, S. F. Acree, Dissociation constants and pH-titration curves at constant ionic strength from electrometric titrations in cells without liquid junction: Titrations of formic acid and acetic acid, RP1537 347

Smith, Wm. O. R. Stair, A tungsten-in-quartz lamp and its applications in photoelectric radiometry, RP1543 449

Solar radiation, ultraviolet, RP1542 434

Sookne, Arnold M., Milton Harris, Mechanical properties of cellulose acetate as related to molecular chain length, RP1513 1

Spectrographic analysis, electrode holder, RP1515 41

Stair, R., W. W. Coblentz, Measurements of ultraviolet radiation in Washington, 1936 to 1942, RP1542 434

——, *Wm. O. Smith,* A tungsten-in-quartz lamp and its applications in photoelectric radiometry, RP1543 449

Stang, Ambrose H., Martin Greenspan, Perforated cover plates for steel columns: Compressive properties of plates have ovaloid perforations and a width-to-thickness ratio of 53, RP1514 15

——, ——, Perforated cover plates for steel columns: Compressive properties of plates having circular perforations and a width-to-thickness ratio of 53, RP1527 177

——, ——, Perforated cover plates for steel columns: Compressive properties of plates having a net-to-gross cross-sectional-area ratio of 0.33, RP1540 411

Steel columns, perforated, mechanical properties of cover plates for:
RP1514 15
RP1527 177
RP1540 411

Steinhardt, Jacinto, Charles H. Fugitt, Milton Harris, Combination of wool protein with weak acids, RP1523 123

Stresses, distribution in steel columns, graphical presentation:
RP1514 15
RP1527 177
RP1540 411

Sucrose, hydrolysis by enzymes, RP1526 159

T

Taylor, William C., Nature of the prismatic dark interstitial material in portland cement clinker, RP1536 329

Page

Thermal expansion of indium, RP1541 427

Thermal expansion of some bronzes, RP1518 75

Thermal expansion of titanium, RP1520 101

Thermal transmission of blankets:
RP1528 203
RP1529 209

Tilton, Leroy W., Sources of error in precise refractometry, RP1535 311

Titanium, thermal expansion, RP1520 101

Titration curves of formic and acetic acids, RP1537 347

Translation waves, effect of turbulence and channel slope on, RP1544 461

Tregoning, J. J., George L. Kalousek, C. H. Jumper, Composition and physical properties of aqueous extracts from portland cement clinker pastes containing added materials, RP1530 215

Tungsten-in-quartz lamp, application in photoelectric radiometry, RP1543 449

Tubrbulence and channel slope, effect on translation waves, RP1544 461

U

Ultraviolet solar radiation, RP1542 434

W

Waves, translation, effect of turbulence and channel slope on RP1544 461

Weber, Charles G., Merle B. Shaw, Martin J. O'Leary, Further experimental study of beater practice in the manufacture of offset papers, RP1532 267

Wells, Lansing S., W. W. Clarke, H. F. McMurdie, Study of the system CaO–Al_2O_3–H_2O at temperatures of 21° and 90° C, RP1539 367

Wilson, William K., Herbert F. Launer, Photochemical stability of papers, RP1517 55

Wool blankets, properties:
RP1528 203
RP1529 209

Wool, combination with weak acids, RP1523 123

Wool, reaction with alkali, RP1516 47

Worthington, Vernon, F. T. Carson, Measuring the degree of curl of paper, RP1522 113

X

X-ray diffraction patterns of hydrated calcium aluminates, RP1539 367

NATIONAL BUREAU OF STANDARDS, WASHINGTON, D. C.

Send me the Mathematical Tables marked X below. I enclose remittance [1] to cover the cost.

Mark X	Title of publication	United States and its possessions, and countries extending franking privilege	Other countries	Amount enclosed
----	MT1. Table of the first ten powers of the integers from 1 to 1000	$0. 50	$0. 65	----
----	MT2. Tables of the exponential function e^x	2. 00	2. 50	----
----	MT3. Tables of circular and hyperbolic sines and cosines for radian arguments	2. 00	2. 50	----
----	MT4. Tables of sines and cosines for radian arguments	2. 00	2. 50	----
----	MT5. Tables of sine, cosine, and exponential integrals, volume I	2. 00	2. 50	----
----	MT6. Tables of sine, cosine, and exponential integrals, volume II	2. 00	2. 50	----
----	MT7. Table of natural logarithms, volume I	2. 00	2 50	----
----	MT8. Tables of probability functions, volume I	2. 00	2. 50	----
----	MT9. Table of natural logarithms, volume II	2. 00	2. 50	----
----	MT10. Table of natural logarithms, volume III	2. 00	2. 50	----
----	MT11. Tables of moments of inertia and section moduli	2. 00	2. 50	----
----	MT12. Table of natural logarithms, volume IV	2. 00	2. 50	----
----	MT13. Table of sine and cosine integrals for arguments from 10 to 100	2. 00	2. 50	----
----	MT14. Tables of probability functions, volume II	2. 00	2. 50	----
----	MT15. The hypergeometric and Legendre functions with applications to integral equations of potential theory	2. 00	2. 50	----
----	MT16. Table of arc tan x	2. 00	2. 50	----
----	MT17. Miscellaneous physical tables—Planck's radiation functions; electronic functions	1. 50	1. 75	----
----	MT18. Table of the zeros of the Legendre polynomials of order 1–16 and the weight coefficients for Gauss' mechanical quadrature formula	. 25	. 30	----
	Total remittance	----	----	

[1] Remittance should be in form of post-office money order, or check, and made payable to the order of the "National Bureau of Standards" in United States currency.

Send to----

Number and Street---- City and State----

(Cut here)

MATHEMATICAL TABLES

Attention is invited to a series of publications prepared by the *Project for the Computation of Mathematical Tables* conducted by the Federal Works Agency, Work Projects Administration for the City of New York under the sponsorship of the National Bureau of Standards. The tables which have been made available through the National Bureau of Standards are listed below.

There is included in this list a publication on the hypergeometric and Legendre functions (MT15), prepared by the Bureau.

MT1. TABLE OF THE FIRST TEN POWERS OF THE INTEGERS FROM 1 TO 1000:

(1938) VIII+80 pages; heavy paper cover. 50 cents.

MT2. TABLES OF THE EXPONENTIAL FUNCTION e^x.

The ranges and intervals of the argument and the number of decimal places in the entries are given below:

Range of x	Interval of x	Decimal given
—2.5000 to 1.0000	0.0001	18
1.0000 to 2.5000	.0001	15
2.500 to 5.000	.001	15
5.00 to 10.00	.01	12

(1939) XV+535 pages; bound in buckram, $2.00.

MT3. TABLES OF CIRCULAR AND HYPERBOLIC SINES AND COSINES FOR RADIAN ARGUMENTS:

Contains 9 decimal place values of sin x, cos x, sinh x and cosh x for x (in radians) ranging from 0 to 2 at intervals of 0.0001.
(1939) XVII+405 pages; bound in buckram, $2.00.

MT4. TABLES OF SINES AND COSINES FOR RADIAN ARGUMENTS:

Contains 8 decimal place values of sines and cosines for radian arguments ranging from 0 to 25 at intervals of 0.001.
(1940) XXIX+275 pages; bound in buckram, $2.00.

MT5. TABLES OF SINE, COSINE, AND EXPONENTIAL INTEGRALS, VOLUME I:

Values of these functions to 9 places of decimals from 0 to 2 at intervals of 0.0001.
(1940) XXVI+444 pages; bound in buckram, $2.00.

MT6. TABLES OF SINE, COSINE, AND EXPONENTIAL INTEGRALS, VOLUME II:

Values of these functions to 9, 10, or 11 significant figures from 0 to 10 at intervals of 0.001 with auxiliary tables.
(1940) XXXVII+225 pages; bound in buckram, $2.00.

MT7. TABLE OF NATURAL LOGARITHMS, VOLUME I:

Logarithms of the integers from 1 to 50,000 to 16 places of decimals.
(1941) XVIII+501 pages; bound in buckram, $2.00.

MT8. TABLES OF PROBABILITY FUNCTIONS, VOLUME I:

Values of these functions to 15 places of decimals from 0 to 1 at intervals of 0.0001 and from 1 to 5.6 at intervals of 0.001.
(1941) XXVIII+302 pages; bound in buckram, $2.00.

[Continued on p. 4 of cover]

[Continued from p. 3 of cover]

MT9. TABLE OF NATURAL LOGARITHMS, VOLUME II:

Logarithms of the integers from 50,000 to 100,000 to 16 places of decimals.
(1941) XVIII+501 pages; bound in buckram, $2.00.

MT10. TABLE OF NATURAL LOGARITHMS, VOLUME III:

Logarithms of the decimal numbers from 0.0001 to 5.0000, to 16 places of decimals.
(1941) XVIII+501 pages; bound in buckram, $2.00.

MT11. TABLES OF THE MOMENTS OF INERTIA AND SECTION MODULI OF ORDINARY ANGLES, CHANNELS, AND BULB ANGLES WITH CERTAIN PLATE COMBINATIONS:
(1941) XIII+197 pages; bound in green cloth. $2.00.

MT12. TABLE OF NATURAL LOGARITHMS, VOLUME IV:

Logarithms of the decimal numbers from 5.0000 to 10.0000, to 16 places of decimals.
(1941) XXII+506 pages; bound in buckram, $2.00.

MT13. TABLE OF SINE AND COSINE INTEGRALS FOR ARGUMENTS FROM 10 TO 100:
(1942) XXXII+185 pages, bound in buckram, $2.00.

MT14. TABLES OF PROBABILITY FUNCTIONS, VOLUME II:

Values of these functions to 15 places of decimals from 0 to 1 at intervals of 0.0001 and from 1 to 7.8 at intervals of 0.001.
(1942) XXI+344 pages; bound in buckram, $2.00.

MT15. The hypergeometric and Legendre functions with applications to integral equations of potential theory. By Chester Snow, National Bureau of Standards. Reproduced from original handwritten manuscript.

(1942) VII+319 pages; bound in heavy paper cover. $2.00.

MT16. TABLE OF ARC TAN X:

Table of inverse tangents for positive values of the angle in radians. Second central differences are included for all entries.

Range of x	Interval between successive arguments
0 to 7	0.001
7 to 50	.01
50 to 300	.1
300 to 2,000	1
2,000 to 10,000	10

(1942) XXV+169 pages; bound in buckram, $2.00.

MT17. Miscellaneous Physical Tables:
Planck's radiation functions (Originally published in the Journal of the Optical Society of America, February 1940); and
Electronic functions.
(1941) VI+58 pages, bound in buckram, $1.50.

MT18. Table of the Zeros of the Legendre Polynomials of Order 1–16 and the Weight Coefficients for Gauss's Mechanical Quadrature Formula.
(Reprinted from Bull. Amer. Mathemical Society, October 1942.)
5 pages. 25 cents.

Payment is required in advance. Make remittance payable to the "National Bureau of Standards," and send with order, using the blank form facing page 3 of the cover.

The prices are for delivery in the United States and its possessions and in countries extending the franking privilege. To other countries the price of MT1 is 65 cents; that of MT2 to MT16, inclusive, is $2.50 each; MT17, $1.75; MT18, 30 cents; remittance to be made payable in United States currency.

Copies of these publications have been sent to various Government depositories throughout the country, such as public libraries in large cities, and colleges and universities, where they may be consulted.

A mailing list is maintained for those who desire to receive announcements regarding new tables as they become available.